CNIC-01016
CNDC-0017
INDC(CPR)-036 / L

COMMUNICATION OF NUCLEAR DATA PROGRESS

No. 14 (1995)

China Nuclear Data Center

China Nuclear Information Centre

Atomic Energy Press

Beijing, December, 1995

EDITORIAL NOTE

This is the fifteenth issue of *Communication of Nuclear Data Progress* (CNDP), in which the achievements in nuclear data field for the last year in P. R. China are carried. It includes the measurements of neutron activation cross sections for $^{64}Zn(n,\gamma)^{65}Zn$, $^{23}Na(n,2n)^{22}Na$, $^{92}Mo(n,p)^{92m}Nb$, $^{94}Mo(n,2n)^{93m}Mo$, $^{98}Mo(n,p)^{98m}Nb$, $Ba(n,x)^{134}Cs$, $^{134}Ba(n,2n)^{133}Ba$, $^{137}Ba(n,p)^{137}Cs$, $^{140}Ce(n,2n)^{139}Ce$, $^{142}Ce(n,2n)^{141}Ce$, $^{179}Hf(n,2n)^{178m2}Hf$ and $^{209}Bi(n,2n)^{208}Bi$ reactions; calculation of neutron induced reactions on nuclides $^{175,\ 176,\ Nat}Lu$ and ^{89}Y (emphatically on γ-production data); a γ-production data intercomparison system and intercomparison of Fe, Cr, Ni γ-production data; evaluations of $n+^{56}Fe$, $^{58,\ 60,\ 61,\ 62,\ 64,\ Nat}Ni(n,\alpha)$, $^{93}Nb(n,2n)$, (n,n') and ^{58}Ni, ^{87}Rb, ^{89}Y, ^{90}Zr, ^{140}Ce, $^{169}Tm(n,2n)$ reaction cross sections; sensitivity of *logft* on ε branching to ground state of ^{197}Au in decay of ^{197}Hg; evaluated particle reflection data base, physical sputtering simulated calculation; progress on parameter and program libraries.

We hope that our readers and colleagues will not spare their comments, in order to improve the publication.

Please write to Drs. Liu Tingjin and Zhuang Youxiang
Mailing Address : China Nuclear Data Center
China Institute of Atomic Energy
P. O. Box 275 (41), Beijing 102413
People's Republic of China
Telephone : 86-10-9357729 or 9357830
Telex : 222373 IAE CN
Facsimile : 86-10-935 7008
E-mail : CIAEDNP@ BEPC 2.IHEP.AC.CN

CONTENTS

I EXPERIMENTAL MEASUREMENT

Activation Cross Section Measurement of $^{64}Zn(n,\gamma)^{65}Zn$ Reaction from 156 to 1150 keV

Chen Jinxiang Shi Zhaomin Tang Guoyou Zhang Guohui

(Institute of Heavy Ion Physics, Peking University, Beijing)

Lu Hanlin Zhao Wenrong Yu Weixiang

(China Institute of Atomic Energy, Beijing)

Introduction

The neutron capture cross sections are important not only for the studies of nuclear reaction mechanism and astrophysics but also for the nuclear technology application. $^{64}Zn(n,\gamma)^{65}Zn$ cross sections are desired for the design of fusion reactor. Up to now, there are a few data for this reaction, but mostly for thermal and fission spectrum neutrons[1]. At the higher neutron energies, no such measurements of $^{64}Zn(n,\gamma)^{65}Zn$ activation cross section have been reported.

In this work, we measured the cross sections for the $^{64}Zn(n,\gamma)^{65}Zn$ reaction in the neutron energies from 156 to 1150 keV by the activation technique and the cross sections of $^{197}Au(n,\gamma)^{198}Au$ reaction were used as a reference for neutron fluence rate measurement. Experimental activation cross sections were given for the first time. The errors of measured results are 5%～8%.

1 Experimental Measurement

The experiments were performed at 4.5 MV Van de Graaf accelerator of the Institute of Heavy Ion Physics at Peking University. The monoenergetic neutrons with energies 156 and 330 keV were obtained from $^{7}Li(p,n)^{7}Be$ reac-

tion on a solid LiF target with 90 $\mu g / cm^2$ in thickness. The 540 ~ 1150 keV neutrons were produced via the $T(p,n)^3He$ reaction on a solid Ti–T target with 1.2 mg / cm^2 in thickness. The energy of the proton beam was varied between 1.6 and 2.1 MeV and the beam current between 6 and 10 μA.

The target samples are natural metallic zinc disks with a diameter of about 20 mm and a thickness of about 0.45 mm. The purity is better than 99.9%. Two gold disks with same size which were used as the neutron fluence monitors were attached in the front and at the back of each zinc sample, respectively. Then they were sandwiched together between the other two gold foils which were used for a resonance absorption of 5 eV background neutrons. Finally, the sample unit was wrapped with cadmium foil of 0.2 mm thickness. The samples were placed in the 0 ° direction relative to the proton beam at a distance of about 1.5 cm behind the target. The irradiation time of a sample were not less than 12 h, some of them up to 20 h. The fluctuation of neutron fluence rate was monitored by a BF_3 long counter placed in the 0 ° direction relative to the proton beam at a distance of about 2 m from the neutron source.

After irradiation, the ^{198}Au activity was measured with a HPGe γ–detector (105 cm^3), while a Ge(Li) γ–ray detector (136 cm^3) was used for other products. The detectors were calibrated using a set of standard gamma sources in the energy range of 0.1 to 1.5 MeV and the efficiency curve was obtained with a least square fit. The peak area analysis of measured γ–ray was done by using the program H developed for an IBM compatible computer.

2 Results

From the measured γ–spectrum, counting rates under the concerned full–energy peaks were obtained. The decay data[2] of the residual nuclei measured in the experiment are listed in Table 1. After the corrections for the detector efficiency, γ–intensity, fluctuation of neutron fluence rate and γ–ray self absorption in the samples, the cross section of $^{64}Zn(n,\gamma)^{65}Zn$ were calculated by using the well–known activation equation. The standard cross sections of $^{197}Au(n,\gamma)^{198}Au$ reaction were taken from ENDF / B–6. The measured values of the cross section are listed in Table 2. The principal contributions of errors and their magnitudes are given in Table 3.

Table 1 Decay data of the residual nuclei

Residual nuclei	Half-life / h	Energy of γ-ray / keV	γ-intensity / %
^{65}Zn	5858.4	1115	50.60
^{198}Au	64.704	412	95.57

Table 2 Cross sections of $^{64}Zn(n,\gamma)^{65}Zn$ reaction

E_n / keV	Cross section / mb
156 ± 10	24.8 ± 1.3
330 ± 20	21.1 ± 1.7
540 ± 40	20.3 ± 0.9
735 ± 54	19.5 ± 0.8
930 ± 62	19.4 ± 0.8
1150 ± 70	18.4 ± 0.9

Table 3 Principal sources of errors

Source of uncertainty	Relative errors / %
Reference cross section	3.0~4.5
γ-counting statistics for ^{65}Zn	1.0~8.0
γ-counting statistics for ^{198}Au	0.6~1.0
γ-detection efficiency for ^{65}Zn	1.0
γ-detection efficiency for ^{198}Au	1.5
^{64}Zn sample weight	0.2
^{197}Au foil weight	0.1

Cross section calculation of $^{64}Zn(n,\gamma)^{65}Zn$ reaction was also done by using the systematics method described in Refs. [3, 4]. The results of the systematics calculation and our experimental data are shown in Fig. 1, which shows that the systematics results are lower than the experimental data and decrease faster than the experimental data as increasing incident neutron energy. J. B. Garg et al.[5] had measured the neutron capture cross section of ^{64}Zn nuclei using the method of time-of-flight, but they gave out only the resonance curves. We took the average values from the curves and drew them in Fig. 1 for comparison. It can be seen from Fig. 1 that Garg's results are higher than our data, but

both data decrease with same trend as increasing the incident neutron energy.

We appreciate Dr. Zhao Zhixiang for the systematics calculation data and thank the China National Nuclear Corporation for the financial support. Acknowledgement is made to the crews of the 4.5 MV Van de Graaff accelerator at Peking University for numerous irradiations.

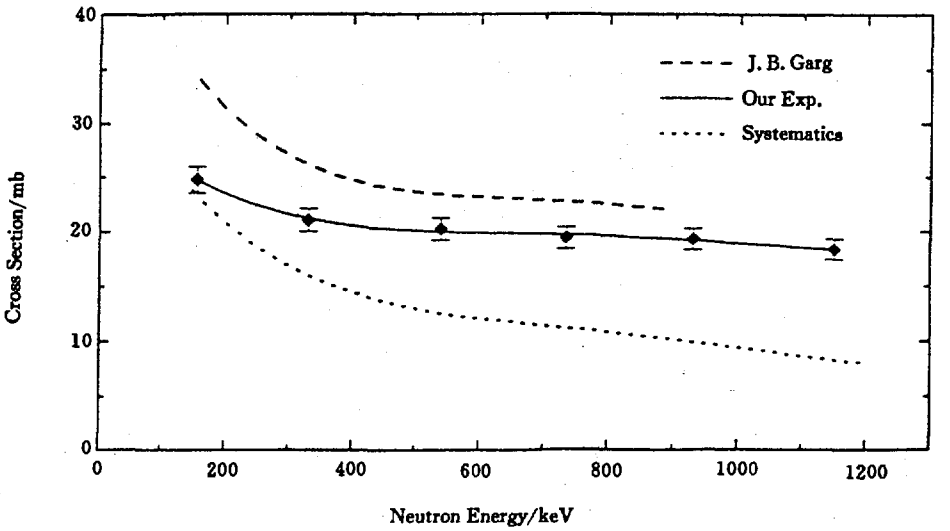

Fig. 1 $^{64}Zn(n,\gamma)^{65}Zn$ cross section

References

[1] D. L. Smith et al., ANL / NDM−123, p. 73, 1991

[2] C. M. Lederer et al., Table of Isotopes, 7th Edition, p. 202

[3] Zhao Zhixiang et al., Chin. J. Nucl. Phys., 11(3), 71, 1989

[4] Zhao Zhixiang, et al., Proceedings of the International Conference Nuclear Data for Science and Technology, Mito, Japan, p. 513 (1988)

[5] J. B. Garg et al., Phys. Rev., 23(2), 683, 1981

Recent Progress on 14 MeV Neutron Activation Cross Section Measurements

Kong Xiangzhong Wang Yongchang Yang Jingkang Yuan Junqian

(Department of Modern Physics, Lanzhou University)

The activation cross section data of 14 MeV neutrons are important for development of fusion reactor. The activation cross sections leading to the production of long–lived radionuclides especially attract the human attention, because they effect a series of problems, such as re–applying the old structure materials of a fusion reactor, reducing its radiation background and disposing the nuclear waste, etc.. Therefore a Coordinated Research Program was organized by the IAEA to measure some activation cross sections leading to the production of long–lived radionuclides in 1988. Since March 1993 we have measured some activation cross sections for the generations of long–lived radionuclides and obtained useful results at the Intense Neutron Generator of Lanzhou University. The results obtained are given in Table 1[1, 2]. Some activation cross sections for the interesting reactions were also measured. The results obtained are given in Tables 2 and 3, respectively.

Table 1 Values of activation cross sections for the generations of long–lived radionuclides

Neutron energy / MeV	Cross section / mb		
	$^{137}Ba(n,p)^{137}Cs$	$^{179}Hf(n,2n)^{178m2}Hf$	$^{209}Bi(n,2n)^{208}Bi$
14.2	10.6 ± 0.9		
14.4		6.04 ± 0.31	
14.6			2279 ± 173

Table 2 Values of activation cross sections for the interesting reactions [3]

Neutron energy / MeV	Cross section / mb				
	$Ba(n,x)^{134}Cs$	$^{134}Ba(n,2n)^{133}Ba$	$^{140}Ce(n,2n)^{139}Ce$	$^{142}Ce(n,2n)^{141}Ce$	$^{23}Na(n,2n)^{22}Na$
13.50 ± 0.07	0.625 ± 0.031	1682 ± 84	1722 ± 96	2050 ± 100	5.60 ± 0.20
14.18 ± 0.07	0.711 ± 0.036	1764 ± 88	1799 ± 100	2080 ± 100	19.9 ± 0.7
14.80 ± 0.11	0.782 ± 0.039	1785 ± 89	1830 ± 110	2043 ± 100	38.2 ± 10.1

Table 3 Values of activation cross sections for the interesting reactions [4]

Neutron energy / MeV	Cross section / mb		
	$^{92}Mo(n,p)^{92m}Nb$	$^{98}Mo(n,p)^{98m}Nb$	$^{94}Mo(n,2n)^{93m}Mo$
13.40 ± 0.05	92.0 ± 3.3	3.4 ± 0.2	0.67 ± 0.04
13.61 ± 0.05	83.8 ± 3.0	3.5 ± 0.2	1.1 ± 0.1
13.80 ± 0.07	82.3 ± 3.0		
14.07 ± 0.07	77.2 ± 2.7	4.6 ± 0.2	2.3 ± 0.2
14.27 ± 007	71.3 ± 2.5		3.7 ± 0.2
14.65 ± 0.11	63.2 ± 2.2	5.5 ± 0.2	5.3 ± 0.3
14.79 ± 0.11	62.3 ± 2.2	6.2 ± 0.2	6.1 ± 0.3

Irradiation of the samples was carried out at the ZF−300−II Intense Neutron Generator at Lanzhou University with a yield of ~ 1 to 3×10^{12} n / s. Neutrons were produced by the $T(d,n)^4He$ reaction with an effective deuteron beam energy of 125 keV and beam current of 20 mA. The tritium−titanium (T−Ti) target used in the generator was ~ 0.9 mg / cm^2 thick. The neutron flux was monitored by a uranium fission chamber so that corrections could be made for small variations in the yield. The neutron energies for various directions were determined by cross section ratios of $^{90}Zr(n,2n)^{89m+g}Zr$ and $^{93}Nb(n,2n)^{92m}Nb$.

The radioactivities of the reaction products were measured by γ−ray spectrometer using a CH8403 coaxial HPGe detector made in China in conjunction with an EG & G ORTEC 7450 Multichannel Analyzer. The efficiency of the detector was calibrated by using the standard γ source, SRM4275, made in U. S. A.[5]. The relative photopeak detection efficiency of the detector was known within an error ± 1.5%. The decay data used in the present work are taken from Ref. [6]. In order to obtain the γ activities, some corrections were made for the effect of neutron fluence fluctuation, γ−ray self−absorption in the

sample, the coincidence sum effect in the investigated nuclide and the counting geometry, etc..

References

[1] Wang Yongchang et al., Atomic Energy Science and Technology (in Chinese), 27(2), 174 (1993)

[2] Yuan Junqian et al., Trends in Nuclear Physics, (in Chinese), 11(1), 65 (1994)

[3] Kong Xiangzhong et al., High Energy Physics and Nuclear Physics (in Chinese), to be published

[4] Kong Xiangzhong et al., Journal of Lanzhou University (in Chinese), to be published

[5] Wang Yongchang et al., High Energy Physics and Nuclear Physics (in Chinese), 14(10), 919 (1990)

[6] E. Browne and R. B. Firestone, Table of Radioactive Isotopes, 1986

II THEORETICAL CALCULATION

The Calculations of γ-Production Data of n + ^{89}Y Reactions in the Incident Neutron Energy Region from 0.1 to 20 MeV

Liu Jianfeng

(Department of Physics, Zhengzhou University, Zhengzhou)

Liu Tingjin

(China Nuclear Data Center, CIAE)

Introduction

The theoretical calculation of the nuclear reaction data for n+^{89}Y is very important. It not only provides the indispensable nuclear reaction data for nuclear engineering but also has important theoretical significance. On the one hand ^{89}Y is a neutron magic-number nucleus and located in the 3P giant resonance region of the neutron strength functions, i. e., the 3P state energy levels of the neutrons are located nearby the neutron binding energy and the 2d state energy levels nearby the ground state. It provides a favorable condition for researching neutron radiative capture reaction mechanisms, especially for non-statistical effects in the neutron radiative captures. On the other hand the neutrons near Fermi surface of ^{89}Y are filled in the $1g_{9/2}$ single particle state. When these neutrons are excited, the isomeric state which makes a great spin difference from the ground state can be formed. The experimental results have shown that the reaction products of n+^{89}Y, e. g. ^{90}Y, ^{89}Y as well as ^{86}Rb all have the isomeric states and this provides a favourable condition for the isomeric state cross section calculations of nuclear reactions. In the seventies, the direct-semidirect reaction mechanism[1] was studied in terms of ^{89}Y, but it

is carried out only in the energy region above 3～ 5 MeV. For the reaction mechanisms[2, 3], which are important blow 3～ 5 MeV, no systematic calculations in terms of ^{89}Y have been done and the γ–production data, such as γ–ray energy spectra, γ–production cross sections as well as γ–ray multiplicities, have not been calculated as well yet. So far only rare isomeric state cross section calculations have been done.

In this paper, using compound nucleus statistical model[4], in which simplified pre–equilibrium correction[5] is made for primary particle emissions in higher energy region, and considering the contributions from non–statistical effects[1～3] in neutron radiative capture processes, the theoretical calculations of the reaction data for n+^{89}Y have been accomplished in the incident neutron energy region from 0.1 to 20 MeV. The γ–production data, such as γ–ray energy spectra, γ–production cross sections and γ–ray multiplicaties, as well as the isomeric state cross sections in (n,x γ) reactions including (n,γ) processes have been investigated emphatically. The calculated results have been compared with the experimental data and a brief discussion has been made. In present work, the reaction cross sections of (n,γ) and (n,xγ) processes have been calculated by resolving the integration equations which describe cascade γ deexcitations. One of the advantages of this method[6] is that the calculated (n,γ) cross sections deduct the contribution of (n,xγ) processes and include the contribution from primary γ transitions to the energy levels above B_n (neutron binding energy). Another advantage is that the ground state cross section and isomeric state cross section of (n,xγ) reactions can be given at the same time, respectively.

1 Formulation

The integration equations, which describe cascade γ deexcitation processes of residual nuclei created after emissions of particles, can be represented as follows :

$$\sigma_c\ (\ E,J,\pi\ ) = \sigma_{c0}\ (\ E,J,\pi\ ) + \int_{\varepsilon}^{E_{max}} \sum_{J'\pi'} \sigma_c\ (\ E',J',\pi'\ )\ \frac{T_\gamma^{E',J',\pi',E,J,\pi}}{T^{E',J',\pi'}}\ \rho\ (\ E,J,\pi\ )\ dE' \qquad (1)$$

$$\sigma_i = \sigma_{i0} + \sum_{j=i+1,\ j\neq k}^{N} \sigma_j \frac{T_\gamma^j}{T^j} S^{ji}$$

$$+ \int_{E_c}^{E_{max}} \sum_{J'\pi'} \sigma_c (E',J',\pi') \frac{T_\gamma^{E',J',\pi',E_i,J_i,\pi_i}}{T^{E',J',\pi'}} dE' \qquad (2)$$

where $\sigma_c(E,J,\pi)$ is total excitation cross section in a unit energy interval in the continuous energy level region with spin J, parity π and energy E in whole cascade γ deexcitation process; $\sigma_{c0}(E,J,\pi)$ is its initial value, for (n,γ) reaction, it is the excitation created by primary γ transitions but for (n,xγ) reaction, it is the excitation created by particle emissions of parent nucleus. σ_i is total excitation cross section of ith discrete level in whole cascade γ deexcitation process and σ_{i0} is its initial value. $\rho(EJ,\pi)$ represents level density. $T(EJ\pi)$ represents total transmission coefficient. $T_\gamma^{E'J'\pi',EJ\pi}$ is γ transmission coefficient from energy level $(E'J'\pi')$ to $(EJ\pi)$. T^j represents total transmission coefficient of jth discrete level and T_γ^j is its γ transmission coefficient. S^{ji} represents γ transition branching ratio from energy level jth to ith. The relation $j\neq k$ in (2) represents that the kth discrete level is an isomeric state. N is discrete level number. E_c is the inferior limit of continuous energy level region. E_{max} is the highest excitation energy of the system.

After $\sigma_c(E,J,\pi)$ and σ_i are calculated by resolving the above equations, the energy distribution of γ production i. e., γ energy spectrum, can be calculated in terms of following relation :

$$\frac{d\sigma^\gamma}{dE_\gamma} = \sum_{i=1}^{N} \sum_{j=i+1,\ j\neq k}^{N} \sigma_j \frac{T_\gamma^j}{T^j} S^{ji} \delta (E_\gamma + E_i - E_j)$$

$$+ \sum_{i=1}^{N} \sum_{J'\pi'} \sigma_c (E_i + E_\gamma, J', \pi')$$

$$\frac{T_\gamma^{E_i+E_\gamma,J',\pi',E_i,J_i,\pi_i}}{T^{E_i+E_\gamma,J'\pi'}} + \int_{E_c+E_\gamma}^{E_{max}} \sum_{J\pi}^{N} \sum_{J'\pi'} \sigma_c (E',J',\pi')$$

$$\frac{T_{\gamma}^{E',J',\pi',E'-E_{\gamma},J,\pi}}{T^{E',J',\pi'}} \rho\ (\ E'-E_{\gamma},J,\pi\ )\ \mathrm{d}E' \tag{3}$$

and the γ production cross section is calculated by

$$\sigma^{\gamma} = \int_0^{E_{max}} \frac{\mathrm{d}\sigma^{\gamma}}{\mathrm{d}E_{\gamma}}\ \mathrm{d}E_{\gamma} \tag{4}$$

while the γ multiplicity is

$$Y^{\gamma} = \frac{\sigma^{\gamma}}{\sigma\ (\mathrm{n,x}\gamma)} \tag{5}$$

where $\sigma(\mathrm{n,x}\gamma)$ represents the reaction cross section of $(\mathrm{n,x}\gamma)$ reaction. At the same time, the ground cross section $\sigma_{\mathrm{nx}\gamma\mathrm{s}}$ and the isomeric cross section $\sigma_{\mathrm{nx}\gamma\mathrm{m}}$ of $(\mathrm{n,x}\gamma)$ reaction can be calculated by

$$\sigma_{\mathrm{nx}\gamma\mathrm{s}} = \sigma_{10} + \sum_{J=2,\ j\neq K}^{N} \sigma_J \frac{T_{\gamma}^{j}}{T^{j}}\ S^{jj}$$

$$+ \int_{E_c}^{E_{max}} \sigma_c\ (\ E',J',\pi'\ )\ \frac{T_{\gamma}^{E',J',\pi',E,J,\pi}}{T^{E',J',\pi'}}\ \mathrm{d}E' \tag{6}$$

$$\sigma_{\mathrm{nx}\gamma\mathrm{m}} = \sigma_{K0} + \sum_{j=K+1}^{N} \sigma_j \frac{T_{\gamma}^{j}}{T^{j}}\ S^{jK}$$

$$+ \int_{E_c}^{E_{max}} \sigma_c\ (\ E',J',\pi'\ )\ \frac{T_{\gamma}^{E',J',\pi',E_K,J_K,\pi_K}}{T^{E',J',\pi'}}\ \mathrm{d}E' \tag{7}$$

and

$$\sigma(\mathrm{n,x}\gamma) = \sigma_{\mathrm{nx}\gamma\mathrm{s}} + \sigma_{\mathrm{nx}\gamma\mathrm{m}} \tag{8}$$

In order to resolve the Eqs. (1) and (2), the values of σ_{i0} and $\sigma_{co}(EJ,\pi)$ must be given. The calculation formulas for them can be found in Ref. [5].

2 The Parameters and Calculated Results

The numerical calculations of reaction data for n+^{89}Y have been performed in the energy region from 0.1 to 20 MeV. In the calculations, Becchetti–Greenless [7] optical potential has been used to calculate the transmission coefficients of neutrons and charge particles and the real part of this potential has been used to calculate the eigen energies and the wave functions of the single particle bound states. Gilbert–Cameron formulas[8] have been used to calculate the energy level densities. The giant dipole resonance parameters of photonuclear reactions[9], the discrete energy level parameters and the isomeric parameters are all taken from the experimental data.

In the calculations, the optical potential parameters of incident neutrons have been adjusted first to make the calculated total and elastic scattering cross sections coincide better with the experimental values, and then the optical potential parameters of all outgoing particles and the energy level density parameters of the corresponding residual nuclei have been adjusted to make the inelastic scattering cross section and other reaction cross sections of (n,xγ) reactions coincide as good as possible with the experimental values. Finally the energy level density parameters of the compound nucleus and the particle–photon coupling potential parameters in direct–semidirect capture processes have been adjusted to make the calculated radiative capture cross sections coincide better with the experimental values.

In Table 1 the optical potential parameters for neutron, proton and α used in the final calculation are shown. In Table 2 the energy level density parameters and the giant dipole resonance parameters of compound nucleus and residual nuclei are given. The calculated total, elastic scattering, (n,2n), (n,p), (n, α) cross sections are in good agreement with the experimental data. Fig. 1 shows the calculated results of the (n,γ) cross sections and the experimental data. In Fig. 2 the calculated (n,γ) cross section of the isomeric state and the experimental data is shown. The calculated nonelastic process γ–production cross section is given in Fig. 3. In Fig. 4 calculated result of the γ–ray energy spectrum at incident neutron energy 1.0 MeV is shown. The experimental data of Figs. 1~4 are all taken from Ref. [10].

3 Conclusion Remarks

(1) Using the compound nucleus statistical model, in which the pre–equilibrium effect and the contributions from the non–statistical effects are considered.

The γ–production data, including the isomeric state cross sections in the (n,x γ) reactions, have been investigated emphatically. The calculated data reproduce corresponding experimental data very well.

(2) The nonstatistical effects of the neutron radiative capture are very important for ^{89}Y. Below 5 MeV, the contributions from the nonstatistical effects are about 10% of the total (n,γ) cross sections and above 10 MeV, they are larger than 90%.

Table 1 The optical potential parameters for n, p and α

Particle	V_R	γ_R	a_R	W_v	$\gamma_{I'}$	$a_{I'}$	W_{SF}	γ_I	a_I	V_{so}	γ_{so}	a_{so}	γ_c
n	$-53.3+0.32E$	1.17	0.75	$0.94-0.176E$ $W_v<0$	1.26	0.58	$-6.32+0.25E$	1.26	0.58	−6.2	1.01	0.75	
P	$-53.81+0.32E$	1.20	0.70	0			$-15.64+0.25E$	1.25	0.73	−4.7	1.20	0.70	1.25
α	$-145.52+0.25E$	0.984	0.75	$-6.26+0.33E$	1.19	0.84	0			0			1.30

Table 2 The level density parameters and giant resonance parameters

	level density parameters					giant resonance parameters		
Nuclide	E_x / MeV	T / MeV	E_0 / MeV	$P_\delta+P_N$ / MeV	a / MeV^{-1}	σ_R / b	Γ_R / MeV	E_R / MeV
^{90}Y	5.1667	0.8771	−0.6867	0.0	9.577	0.2110	4.5	16.46
^{89}Y	5.1154	1.0039	−0.1253	0.93	8.979	0.2260	4.25	16.74
^{89}Sr	5.4254	0.8753	0.1352	1.24	9.428	0.2260	4.25	16.74
^{86}Rb	4.2442	0.8361	−1.2230	0.0	9.590	0.2484	4.5	15.54
^{88}Sr	6.3746	0.9018	1.0959	2.17	9.031	0.2542	4.5	15.47
^{87}Sr	5.4641	0.8381	0.0371	1.24	10.125	0.2513	4.5	15.50
^{87}Rb	5.1541	0.8980	−0.1665	0.93	9.1123	0.2513	4.5	15.50
^{88}Y	4.2046	0.8388	−1.1859	0.0	10.089	0.2542	4.5	15.47
^{85}Rb	5.7247	0.7955	0.1439	1.46	11.0385	0.2456	4.5	15.58

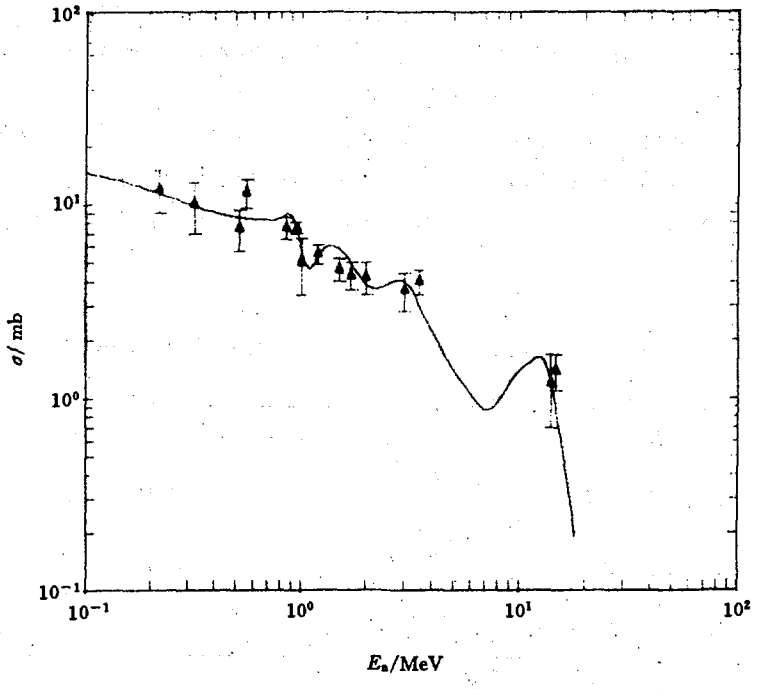

Fig. 1 Calculated (n,γ) cross sections and the experimental data

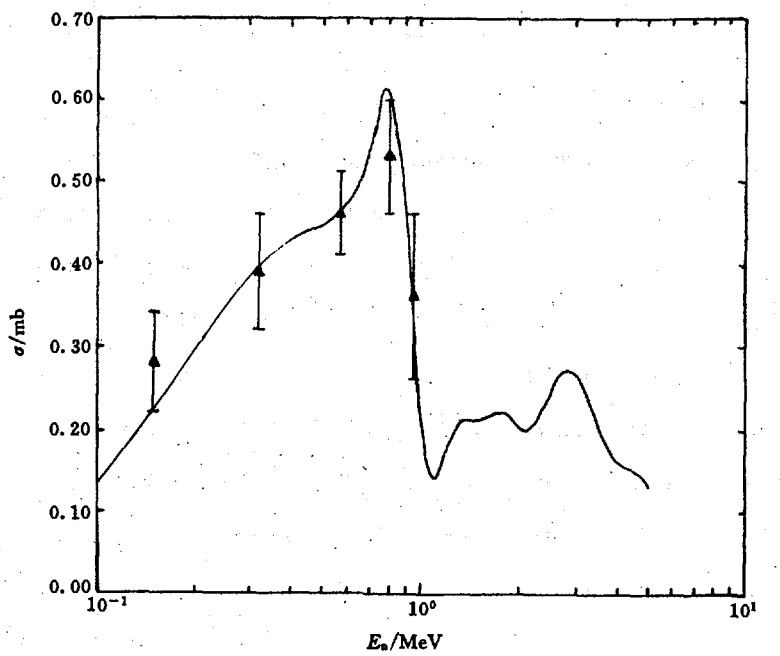

Fig. 2 Calculated (n,γ) cross sections of the isomeric state and the experimental data

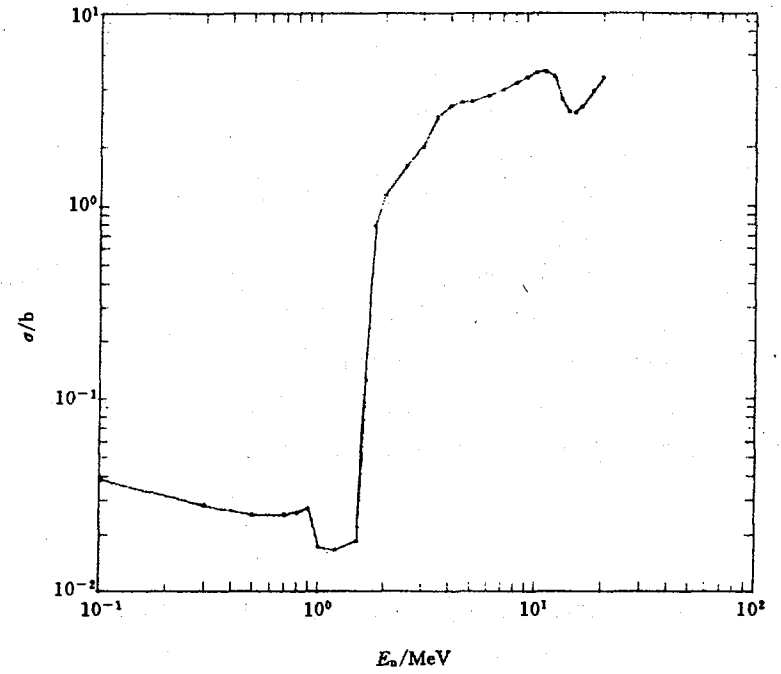

Fig. 3 Calculated nonelastic process γ–production cross sections

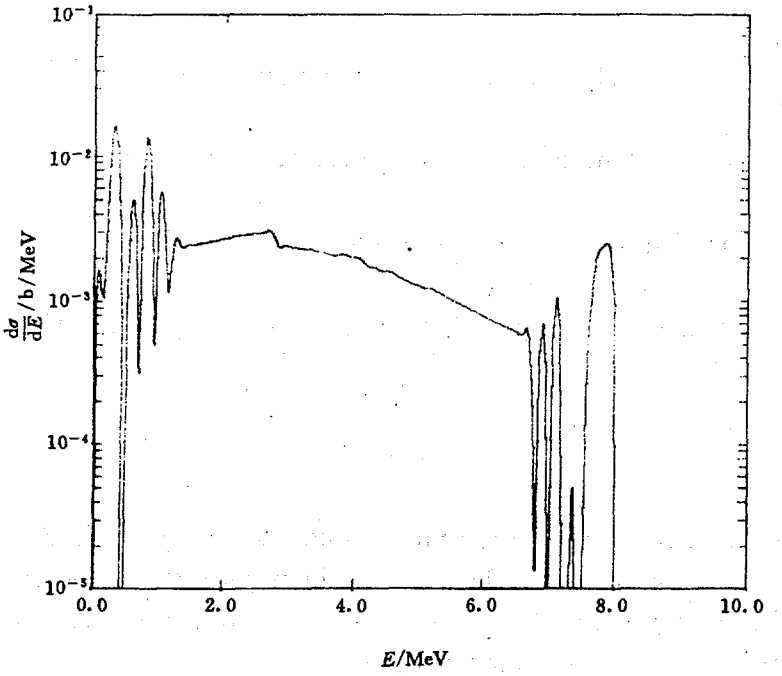

Fig. 4 Calculated γ–ray energy spectrum at incident energy 1.0 MeV

References

[1] G. E. Brown, Nucl. Phys., 57, 339 (1964)
[2] Y. K. Ho et al., Nucl. Phys., A406, 1 (1983)
[3] Liu Jianfeng et al., High Energy Physics & Nucl. Phys., 4, 349 (1991)
[4] Hu Jimin et al., Nuclear Theory, Atomic Energy Press, (1987)
[5] Liu Jianfeng et al., CNDP, 10, 28 (1993)
[6] Liu Jianfeng et al., High Energy Physics & Nuclear Physics, to be published
[7] F. D. Becchetti et al., Phys. Rev., 182, 1190 (1969)
[8] A. Gilbert et al., Can. J. Phys., 43, 1446 (1965)
[9] S. S. Dietrich et al., Atomic Data & Nuclear Data Tables, 38, 199 (1988)
[10] Mclane et al., Neutron Cross Sections, Vol. 2, (1988)

Calculation and Analysis of Neutron Induced Reactions on ^{175,176}Lu and ^{Nat}Lu in Energy Region 1 keV ~ 20 MeV

Han Yinlu Shen Qingbiao

(China Nuclear Data Center, CIAE)

Sun Xiuquan Xiao Ling Zhang Zhengjun

(Physics Department, Northwest University, Shaanxi)

Abstract

A set of neutron optical potential parameters for 1 keV $< E_n <$ 20 MeV is obtained on the basis of the relevant experimental data, and all cross sections of neutron induced reaction on $^{175, 175, Nat}$Lu are calculated. The calculated results are compared with experimental data.

Introduction

The cross sections of neutron induced reactions on ^{175,176,Nat}Lu are important for nuclear science and technology. Because the experimental data are less, the theoretical calculation is necessary and interesting. The purpose of this paper is to report the calculated results of ^{175,176,Nat}Lu at 1 keV $< E_n <$ 20 MeV.

1 The Parameters of Theoretical Models

The code APOM94[1] and NUNF[2] are used in our calculations.

The nuclear discrete levels are taken from Ref. [3]. The parameters of nuclear levels densities and giant dipole resonance are taken from Ref. [4].

First, the code APOM94, by which the best neutron optical potential parameters can be searched automatically with fitting the relevant experimental total, elastic scattering cross sections and angular distributions, is used to obtain a set of optimum neutron optical potential parameters of Lu. Because there are no experimental data of elastic cross sections and elastic scattering angular distributions for Lu, so we choose neutron elastic cross sections[5] and elastic scattering distributions[5, 6] of Hf, which is neighbors nuclei of Lu. A set of optimum neutron optical potential parameters of Lu are obtained as fellows :

$$V = 51.4429 + 0.1546E - 0.0206E^2 - 24.0\ (N-Z)/A$$
$$W_S = \max\{0.0, 9.1002 - 0.3507E - 12.0\ (N-Z)/A\}$$
$$W_V = \max\{0.0, -1.2155 + 0.1940E + 0.016E^2\}$$
$$U_{SO} = 6.2$$
$$r_R = 1.1906,\ r_S = 1.3203,\ r_V = 1.5881,\ r_{SO} = 1.1906$$
$$a_R = 0.5789,\ a_S = 0.6687,\ a_V = 0.3615,\ a_{SO} = 0.5789$$

Then, using this set of neutron optical potential parameters, and giant dipole level density parameter adjusted proton and alpha particle optical potential parameters, level density and giant dipole resonance parameters, all reaction cross sections are calculated by using the code NUNF. The direct inelastic scattering data are calculated by code DWUCK4[7]. The exciton model parameter K is taken as 1500 MeV^3.

2 Calculated Results and Analyses

Fig. 1 shows the comparison of neutron total cross section for ^{Nat}Lu in energy region 1 ~ 20 MeV between the theoretical values (solid line) and experimental data taken from Ref. [8]. The calculated results are in good agreement with the experimental data. The comparisons for theoretical calculated results and experimental data[9~15] of $^{175}Lu(n,\gamma)$, $^{176}Lu(n,\gamma)$ and $^{Nat}Lu(n,\gamma)$ reaction cross sections are given in Fig. 2 to Fig. 4, respectively. The calculated values are in agreement with experimental data in energy region 1 keV ~ 100 keV, but for $E_n > 100$ keV, the calculated values are lower than experimental data. The comparison of theoretical calculated results and experimental data[16~19] of $^{175}Lu(n,2n)$ and $^{175}Lu(n,3n)$ reactions are given in Fig. 5 and Fig. 6, respectively. The agreement between the calculated values and experimental data is good in the whole energy range. Fig. 7 illustrates (n,tot), (n,non), (n,el), (n,γ), (n,in), (n,p), (n,α), (n,t), (n,np), (n,2n), (n,nα) and (n,3n) reaction cross sections of ^{Nat}Lu, the calculated (n,p) and (n,α) cross section curves pass through the existent experimental error bars[20~22], respectively.

3 Conclusions

Based on the available experimental data of Lu and neighbour nuclei Hf, we obtain a set of optimum neutron optical potential parameters for 1 keV $< E_n <$ 20 MeV. With adjusted proton and alpha particle optical potential parameters, level density and giant dipole resonance parameters as well as K, the all cross sections of neutron induced reaction on $^{175, 176, Nat}Lu$ are obtained. The calculated nuclear data are in good agreement with the experimental data.

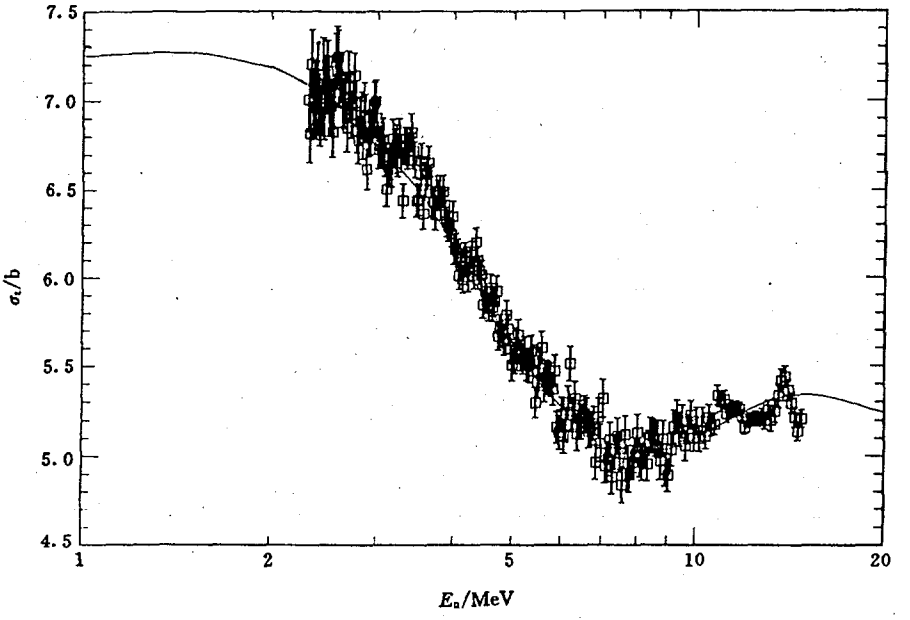

Fig. 1 The total cross section of n+^{Nat}Lu

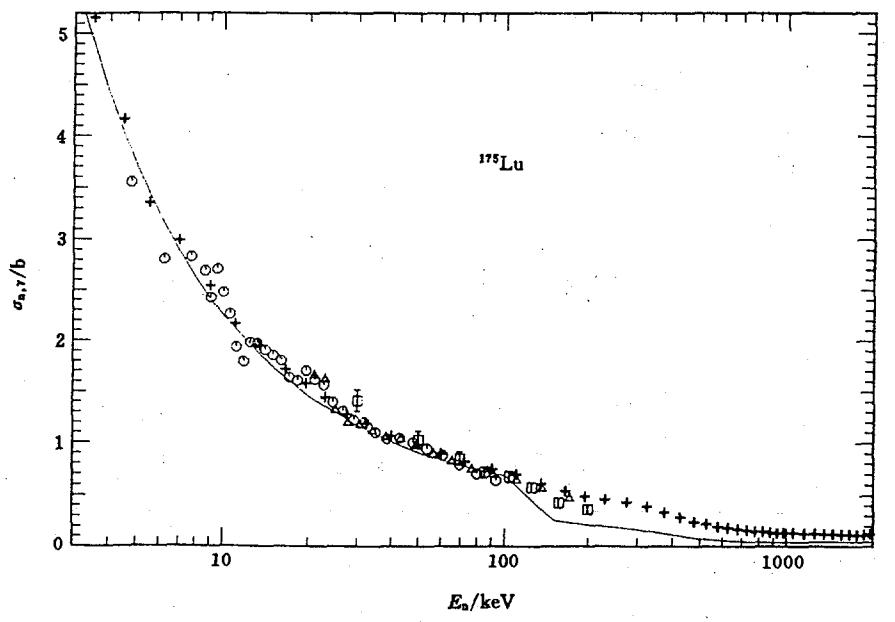

Fig. 2 The cross section of ^{175}Lu(n,γ) reaction

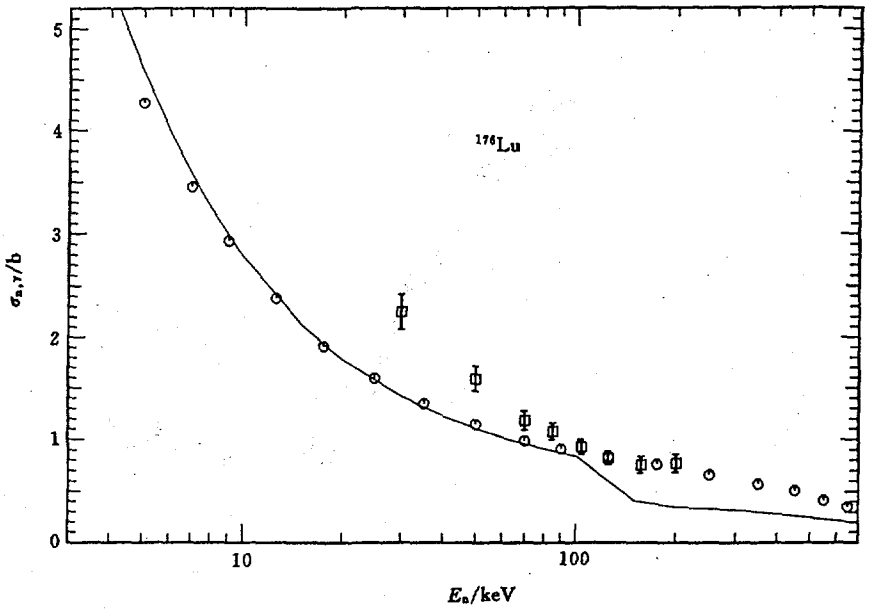

Fig. 3 The cross section of ^{176}Lu(n,γ) reaction

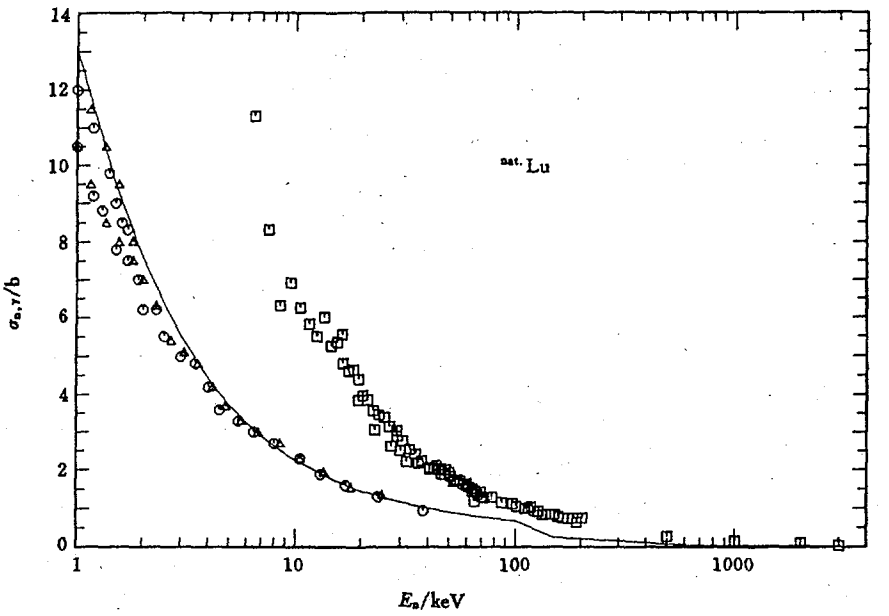

Fig. 4 The cross section of ^{Nat}Lu(n,γ) reaction

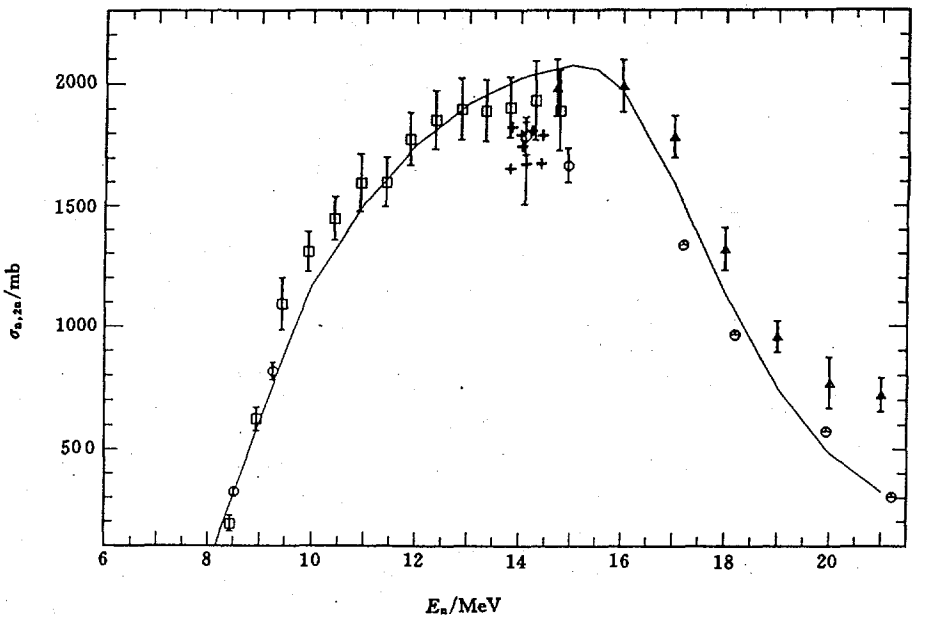

Fig. 5 The cross section of ^{175}Lu(n,2n) reaction

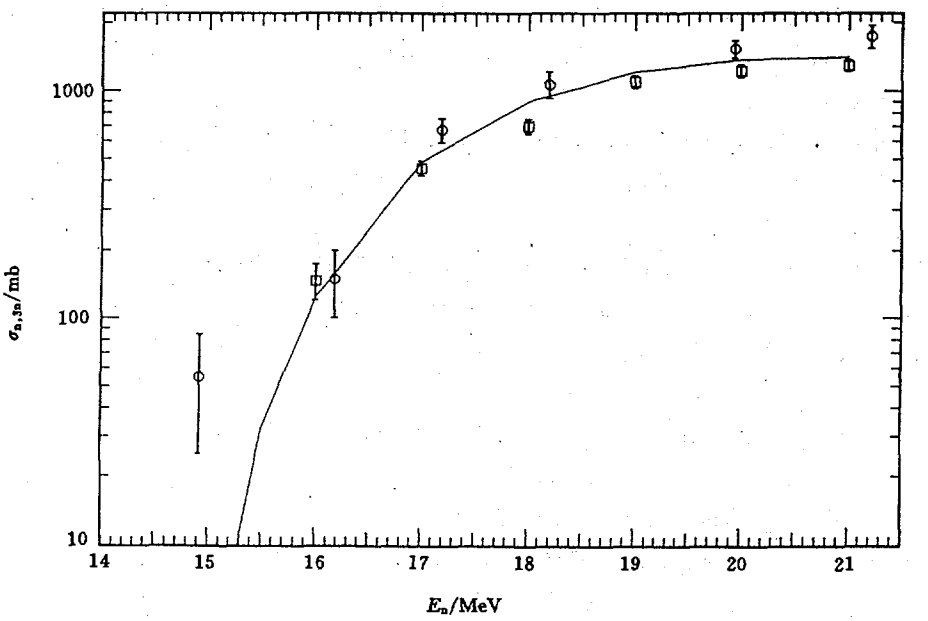

Fig. 6 The cross section of ^{175}Lu(n,3n) reaction

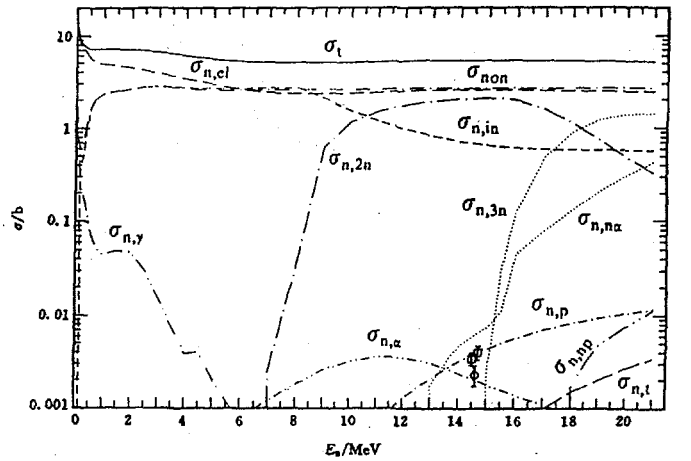

Fig. 7 The cross section of n+^{Nat}Lu reaction

References

[1] Sheng Qingbiao, Commu. Nucl. Data Progress 7, 43(1992)

[2] Zhang Jingshang, Commu. Nucl. Data Progress 7, 14(1992)

[3] Su Zongdi et. al., Commu. Nucl. Data Progress 12, 83(1994)

[4] Su Zongdi et. al., Chin. J. Nucl. Phys. 8, 149(1986); INDC(CPR)-2, 1986

[5] G. L. Sherwood et.al., Nucl. Sci. and Eng. 39, 67(1970)

[6] B. Holmqvist et. al., AE-430, 1971

[7] P. D. Kunz, "Distorted Wave Code DWUCK4", University of Colorado

[8] D. G. Foster and JR. D. W. Glasgow, Phys. Rew. C3, 576(1972)

[9] R. L. Macklin et. al., LA-7479-MS,78

[10] R. L. Macklin and J.H. Gibbons, Phys. Rev. 159, 1007(1967)

[11] H. Beer et. al., Astrophysical Journal S46, 259(1981)

[12] H. Beer et. al., Phys. Rev. C30, 464(1984)

[13] J. H. Gibbons et. al., Phys. Rev. 122, 182(1961)

[14] J. Voignier et. al., Nucl. Sci. and Eng. 93, 43(1986)

[15] V. A. Konks et. al., Jadernaja Fizika 7, 493(1968)

[16] D. R. Nethaway, Nucl. Phys. A190, 635(1972)

[17] L. R. Veeser et. al., Phys. Rev. C16, 1792(1977)

[18] B. P. Bayhurst et. al., Phys. Rev. C12, 451(1975)

[19] J. Frehaut, et. al., CEA-R-4627, 1974

[20] S. M. Qaim, Nucl. Phys. A224, 319(1974)

[21] R. F. Coleman et. al., Proc. Phys. Soc. 73,215(1959)

[22] T. Sato et. al., J. Nucl. Sci. and Tech. 12, 681(1975)

III DATA EVALUATION

A System for the γ–Production Data Intercomparison and the Intercomparison of γ–Production Data for Fe, Cr, Ni from Major Evaluated Data Libraries

Liu Tingjin Wang Cuilan Sun Zhengjun

(China Nuclear Data Center, CIAE)

Liu Wei

(Institute of High Energy Physics)

The γ–production data are very important for the nuclear engineering, especially for radioactive shielding. There are γ–production data in the major evaluated nuclear data libraries[1], such as ENDF / B–6 (B6), JENDL–3 (J3), JEF–2 (JE2), BROND–2 (BR2) and CENDL–2.1 (C2) for important nuclides, especially for structure and shielding materials. And meanwhile, quite lots of measured data have been compiled in EXFOR format.

To intercompare the γ–production data from the major evaluated data libraries, a system has been developed and used to Fe, Cr, Ni data from C2, B6, J3, JE2 and BR2.

1 The γ–Production Data Intercomparison System ICPLG

The system can be used to process and plot the γ–production data in ENDF / B–6 format[2], including γ–production multiplicity (file 12), cross section (file 13), spectrum (file 15) and corresponding experimental data in EXFOR format[3]. In fact, ICPLG is only a subsystem of the intercomparison system ICPL for complete evaluated nuclear data (another subsystem is ICPLN[4] for neutron data). The flow chart of ICPL is shown in Fig. 1.

The main functions of the system ICPLG are as follows :

(1) Data Retrieval

The data to be intercompared are retrieved directly from evaluated libraries and EXFOR library.

(2) Transition Probability Array Processing

Using the transition probability arrays retrieved from file 12, the multiplicity M of Nth level is calculated from

$$M_N = \sum_{i=0}^{N-1} P_{N,i} \ (\ 1 + M_i \ ) \tag{1}$$

where $0 < i < N-1$, $M_0 = 0$, and $1 < N < NS$, NS is the highest level to be excited.

And corresponding γ–production cross section of Nth level

$$\sigma^{\gamma}_{N} \ (E_n) = \sigma^{n}_{N} \ (E_n) \ M_N \tag{2}$$

where, $\sigma^{n}_{N}(E_n)$ is the neutron cross section of inelastic scattering to this level, retrieved from file 3.

The γ energy and production cross section from Nth level to jth level, including the contribution of all levels higher than N are

$$E_\gamma = E_N - E_j \tag{3}$$

$$\sigma^{\gamma}_{N,j} = (\ \sigma^{\gamma}_{N} + \sigma^{\gamma}_{N<NS} \ ) \ P_{N,j} \tag{4}$$

where

$$\sigma^{\gamma}_{N<NS} = \sum_{k=N+1}^{NS} \sigma^{\gamma}_{k} \ P_{k,N}$$

$$P_{N,i} = \begin{cases} TP_{N,i} \ (\ LG = 1 \ ) \\ TP_{N,i} \ \times GP_{N,i} \ (\ LG = 2 \ ) \end{cases}$$

$TP_{N,i}$, $GP_{N,i}$ and LG are defined in ENDF / B format[5], and can be read from file 12.

(3) γ–Production Cross Section and Absolute γ Spectrum

The γ–production cross section can be read from file 13, or calculated by using multiplicity $M(E)$ retrieved from file 12 and neutron cross section $\sigma^{n}(E)$

retrieved from file 3

$$\sigma^{\gamma}(E_n) = M(E_n)\ \sigma^{n}\ (E_n) \tag{5}$$

The absolute γ–production spectrum

$$\frac{d\sigma^{\gamma}(E_n,E_\gamma)}{dE_\gamma} = \sigma^{\gamma}\ (E_n)\ f\ (E_n,E_\gamma) \tag{6}$$

where $f(E_n,E_\gamma)$ is the normalized probability at incident neutron energy E_n and outgoing γ energy E_γ, retrieved from file 15, or file 6. In the latter case, the double differential cross section data need to be transformed to spectrum in 4π space.

(4) γ Emission Cross Section and Spectrum

To compare the evaluated γ–production data with each other and with experimental data, the total γ emission cross section and spectrum are calculated by summing all reaction channel data, according to formulas (7) and (8) for different MT_i in one MAT file

$$\sigma^{\gamma}_{emi}\ (E_n) = \sum_{MT_i}\ \sigma^{\gamma}_{MT_i}\ (E_n) \tag{7}$$

$$\frac{d\sigma^{\gamma}_{emi}\ (E_n,E_\gamma)}{dE_\gamma} = \sum_{MT_i}\ \frac{d\sigma^{\gamma}_{MT_i}\ (E_n,E_\gamma)}{dE_\gamma} \tag{8}$$

The summing must be done at the same energy point E_n and E_γ, so they must interpolated for all given incident neutron energy points and γ energy points according to the given interpolation modes in the files. The interpolation for γ spectrum in two dimension space is quite complicated and in some cases, the interpolated values may be unreasonable. What's more, when the needful neutron energy is interpolated from E_{n1} and E_{n2}, and the interpolation modes are different for E_{n1} and E_{n2}, it is made more complicated.

The discrete γ–ray calculated according to formulas (3) and (4) must be added in γ emission spectrum, and to compare with experimental data, the Gaussian extension must be done for them

$$P_i(E_j') = \frac{\sigma_i(E)}{\sqrt{2\pi}\ \sigma} \exp\ [\ -\frac{(E_j' - E_i)^2}{2\sigma^2}\ ] \tag{9}$$

where i means ith discrete γ–ray line, E_j' is γ energy at jth point, and σ is the extension width and taken as 2 keV, which is the energy resolution of γ–detector in general case.

(5) The Natural Element Data

In some libraries, such as ENDF / B–6, the evaluated data are given for isotopes not for natural element. In this case, the natural element data can be obtained from the sum of the product of every isotope' data retrieved from different MAT file and its abundance :

$$\sigma^{\gamma}_{\text{nat}}(E_n) = \sum_{MAT_i} a_i\ \sigma^{\gamma}_{MAT_i}(E_n) \tag{10}$$

$$\frac{d\sigma^{\gamma}_{\text{nat}}(E_n, E_\gamma)}{dE_\gamma} = \sum_{MAT_i} a_i \frac{d\sigma^{\gamma}_{MAT_i}(E_n, E_\gamma)}{dE_\gamma} \tag{11}$$

It can be seen that the interpolation for E_n, E_γ are also necessary, which is similar to those discussed in section (4).

If the data are given for isotopes, and the γ emission cross section and spectrum need to be compared; in this case, the natural element data for each reactions (MT) can be calculated either according to formulas (10) and (11), then the (7) and (8), or conversely first emission data for each isotope, then the natural element data.

(6) Plotting

The processed data are plotted. The x abscissa is selected and given by users, the maximum and minimum as well as the coordinate scale for ordinate are determined automatically. The curves for spectra can be plotted with curve or histogram according to the requirement, and the histogram methods are somewhat different due to the different interpolation modes for E_γ. The plot can be output with different devices, such as graphic terminal screen, printer or laser jet etc..

2 The Intercomparison of γ Production Data

Using the intercomparison system ICPLG, the γ–production data from CENDL–2.1, BROND–2, ENDF / B–6, JENDL–3 and JEF–2 have been compared with each other and with corresponding EXFOR experimental data. The γ–production cross sections and spectra for each reaction channels (MT) and total emission cross sections and spectra with corresponding experimental data were plotted in great detail. Because the γ–production cross sections and spectra for each reactions are not given in all libraries (As a whole; the γ–production cross sections and spectra for each reaction are given in ENDF / B–6, JEF–2 libraries, but only nonelastic (MT = 3), (n,γ) γ–production cross sections and spectra are given in JENDL–3, CENDL–2.1 and BROND–2) and the experimental data, in general, are only total γ emission cross sections and spectra, the intercomparisons of the emission cross sections and spectra are more significant. Through the intercomparisons, some notable features, differences and problems have been found.

(1) γ–Production Cross Section

I The emission cross sections of Ni are consistent very well with each other in the neutron energy region $E_n > 2$ MeV;

II For Fe, the γ emission cross section of JENDL–3 (CENDL–2.1) is higher than the others in the energy region $E_n > 7$ MeV, for example, at 20 MeV 6b for JENDL–3, about 2b for ENDF / B–6, BROND–2 and JEF–2 (Fig. 2);

III For Cr, γ emission cross section of BROND–2 is an about 2b step at $E_n = \sim 4$ MeV (Fig. 3), it seems unreasonable.

(2) γ Spectra for Fe

I For the γ emission spectrum (sum of each reaction) of BROND–2 in the energy range $E_n > 6$ MeV, the highest γ energy is limited to 10.5 MeV for all of spectra at $E_n = 10.5$–20 MeV (Fig. 4);

II For BROND–2, in the neutron energy region $E_n < 4$ MeV, there is no continuous gamma, only some discrete γ–ray lines in the spectra (Fig. 5);

III For JENDL–3, the spectra at $E_\gamma \approx 0.01$–0.7 MeV are 100 times smaller than the others in the neutron energy $E_n < 4$MeV (Fig. 5), but 10 times larger than the others in $E_n > 10$ MeV.

(3) γ Spectrum for Cr

I In BROND–2, the γ spectra are given only for (n,γ) reaction at $E_n < 4.2$ MeV and nonelastic channel at $E_n \geqslant 4.2$ MeV, in any case, the γ spectra are not complete, only in the energy region ($E_\gamma = \sim 0.4$–10.5 MeV) (Fig. 6);

II The high energy part($E_\gamma > \sim 10$ MeV) of ENDF / B–6 is harder than JEF–2, and JEF–2 harder than JENDL–3 and CENDL–2.1 (Fig. 7);

III The low energy part ($E_\gamma < \sim 0.5$ MeV) of ENDF / B–6 is 10 times

smaller than the others in $E_n \leqslant 4$ MeV (Fig. 8), and is 5 times larger in $E_n \geqslant 8$ MeV.

(4) γ Spectrum for Ni

I For BROND-2, as the same as Cr, the γ spectra are not complete, only given in γ energy region $E_\gamma = 0.5-10.5$ MeV;

II As the same as Cr, the high γ energy part ($E_\gamma > \sim 10$ MeV) of ENDF / B-6 is harder than the others (Fig. 9);

III The low γ energy part ($E_n < \sim 0.5$ MeV) of JENDL-3 is 10 times larger than ENDF / B-6 (JEF-2) in $E_n \leqslant 4$ MeV (Fig. 10), but is in good agreement between JENDL-3 and ENDF / B-6 in $E_n \geqslant 8$ MeV.

3 Conclusion Remarks

The intercomparison system ICPLG for γ-production data has been developed and used to Fe, Cr, Ni data, which are very important structural and shielding materials. The system has strong data processing function and can automatically select the plot parameters, the evaluated and experimental data can be directly retrieved. It is a powerful tool for γ-production data evaluation and improvement of the evaluated data libraries.

As regards to the γ-production data of Fe, Cr, Ni, the following discrepancies and common problems need to be paid attention to, which may be not only for these nuclides, but also for the others :

(1) There are some discrepancies for γ-production cross section in low ($E_n < 0.7$ MeV) and high ($E_n > 7$ MeV) neutron energy regions;

(2) The high γ energy part ($E_\gamma > 10$ MeV) of γ emission spectrum for B6 is harder than others;

(3) There are larger discrepancies at the low energy part ($E_\gamma < \sim 0.5$ MeV) of γ emission spectra;

(4) The γ spectra of BR2 are not complete, the γ energy is only limited to $E_\gamma = \sim 0.5-10.5$ MeV, and also the γ-production cross section need to be improved, because there is a unreasonable step at $E_n = \sim 2$ MeV.

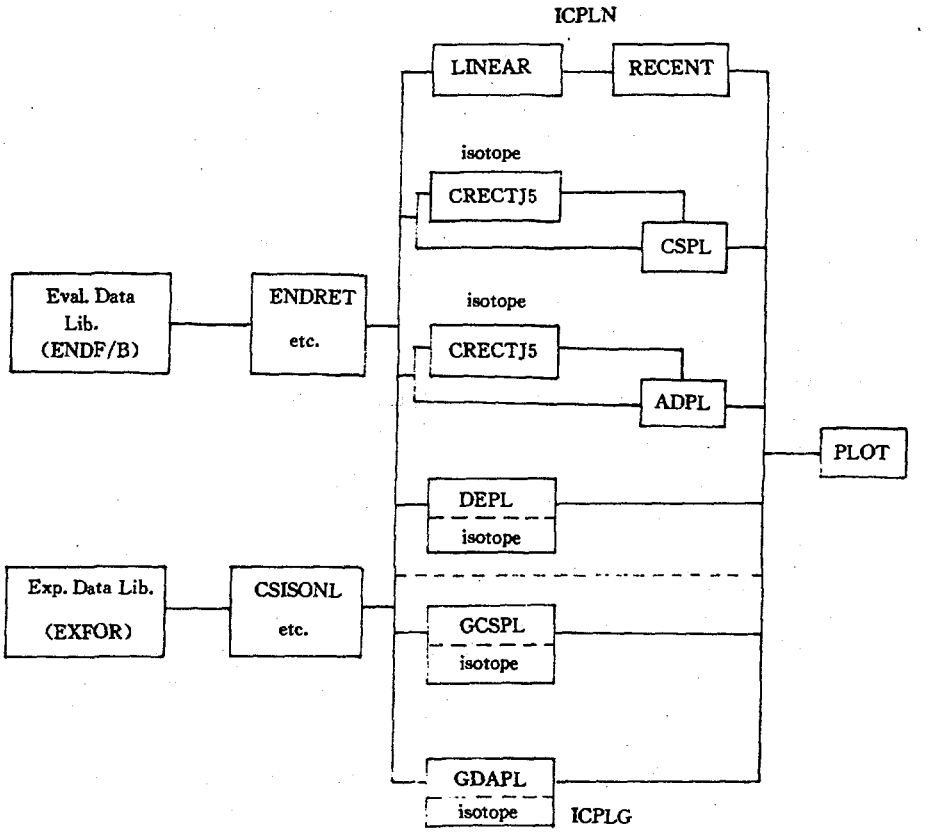

Fig. 1 Flow chart of the intercomparison system ICPL

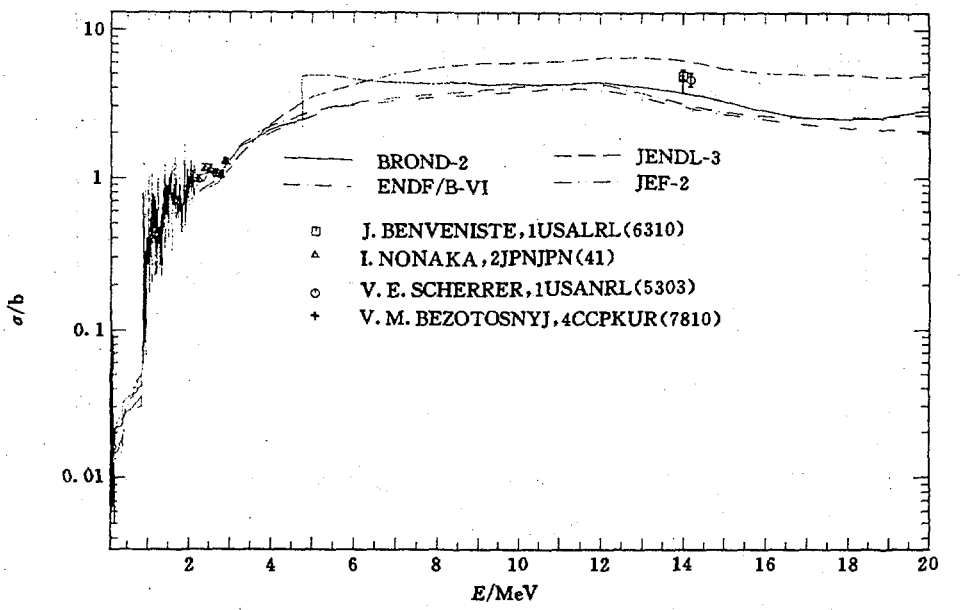

Fig. 2 γ emission cross section for Fe

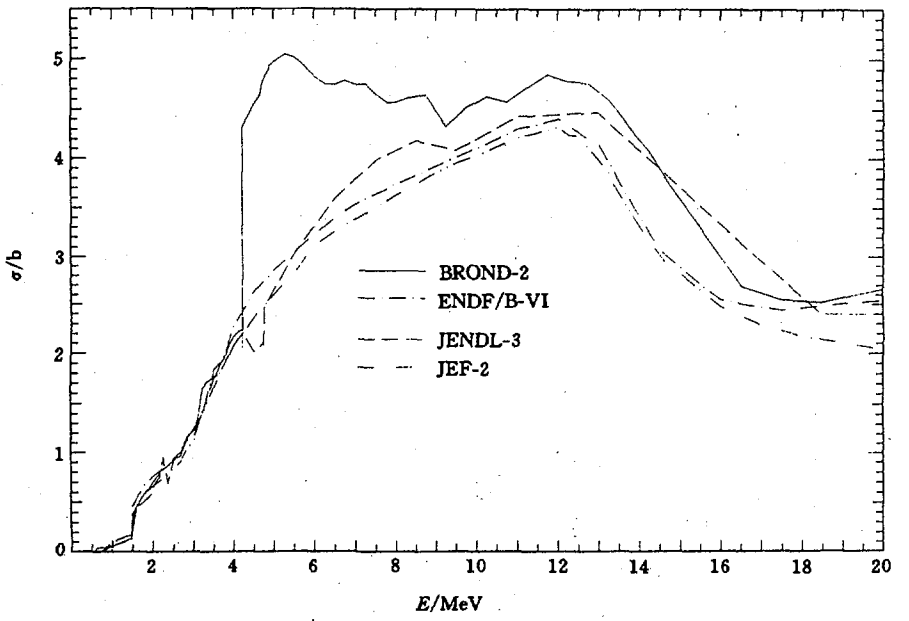

Fig. 3 The γ emission cross section for Cr

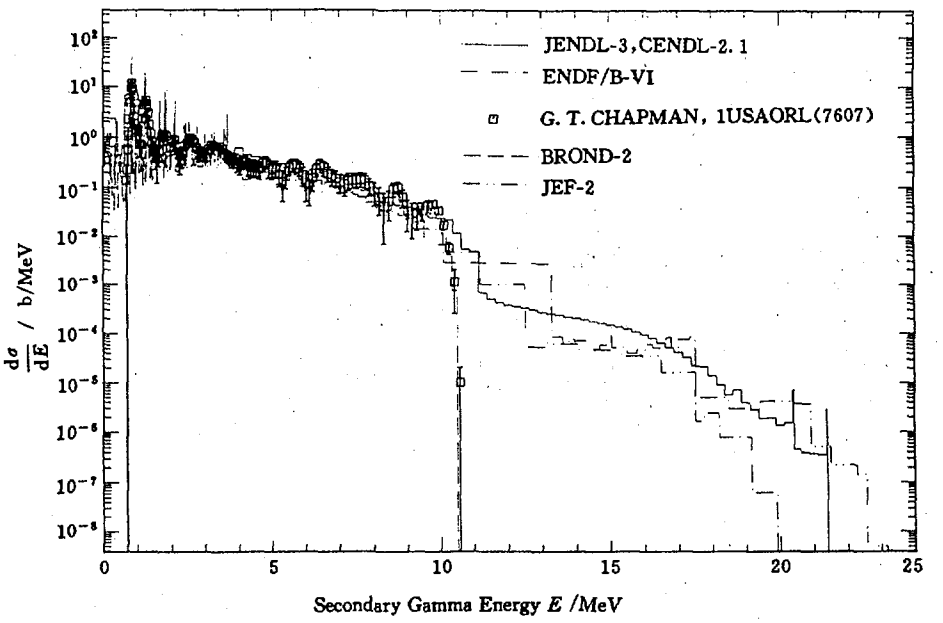

Fig. 4 The γ emission spectrum of Fe at E_n = 13.5 MeV

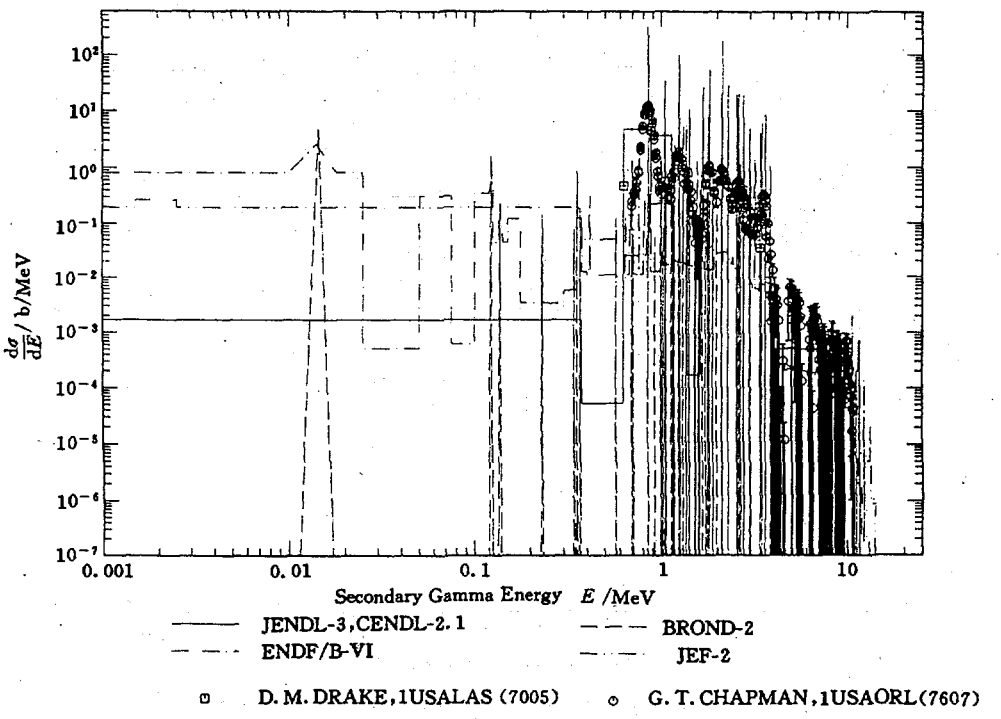

Fig. 5 The γ emission spectrum of Fe at E_n = 4.0 MeV

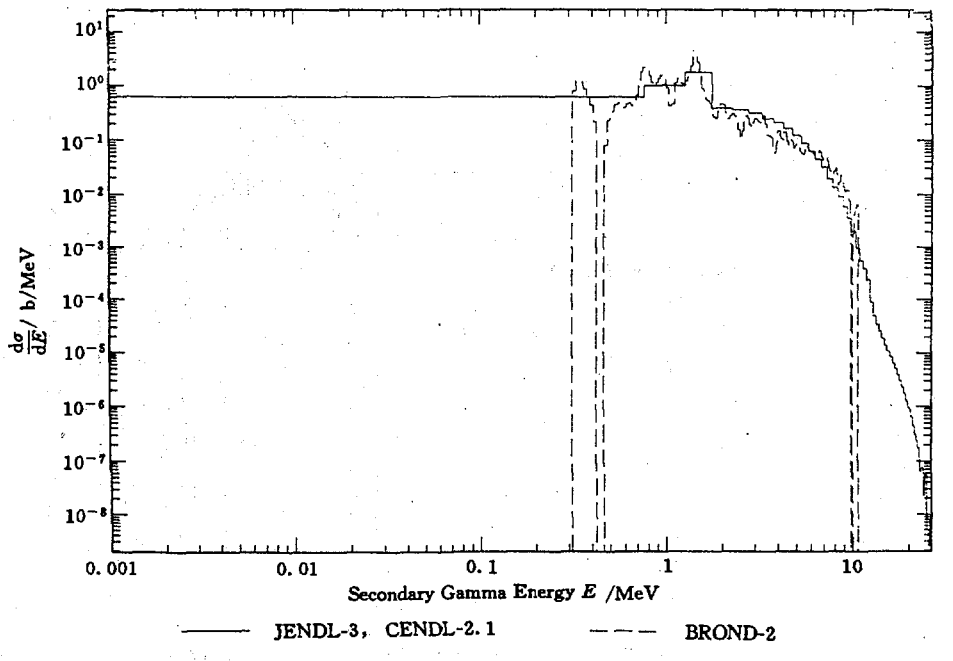

Fig. 6 The γ-production spectrum of Cr(n,non) reaction at E_n = 17.0 MeV

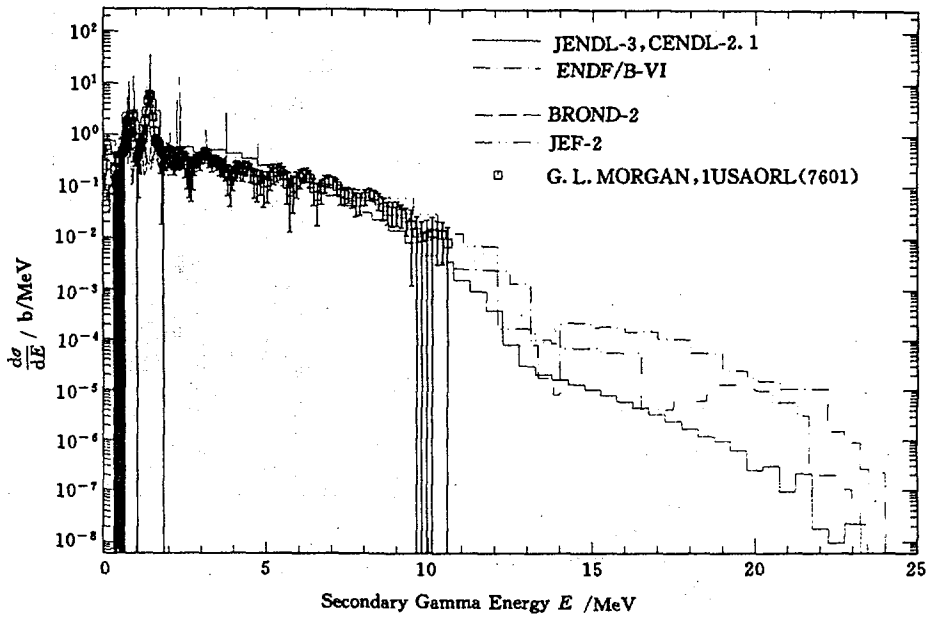

Fig. 7 The γ-emission spectrum of Cr at E_n = 14.0 MeV

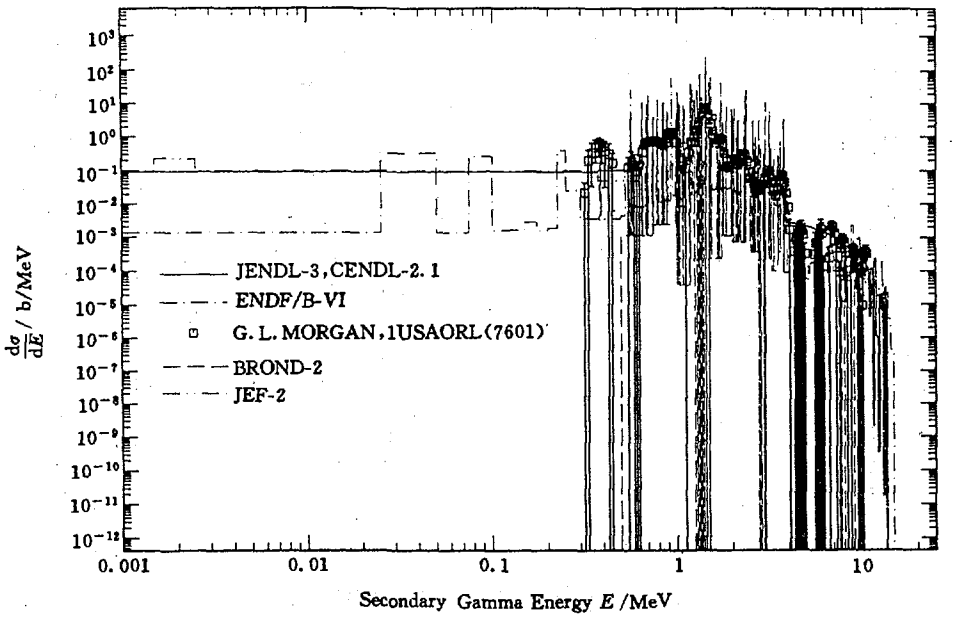

Fig. 8 The γ-emission spectrum of Cr at E_n = 4.0 MeV

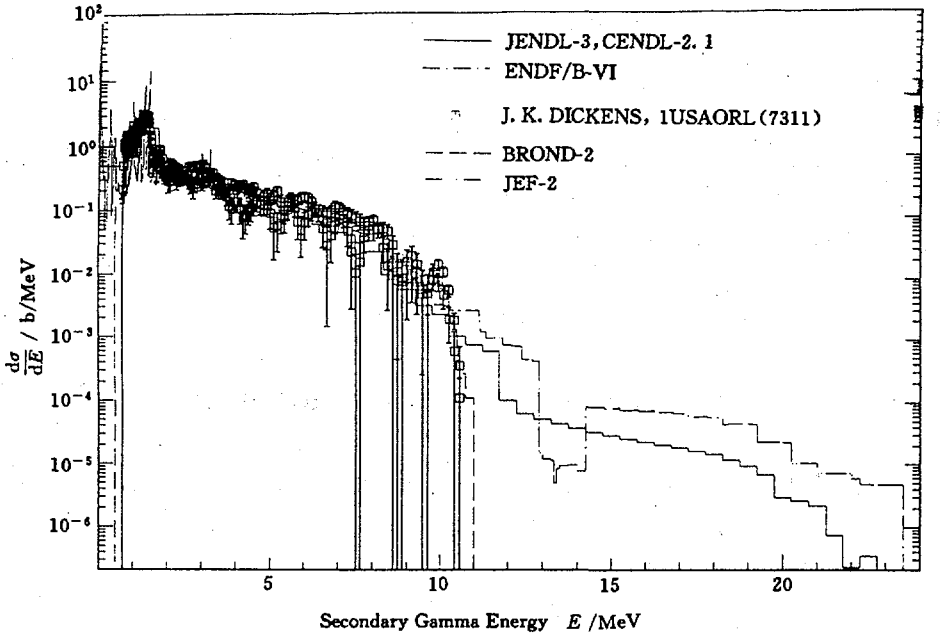

Fig. 9 The γ-emission spectrum of Ni at E_n = 14.0 MeV

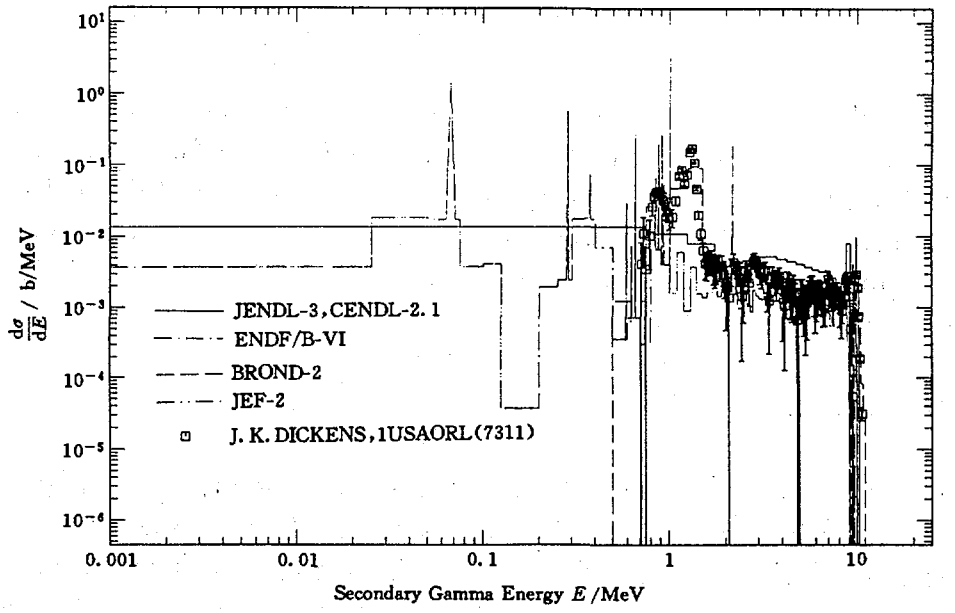

Fig. 10 The γ-emission spectrum of Ni at E_n = 1.0 MeV

References

[1] H. D. Lemmel, IAEA-NDS-107 (Rev. 8) (1993)

[2] P. F. Rose et al., EDF-102 (1988)

[3] H. D. Lemmel, IAEA-NDS-3 (1989)

[4] Liu Tingjin et al., Proc. of Symposium on Nuclear Data Evaluation Methodology, p. 37, BNL, USA (1992)

[5] P. F. Rose and C. L. Dunford, ENDF / 102 (1988)

A Simultaneous Evaluation of Neutron Induced Reaction Cross Sections for ^{56}Fe at E_n = 14.1 MeV

Zhou Delin

(China Nuclear Data Center, CIAE)

Abstract

A simultaneous evaluation of neutron induced reaction (i. e., (n,total), (n,n), (n,non), (n,n′), (n,2n), (n,nα), (n,np), (n,γ), (n,p), (n,d), (n,α), (n,n−em), (n,p−em), (n,d−em) and (n,α−em) reaction) cross sections on ^{56}Fe at E_n = 14.1 MeV is carried out. The evaluated cross sections are compared with the corresponding measured values and the evaluations for CENDL-2, ENDF / B-6, JEF-2.2, JENDL-3 and BROND-2.

Introduction

We have provided comprehensive evaluations for particle (n, p, d, α) emission and related partial reaction cross sections of all isotopes of Fe, Cr and Ni respectively as 'benchmarks' for the 'Intercomparisons of Evaluations (Calculations) of 14.1 MeV Particle Emission Data of Cr, Fe, Ni for Various Libraries' for IAEA / FENDL advisory group meeting[1]. There, by 'comprehensive evaluation' we meant that it was carried out based on the evaluations of the particle emission and related reaction cross sections performed individ-

ually, and considering the constraint relations :

$$\sigma(\text{total}) = \sigma(\text{n}) + \sigma(\text{n}') + \sigma(2\text{n}) + \sigma(\text{n}\alpha) + \sigma(\text{np}) + \sigma(\text{p}) + \sigma(\text{d}) + \cdots$$
$$\sigma(\text{non}) = \sigma(\text{n}') + \sigma(2\text{n}) + \sigma(\text{n}\alpha) + \sigma(\text{np}) + \sigma(\text{p}) + \sigma(\text{d}) + \cdots$$
$$\sigma(\text{n-em}) = \sigma(\text{n}') + 2 \times \sigma(2\text{n}) + \sigma(\text{n}\alpha) + \sigma(\text{np})$$
$$\sigma(\text{p-em}) = \sigma(\text{np}) + \sigma(\text{p})$$
$$\sigma(\alpha\text{-em}) = \sigma(\text{n}\alpha) + \sigma(\alpha)$$
$$\sigma(\text{d-em}) = \sigma(\text{nd}) + \sigma(\text{d})$$

Actually, in Ref. [1], for getting evaluated values, the measured data for (n,n'), (n,2n) reactions and for n–em, p–em, and α–em cross sections have been reviewed and analysed carefully, and for some reasons, some other cross sections (σ(non), σ(p), σ(γ), for example) and the ratios of some cross sections (σ(np) / σ(p), $\sigma(\text{n}\alpha) / \sigma(\alpha)$ for example) were quoted from available evaluations. And we have pointed out that 'the nonelastic scattering cross sections as well as the total inelastic scattering cross sections for the main isotopes remain to be improved'. And also pointed out that 'a simultaneous evaluation of total cross section, nonelastic scattering cross section, elastic scattering cross section, etc., on an experimental data base might be a way for further improving the evaluation of these data '[1].

So, at first, it is important to have reliable evaluation(s) for total, nonelastic and / or elastic scattering cross sections. Since the large component of the direct inelastic scattering to the first excited state (846 keV) of ^{56}Fe, more difficulties exist in the elastic and nonelastic scattering cross section measurements, then more difficulties exist in the evaluation work.

1 Individual Evaluations of Various Reaction Cross Sections

1.1 Total Cross Section

Five measurements of total cross section are available by using white neutron source or 'spot' thick target Li(d,n) neutron source by Cierjacks et al. (68), Perey et al. (72), Schwartz et al. (74), Larson et al. (80) and Foster et al. (71) respectively. Total cross sections at 14.1 MeV are obtained via smoothing the measured points around 14 MeV from EXFOR data base. Four measurements performed by Perey et al., Cierjacks et al., Larson et al. and Foster et al. are adopted for this work.

1.2 Elastic Scattering Cross Section

Except Tak92, all those measurements in which the cross sections of elastic and inelastic scattering to 1st excited state are analysed and provided simultaneously are in good agreement with each other[2]. Although the elastic scattering cross section of Tak92 is also in agreement with others within its large quoted error, it is too low to compare with the differences of the measured total and nonelastic scattering cross sections. Anyway, five measurements including Tak92 (i. e., Sch94, Tak92, Elk82, Hya75, Coo52)[2] are adopted in this work.

1.3 Nonelastic Scattering Cross Section

The measurements of nonelastic scattering cross section at 14 MeV were often carried out by using spherical transmission method in 1950's and early 1960's. It seems that in almost all these nonelastic scattering measurements the large inelastic scattering cross section (totaled up to 74.0 ± 5 mb, mainly from direct interaction) to 1st excited state was not corrected properly. Three such measurements for which the detector bias have been mentioned explicitly are adopted in this evaluation after correcting them to 'real' nonelastic scattering cross section :

(1) Mac57[3]. The measured values of nonelastic scattering cross section depend on the thresholds of the detector as shown in Table 1 :

Table 1 Nonelastic scattering cross section measured by MacGregor et al.[3] at 14.2 MeV energy spread 300 keV

E(thr) / MeV	13.1	12.75	12.6	12.35	12.0	11.4	11.0	10.5	9.4	7.7
σ(non) / b	1.39	1.37	1.35	1.36	1.36	1.36	1.33	1.34	1.30	1.21

In this case, 1.36 ± 0.03 b is reported by the authors. Obviously the component of inelastic scattering to 1st excited state was not included. So a value of 74.0 mb should be add to 1.360 and then 1.434 b obtained.

(2) Fle56[4]. In this measurement the neutrons from inelastic scattering to 1st excited state were detected as neutrons of elastic scattering considering that its detector were biased at 9 ~ 12 MeV. 74.0 mb should be added to its results of 1.380 ± 0.020 mb then 1.454 ± 0.02 b is obtained.

(3) Gra53[5]. The detector biased at 2 / 3 of the primary neutron energy. To add the contribution of the inelastic scattering to 1st excited state to its meas-

ured value then result in 1.344 ± 0.04 b.

1.4 Total Inelastic Scattering

Fortunately the most important isotopes of Fe, Cr and Ni are even–even nuclides. So the total inelastic scattering cross sections of these nuclides can be obtained from γ–production cross sections to 2^+ to ground state. Actually about 90% (95 % for ^{56}Fe) of the inelastic scattering processes are de–excited through 2^+ to ground state [6].

For ^{56}Fe, eight measurements of γ–production data[6~13] are available as shown in Table 2. After correcting the incident neutron energy to 14.1 MeV and gamma detection angle to 125 degree, the measurements (i. e., Abb73, Suk70, Lar85, and Xin88) which are in agreement with each other are adopted.

Table 2 Measured total inelastic scattering cross section of ^{56}Fe

	Orp75 [7]	Lac74 [8]	Eng67 [9]	Abb73 [10]	Suk70 [11]	Lar85 [6]	Xin88 [12]	Yan88 [13]
E_n / MeV	14.1	14.1	14.7	14.2	14.1	14.1	14.2	14.7
Angle / deg.	125	125	90	125	90	–	55	90
Sig / (mb / sr)	36.5	70 ± 7	57.6 ± 6	57.4 ± 6	52 ± 8			67.14 ± 3.4
Sig (125)	36.5	70	66.2	57.4	59.8		58.9	71.5
Sig (14.1)	36.5	70	77	59.0 ± 6	59.8 ± 9	60.0 ± 6	60.5 ± 6	83.4
Sig (total)	482	924	1016	778 ± 78	789 ± 118	792 ± 79	798 ± 79	1100
Adopted				778 ± 78	789 ± 118	792 ± 79	798 ± 79	

1.5 (n,2n) Reaction Cross Section

The experimental data of (n,2n) reaction cross section for Fe around 14 MeV by using various methods have been collected as far as possible[14~19]. The measurements of Refs. [16~ 18] are in agreement with each other. (see Table 3). As pointed out by Pavlik and Vonach [20], Frehaut et al.'s measurements are underestimated systematically by about 10%. Considering this point, and

Table 3 Measured Fe(n,2n) reaction cross section

	Frc80 [14]	Qai77 [15]	Ach77 [16]	Koz78 [17]	Sal72 [18]	Ash58 [19]
	Fc	^{56}Fc	Fc	Fc	Fc	Fe
E_n / MeV	14.1	14.7	14.7	14.6	14.36	14.1
Sig / E_n	385 ± 30	440 ± 40 *	485 ± 39	480 ± 50	460 ± 40	480 ± 40
Sig (14.1)	385	374	412	416	423	480
Adopted	423	374	412	416	423	407
^{56}Fc*	434 ± 30	374 ± 40	422 ± 40	426 ± 45	434 ± 37	417 ± 40

* All values measured on Fe are corrected to ^{56}Fe supposing the (n,2n) cross sections for ^{54}Fe, ^{57}Fe and ^{58}Fe are 5., 1000., 1000. mb respectively.

through the comparisons of the measurements of Ashby et al. with other measured or evaluated ones as shown in Table 4, we may conclude that Ashby et al.'s measurements are overestimated by about 20% systematically.

Table 4 Comparisons of Ashby's measurements with others at 14.1 MeV

	Ashby	Frehaut	Ryves	Zhou	Ashby / other
Mn	900			755	1.19
Co	870			720	1.21
Cu	740			609	1.21
Au	2520		2073		1.22
Pb	2650			2252	1.18
Ti	520	340			1.39
V	640	460			1.26
Fe	480	380			1.26
Cu	740	560			1.32
Zr	1250	910			1.37
Mo	1590	1100			1.31
Ta	2560	1910			1.34
W	2800	1920			1.33
Bi	2520	2014			1.25

After a correction of 10% and 20% to the values to neutron energy of 14.1 MeV measured by Frehaut et al. and Ashby et al. was made respectively, all measurements are in agreement except Qaim's measurement (by activation method) which by about 10% lower than others. One may notice that around 14 MeV an overestimation of 2% of the neutron energy could cause 8%

underestimation of the (n,2n) reaction cross section. Anyway, it is difficult to make sure that what caused this discrepancy, the data set shown in last row of Table 3 are all adopted in this evaluation.

1.6 Neutron Emission Cross Section

An evaluation of angle–energy–integrated neutron emission cross section for Fe at 14.1 MeV has been performed[1]. The evaluated value of 1610 mb for Fe is adopted for this evaluation. After correcting it, a value of 1653 mb for ^{56}Fe is obtained.

1.7 Charged Particle (p, α, d) Emission Data

A series of total (angle–energy–integrated) p–emission and α–emission cross sections have been reported by[21~24] from the measurements of emission spectra. And a series of total α–emission cross section measurements have been performed by Kneff et al. by using isotope–dilution gas mass spectrometer[25].

Intercomparison of these measurements, and comparisons of these measurements with those measured by activation method demonstrate that almost all Grimes' measurements on p–emission cross sections are higher by about 10% systematically than others, as shown in Table 5. So in present evaluation for p–emission cross section, the Grimes' measurement for ^{56}Fe is adopted after 10% reduction.

As shown in Table 6, Grimes' results of α–emission cross section measurements coincide with comparable ones measured by activation method; and most of the Kneff's measurements are about 10 percent higher than Grimes' and Fisher's measurements as well as other comparable ones measured by activation method. In the present evaluation for α–emission cross section, Grimes', Fisher's and Kneff's (after 10% reduction) are adopted.

A more recent measurement from threshold to over 30 MeV on α–emission including spectrum and angular distribution is carried out using the spallation source at WNR / LAMPF and detector telescopes consisting of a low–pressure gas proportional counter and a large area silicon detector[26]. The result of this measurement at 14.1 MeV (42 ± 2 mb) also adopted in present work is in good agreement with Grimes et el.'s measurement and the evaluated value obtained in[1].

Only one measured value of (d–em) cross section is available[21]. This measurement is adopted in this evaluation as (n,d–em), also as (n,d) reaction cross section.

Table 5 Comparisons of measured results of measured and evaluated p–emission cross section and evaluated at 14.8 MeV

	Grimes et al.	Zhou et al. or others				Grimes / others
	(p–em)	(n,p)	(n,np)	(n,2p)	(p–em)	
^{48}Ti	85	62	16.8		78.8	1.16
^{50}Cr	830	294	291	5	590	1.40
^{54}Fe	900	280	362	17	659	1.36
^{58}Ni	1002	937	937	20	957	1.05
^{60}Ni	325	142	79		221	1.47
^{63}Cu	320	125	150		275	1.16
^{65}Cu	44	20	22		44	1.00
^{92}Mo	967	37	744		781	1.24
^{96}Mo	64	24	6		30	1.78

Table 6 Comparisons of measured results of α–emission cross section

	Kneff et al.	Grimes et al.	Fishers et al.	Eval. or meas. by other meth.	
				(n,α)	(n,nα)
^{51}V	18.5 ± 1.1 #	17 ± 0.2 #		17.0 ± 0.2	0.07 ± 0.01 #
^{27}Al	143 ± 7 #	121 ± 25 #		115.5 ± 1.2	– #
^{59}Co	40 ± 3 #		33 ± 1.7 *	31 ± 1 #	
Mg	28 ± 2 #		24.4 ± 1.3 *		
			(23.4 ± 1.5 #)		
^{56}Fe	46 ± 3 #	41 ± 7 #	44 ± 3 *		
	(45.3 ± 3 *)	(40.4 ± 2 *)			

E_n = 14.8 MeV, * E_n = 14.1 MeV

1.8 Partial Cross Sections Relevant to Charged Particle Emission

As a standard, ^{56}Fe(n,p) cross section has been well measured and evaluated and an evaluated value of 114.5 mb at 14.1 MeV is adopted for this work. Incorporating with evaluated p–em and α–em cross sections and the shapes of the excitation function of (n,p), (n,np), (n,α) and (n,nα) reactions, the rest of the partial cross sections relevant to charged particle emission are determined for this evaluation.

1.9 (n,γ) Reaction Cross Section

For the minor reaction cross section $\sigma(\gamma)$, a selected evaluation (calcula-

tion) of 0.74 mb at 14.1 MeV is used in present evaluation.

1.10 Uncertainties of the Adopted Data

Generally, the uncertainties reported by the authors are quoted. For some measured cross sections, such as (n,2n) cross sections by Frehaut et al. and Ashby et al., p–emission cross section by Grimes et al., α–emission cross section by Kneff et al., have been modified to more reliable values in present evaluation, so their uncertainties have been reduced properly.

2 Simultaneous Evaluation of All Measurable Cross Sections

Based on the analyses and evaluations on the measured cross section for all (totalled 15) reactions, i. e., (n,n), (n,n′), (n,2n), (n,nα), (n,np), (n,γ), (n,p), (n,d) ((n,d–em) in the present case), (n,α), as well as (n,total), (n,non), (n,n–em), (n,p–em), (n,α–em) and (n,d–em) individually (i. e., independently as far as possible), a simultaneous evaluation is carried out by using a least squares code LSCC with the constraints given above.

All measured cross sections and their uncertainties of 15 (for ^{56}Fe, actually 14) reactions adopted for this evaluation are used as input data set : measurement vector Y^* and its covariance V_y^*. It is supposed that all measured cross sections are independently (uncorrelated), except p–emission and α–emission relevant cross sections σ(p), σ(np) and σ(α), σ(nα), they are deduced from the measured emission cross sections, so σ(p) and σ(α) are correlated with σ(np) and σ(nα) respectively, and four total inelastic scattering measurements are correlated via the common correction factor 1.05[6].

The output of LSCC consists of the evaluated values of all reaction cross sections mentioned above and their covariances, as showing in Table 7. The comparisons of the evaluated values with the corresponding measurements as well as the evaluations for various libraries are shown in Fig. 1 and Table 8. From Fig. 1 we can see that all evaluated values are consistent with all measured data in quoted error.

Table 7 Results of simultaneous evaluation

(1) total and partial cross sections (mb)

total	elast.	incl.	n,2n	n,nα	n,np	n,γ	n,p	n,d	n, α
2561	1158	779.7	418.6	1.448	40.34	0.740	114.5	7.965	40.04

(2) Covariance

1.7E+02	8.7E+01	7.0E+01	6.3E+00	7.3E−03	1.1E+00	1.1E−03	1.5E−01	4.0E−01	5.5E−02
8.7E+01	2.7E+02	−1.7E+02	−1.5E+01	−1.8E−02	−2.7E+00	−2.7E−03	−3.7E−01	−9.5E−01	−1.3E−01
7.0E+01	−1.7E+02	4.5E+02	−1.8E+02	−2.4E−01	−2.3E+01	−1.6E−02	−1.8E+00	−5.8E+00	−7.3E−01
6.3E+00	−1.5E+01	−1.8E+02	2.1E+02	−4.4E−02	−3.1E+00	−1.5E−03	−7.4E−02	−5.3E−01	−5.4E−02
7.3E−03	−1.8E−02	−2.4E−01	−4.4E−02	6.9E−01	−4.1E−03	−1.7E−06	−4.9E−05	−6.1E−04	−3.8E−01
1.1E+00	−2.7E+00	−2.3E+01	−3.1E+00	−4.1E−03	3.2E+01	−2.6E−04	−5.7E+00	−9.4E−02	−1.2E−02
1.1E−03	−2.7E−03	−1.6E−02	−1.5E−03	−1.7E−06	−2.6E−04	2.2E−02	−3.6E−05	−9.3E−05	−1.3E−05
1.5E−01	−3.7E−01	−1.8E+00	−7.4E−02	−4.9E−05	−5.7E+00	−3.6E−05	5.0E+00	−1.3E−02	−1.9E−03
4.0E−01	−9.5E−01	−5.8E+00	−5.3E−01	−6.1E−04	−9.4E−02	−9.3E−05	−1.3E−02	7.8E+00	−4.6E−03
5.5E−02	−1.3E−01	−7.3E−01	−5.4E−02	−3.8E−01	−1.2E−02	−1.3E−05	−1.9E−03	−4.6E−03	1.4E+00

Table 8 Comparisons of this evaluations with the evaluations for various libraries[27]

MT	This work		CENDL−2	JEF−2.2	ENDF/B−6	JENDL−3.2	BROND−2
	14.1	14.0	14.0	14.0	14.0	14.0	14.0
3 1	2561.	2573.	2550.	2570.	2596.	2574.	2590.
3 2	1158.	1167.	1157.	1192.	1205.	1137.	1266.
3 3	1403.	1405.	1400.		1391.	1427.	
3 4	779.7	798.9	773.8	688.0	774.4	769.3	692.1
3 16	418.6	405.3	416.2	414.4	402.0	439.1	419.0
3 22	1.448	1.324	.8186		1.297	0.840	
3 28	40.34	37.53	38.49		46.71	70.94	
3102	.7399	.7279	.7300	.2138	.7300	.0995	.8100
3103	114.5	116.8	115.2	118.8	115.1	114.0	114.0
3104	7.965	7.694	7.436	.9235	6.300	−	
3107	40.04	40.09	40.18	45.00	44.30	40.90	38.00
3201		1648.	1646.		1626.	1719.	
3203		154.3	153.7		161.8	184.9	
3207		41.41	41.00		45.60	41.74	

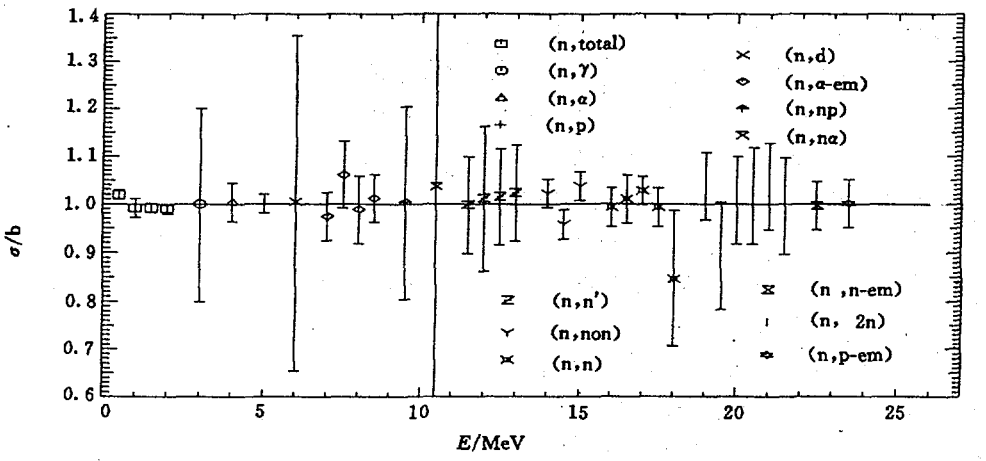

Fig. 1 Comparisons of evaluated values with measured data

3 Discussion and Conclusion

One may notice that Perey et al.'s total cross section measurement at 14.1 MeV is higher by 2.8% ~ 3.0% (about 70 mb) than other three measurements which are in very good agreement with each other and consistent with Qaim's measurement of (n,2n) reaction cross section by activation method. One may also notice that all individual evaluations mentioned above favour Perey et al.'s measurement at least the results near 14.1 MeV. Before solving and / or explaining the discrepancies existed in total and other reaction cross section measurements, a simultaneous evaluation just like this work should be the most reasonable way to compromise and optimize the evaluated data set based on wide-spread available experimental information.

References

[1] Zhou Delin et al., Proc. of Inter. Conf. on Nucl. Data for Sci. and Tech., Julich, p. 942, 1991; Zhou Delin et al., A progress report to AGM on FENDL, A report to AGM on FENDL, final report for IAEA Contract No. 5962 / R1 / RB

[2] D. Schmidt et al., p. 907, Proc. of Inter. Conf. on Nucl. Data for Sci. and Tech., Gaitlinburg, 1994

[3] M. H. MacGragor et al., Phys. Rev. 108, 726 (1957)
[4] N. N. Flerov et al., A. E. 1, 5, 155 (1956)
[5] E. R. Graves et al., Phys. Rev. 97, 1205 (1955)
[6] D. Larson et al., 85Santa Fe, 1, 71 (1985)
[7] V. J. Orphan et al., NSE 57, 309 (1975)
[8] J. Lachkar et al., NSE 55, 168 (1974)
[9] F. C. Engesser et al., J. Nucl. Energy 21, 487 (1967)
[10] U. Abbondanno et al., J. Nucl. Energy 27, 227 (1973)
[11] B. I. Sukhanov et al., YF 11, 33 (1970)
[12] Xing Jinqiang et al., CNP 10, 284 (1988)
[13] Yan Yiming et al., CNP 10, 266 (1988)
[14] J. Frehaut et al., Report BNL–NCS–51245, p. 399 (1980)
[15] S. Qaim et al., 77Geel, p. 327
[16] G. Achampaugh et al., 77BNL, p. 231
[17] U. Kozyr' et al., YF 27, 616 (1978)
[18] O. Sal'nikov et al., YF 12, 1132 (1972)
[19] V. Ashby et al., Phys. Rev. 111, 616 (1958)
[20] A. Pavlik et al., Physics Data Nr. 13–4 Fachinformationszentrum Karlsruhe (1988)
[21] S. Grimes et al., Phys. Rev. C19, 2127 (1979)
[22] R. Fishers et al., Phys. Rev. C30, 72 (1984)
[23] E. Wattecampes et al., EUR–8355, p. 156 (1983)
[24] G. Doyla et al., Report CONF–740376 (1976)
[25] D. Kneff et al., NSE 92, 491 (1986)
[26] S. M. Sterben et al., same as Ref. 2, p. 314
[27] JEF Report 14 and CENDL–2

Evaluation of Neutron Activation Cross Sections for $^{93}Nb(n,2n)^{92m}Nb$ and $^{93}Nb(n,n')^{93m}Nb$ Reactions from Threshold to 20 MeV

Yu Baosheng

(China Nuclear Data Center, CIAE)

Introduction

Niobium is a very important structure material in nuclear fusion engineering. The activation cross sections of neutron interaction with ^{93}Nb must be considered for the evaluation of radiation safety, radiation induced material damage. Meanwhile, knowledge of the neutron (n,2n) and (n,n′) reactions have been used for the neutron dosimetry. The dosimetry reaction of $^{93}Nb(n,n')^{93m}Nb$ is characterized by the low threshold energy less than 0.1 MeV and the long half-life of 13.6 a. Because of the appropriate half life of the ^{92m}Nb (10.15 day) produced from $^{93}Nb(n,2n)$ reaction and its high threshold energy about 9 MeV, it is suitable for high energy neutron monitor. On the other hand, the reaction is a good standard cross section in relevant measurement. Therefore, the development of activation cross sections information will largely meet the demands for neutron activation, dosimetry and radiation safety and material damage research etc.

1 Evaluation for $^{93}Nb(n,2n)^{92m}Nb$ Reaction

All the measurements were carried out by activation technique. The available measured data of $^{93}Nb(n,2n)^{92m}Nb$ reaction exist below 20 MeV. The list of experiments for $^{93}Nb(n,2n)^{92m}Nb$ reaction[1~37] is given in Table 1 and Fig. 1. Most of the experimental data up to 1994 were collected. Many data were retrieved from EXFOR master files of International Atomic Energy Agency, enriched with new information as well as CIAE, SIU (China Southwest Institute of Nuclear Physics and Chemistry) experimental results.

Among 37 data sets, there are 33 data sets measured around 14 MeV. In this evaluation all collected cross section data around 14 MeV were adjusted to

equivalent 14.6 MeV cross section, based on the shape of the excitation curve for ^{93}Nb(n,2n) ^{92m}Nb reaction. In order to obtain the factors of energy adjustment values, the data of D. L. Smith et al.[38] were used.

The data around 14 MeV were also renormalized with standard cross section taken from Ref. [32].

The relevant cross section and energy adjusted factors R_1 and R_2 are also given in Table 1. separately, in which σ_0 and σ represent the original and adjusted cross sections, respectively.

The abundance of isotope ^{93}Nb in natural is 100%. The half–life of ^{92m}Nb is 10.15 d, the gamma ray associated with the decay of ^{92m}Nb is emitted as almost single quantum of 934 keV with a branching ratio 99 %. The characters of gamma ray of ^{92m}Nb quantum and positron yields, corrections due to change in half–lives of radioactive nuclei are negligible.

After adjustment, the first–step evaluation was done for 33 cross section values at 14.6 MeV. Some data should be rejected due to the larger discrepancies with others and exceeding the averaged value by three standard deviation.

The secondary step was made by averaging the adjusted data with the weighted factor. The weighted factors in the evaluation were based on the given errors by authors and quoted errors by us. Present evaluated data is 460.2 ± 4.9 mb at 14.6 MeV, as shown in Fig. 2.

Above 14 MeV, the new measured data by Wang Yongchang [3], Lu Hanlin[32], D. C. Santry[33], Y. Ikeda[35], are in good agreement with the obtained recommended value by us at 14.6 MeV.The measured data by Y.Ikeda[35], S. Chiba[37] provided the activation cross sections in the so–called "gap" energy region from 9 to 13 MeV using the activation method with monoenergetic neutron produced by the ^{1}H(^{11}B,n)^{11}C reaction at JAERI. The more accurate measurements mentioned–above update the evaluation in energy region from 13 to 20 MeV where larger discrepancies existing data sets.

Below 14 MeV, The data obtained by D. C. Santry[33], D. L. Smith[36], S. Chiba[37], supersede all earlier measured data and the data measured by D. C. Satry[33] supplement the data in low energy.

The project from NEANDC working group on activation cross sections showed that the data measured by D. L. Smith and W. Mannhart[36] are very important. In their measurement, the neutron yields from both "gas–out" effect and breakup were accurately determined. And it was noted that both effects increase with the neutron energy and strongly depend on the threshold of the specific reaction. In the measurement, both "gas–out" effect and breakup neutron were subtracted and the accurate cross sections were obtained.

Those experimental data mentioned above are looked upon as quite ade-

quate for most competent shape of excitation function for ^{93}Nb(n,2n) ^{92m}Nb reaction from threshold to 20 MeV. The evaluated result was obtained on the basis of the data mentioned above by using a program of orthogonal polynomial fitting.

The uncertainties for the ^{93}Nb(n,2n)^{92m}Nb reaction were estimated from experimental errors and the spread of measured data around evaluated data, and given in file 33.

Recently, evaluation of neutron activation cross section combined with the new measured data reached some points :

(1). The measured data by D. C. Santry[33], D. L. Smith and Manhart[36] show that the accurate data are significant and reasonable, especially change the trend of shape in threshold to 13 MeV. This evaluation improved the previous work[32].

(2). Above 13 MeV, in present evaluation the results of available measurements were taken and renormalized at 14 MeV. It seems no changes appear from our original evaluated data.

(3). Present evaluation updates mainly original data[38] from threshold to 13 MeV. The comparison is shown in Fig. 3.

2 Evaluation for ^{93}Nb(n,n′)^{93m}Nb Reaction

In spite of the importance of the ^{93}Nb(n,n′)^{93m}Nb reaction, experimental data of the cross section is sparse and uncertainties of the data are large due to the difficulty of activation measurement. For a few measured data, the larger discrepancies were recognized.

The measured data selected are as follows :

1981	T. B. Ryves [39]	at	14.3 MeV
1988	D. B. Gayther [40]	in	1.09～5.76 MeV
1988	M. Wagner [41]	at	2.83 MeV
1988	M. Wagner [42]	at	7.91 MeV
1993	M. Wagner [43]	in	5.91 to 7.91 MeV.

The new measured data by Wagner[43] are consistent with his previous measured value around 8 MeV and the measured value by Gayther[40] around 6 MeV within uncertainty.

The measured data and the tendency of evaluated data from ENDF / B–6 were considered between 8～ 12 MeV. The evaluated results from threshold to 20 MeV were obtained by using a program of orthogonal polynomial fitting

based on the data mentioned above. The results are shown in Fig. 4.

Acknowledgements

The authors are indebted to IAEA (International Atomic Energy Agency), CNNC (Chinese National Nuclear Corporation) and CIAE for their supports, and thank to Drs. A. B. Pashchenko, T. Benson, O. Schwerer, Lu Hanlin and Zhao Wenrong for kind helps and suggestions.

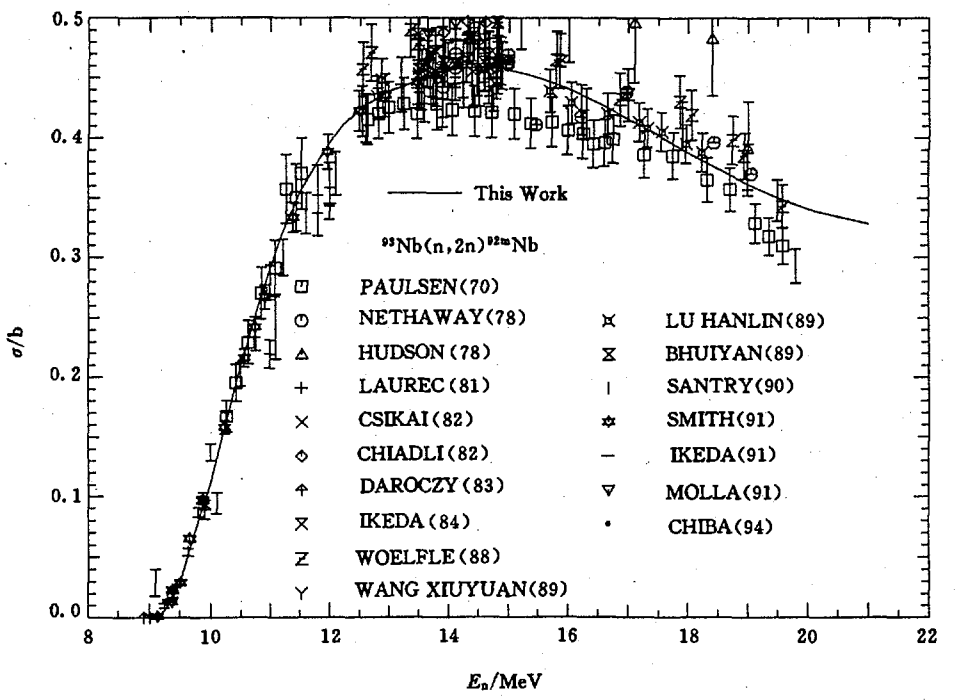

Fig 1 Comparison between evaluated & measured data

Table 1 Collected Data and Relevant Information for $^{93}Nb(n,2n)^{92m}Nb$

Year	Author	E_n / MeV	σ_0 / mb	$\Delta\sigma$ / mb	n flux	R_1	R_2	σ / mb
1959	H.Vonach	14.1	430.0	70.0	$^{27}Al(n,\alpha)$	0.9999		430.0
1960	H.A.Tewes	14.5	466.0	93.2	H(n,n)	0.9999		467.0
1961	V.L.Glagolev	14.7	560.0	60.0	$^{63}Cu(n,2n)$	1.0005		560.3
1962	F.Strohal	14.6	318.0	18.0	$^{27}Al(n,\alpha)$	1.0000	1.0070	320.2
1962	D.R.Kochler	14.7	360.0	120.0	$^{63}Cu(n,2n)$	1.0005		360.2
1963	E.T.Bramlitt	14.7	499.0	91.0	$^{27}Al(n,\alpha)$	1.0005	1.0044	501.5
1965	R.Rieder	14.7	464.0	23.2	$^{27}Al(n,\alpha)$	1.0005		464.2
1966	G.T.Western	14.7	400.0	20.0	ASSOP	1.0005		400.2
1966	D.G.Vallis	14.7	502.0	25.0	$^{27}Al(n,\alpha)$	1.0005	0.9542	479.2
1970	L.Husain	14.8	455.0	32.0	$^{56}Fe(n,p)$	1.0036	1.0429	476.2
1970	W.D.Lu	14.4	578.0	30.0	$^{56}Fe(n,p)$	0.9998	1.1180	646.1
1970	A.Paulsen	14.71	421.0	21.0	PRT	1.0005		421.2
1970	M.Bormann	14.82	491.0	29.5	H(n,n)	1.0043		493.1
1971	S.M.Qaim	14.7	512.0	46.0		1.0005		512.3
1972	D.R.Nethaway	13～14.9			$^{27}Al(n,\alpha)$			
1976	E.Holub	14.6	484.0	50.0		1.0000		484.0
1978	D.R.Nethaway	14.8	450.0	30.0	$^{27}Al(n,\alpha)$	1.0036	1.0107	456.5
1978	C.G.Hudson	14.1	542.0	43.0	$^{27}Al(n,\alpha)$	0.9999		541.9
1981	J.Laurec	14.1	463.0	18.0	$^{27}Al(n,\alpha)$	0.9999	1.0108	467.9
1981	T.B.Ryves	14.68	453.0	11.0	$^{56}Fe(n,p)$	1.0004	1.0442	473.2
1982	J.Csikai	14.66	458.0	30.0	$^{27}Al(n,\alpha)$	1.0003	0.9428	431.9
1982	A.Chiadli	14.6	496.0	32.0	$^{27}Al(n,\alpha)$	1.0000	1.0114	501.7
1982	R.C.Harper	14.2	527.0	47.0	ASSOP	0.9996		526.8
1983	S.Daroczy	8.92～9.9						
1984	I.Garler	14.75	494.8	20.2	$^{235}U(n,f)$	1.0021		496.3
1984	Y.Ikeda	14.78	463.0	19.9	$^{27}Al(n,\alpha)$	1.0030		464.4
1985	K.Kobayashi	14.1	477.1	15.6		0.9999		477.1
1986	Y.S.Kim	14.6	455.0	11.0	$^{27}Al(n,\alpha)$	1.0000	1.0114	460.2
1988	R.Woelfle	14.41	487.0	23.0		0.9999		486.9
1989	S.I.Bhuiyan	14.8	496.0			1.0036		497.8
1989	Wang Yongchang	14.67	458.7	24.3	$^{27}Al(n,\alpha)$	1.0004	0.9964	457.2
1989	Lu Hanlin	14.6	457.0	18.0	ASSOP	1.0000		457.0
1990	D.C.Santry	14.5	444.0	18.0	$^{32}P(n,p)$	0.9999		443.0
1991	N.T.Molla	14.58	483.0	45.0	$^{27}Al(n,\alpha)$	0.9999		482.9
1991	Y.Ikeda	11～13.2			$^{197}Au(n,2n)$			
1991	D.L.Smith	9.38～9.8			$^{238}U(n,f)$			
1994	S.Chiba	9.1～11.8						

R_1 : Adjusted factor for neutron energy; R_2 : Adjusted factor for relevant cross section

ASSOP : Associated alpha particle method; PRT : Proton recoil telescope counter

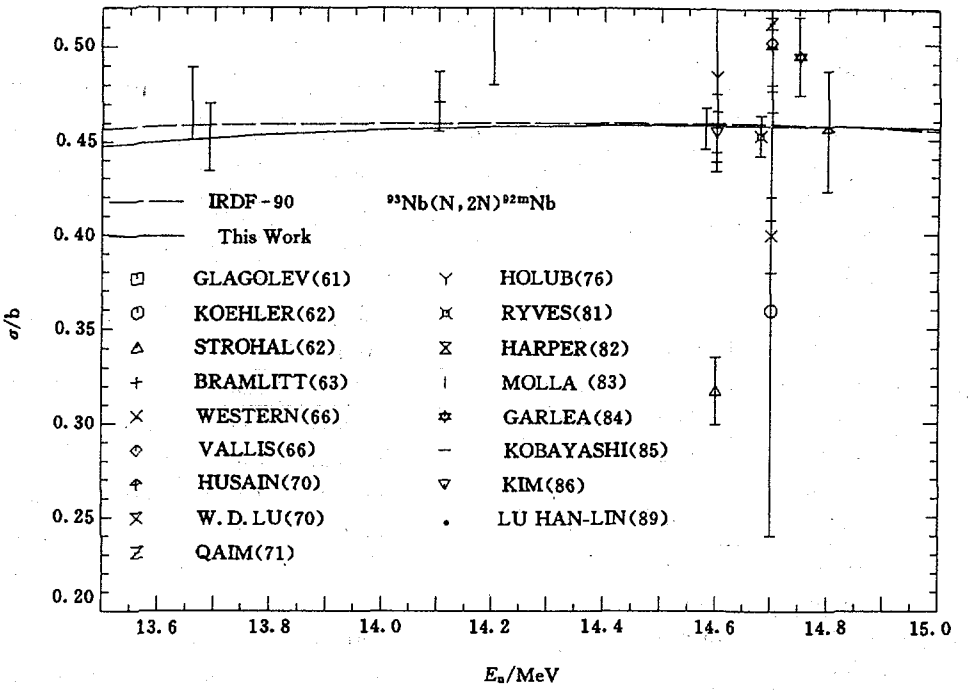

Fig 2 Comparison between evaluated & measured data

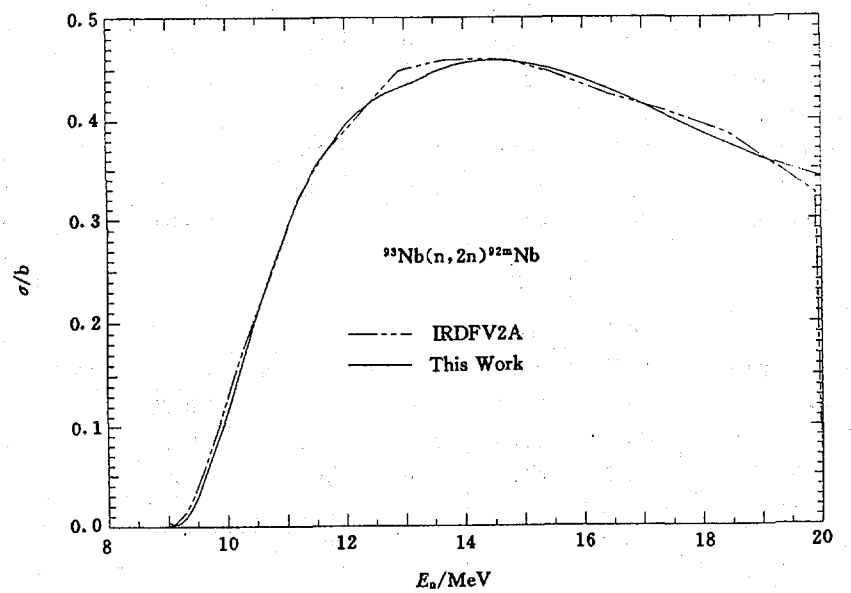

Fig 3 Comparison between evaluated data

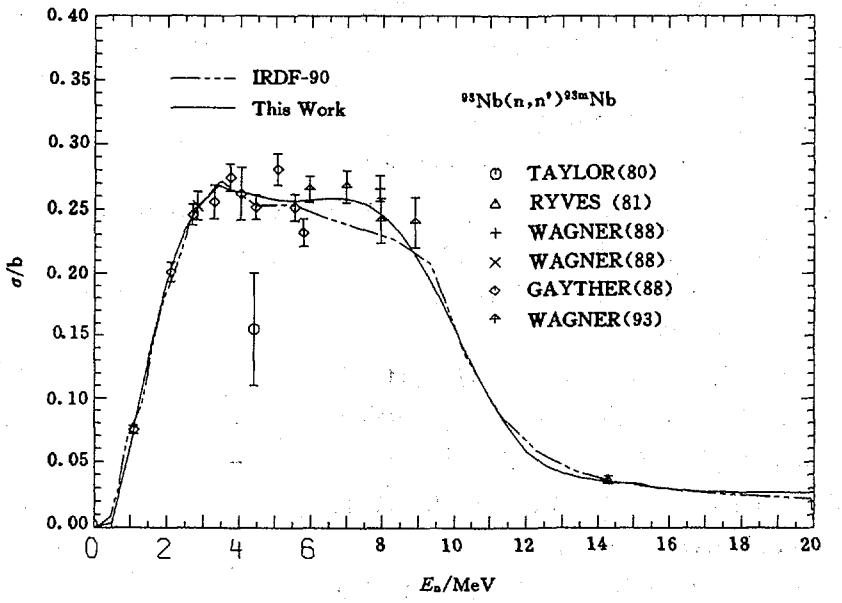

Fig 4 Comparison between evaluated & measured data

References

[1] H. Vonach et al., EXFOR Data No. 20087006

[2] H. A. Tewes et al., UCRL-6028-T (1960)

[3] V. L.Glagolev et al ., EXFOR Data No. 40789003

[4] F. Strohal et al., Nucl. Phys., 30, 49(1962)

[5] D. R. Kochler et al., NP11667(1962)

[6] E. T. Bramlitt et al., Phys. Rev., 131, 2649(1963)

[7] R. Rieder et al., EANDC(OR)-38 (1965)

[8] G. T. Western et al., AFWL-TR-65-216 (1966)

[9] D. G. Vallis ., AWRE-0-76 / 66, (1966)

[10] L. Husain et al., Phys. Rev., C1, 1233(1970)

[11] W. D. Lu et al., Phys. Rev., C1, 350(1970)

[12] A. Paulsen et al., Z. Phys., 238, 23(1970)

[13] M. Bormann et al., Nucl. Phys., A157, 481(1970)

[14] S. M. Qaim et al., EXFOR Data No. 20554011

[15] D. R. Nethaway et al., Nucl. Phys., A190, 635(1972)

[16] E. Holub et al., EXFOR Data No. 30348010

[17] D. R. Nethaway et al., EXFOR Data No. 10709004

[18] C. G. Hudson et al., Annual of Nuclear Energy 5, 589(1978)
[19] J. Laurec et al., CEA-R-5109 (1981)
[20] T. B. Ryves et al., Nucl. Phys., G7, 4, 529(1981)
[21] J. Csikai et al., Proc. of Conf. on Nuclear Science and Technology, Antwerp, 414(1982)
[22] A. Chiadli et al., EXFOR Data No. 30697002
[23] R. C. Harper et al., EXFOR Data No. 12730004
[24] S. Daroczy et al., Proc. of Conf. on Neutron Physics, Kiev, 191(1983)
[25] I. Garlea et al., EXFOR Data No. 30813004
[26] Y. Ikeda et al., EXFOR Data No. 21945002
[27] K. Kobayashi et al., NEANDC(J)116 (1985)
[28] Y. S. Kim et al., EXFOR Data No. 30737004
[29] R. Woelfle et al., Appl. Radiat. Isot., 39, 407(1989)
[30] S. I. Bhuiya et al., EXFOR Data No. 30936003
[31] Wang Yongchang et al., EXFOR Data No. 30935003
[32] Lu Hanlin et al., INDC(CPR)16 (1989)
[33] D. C. Santry et al., Can. Journal Phys., 68, 582(1990)
[34] N. T. Molla et al., Proc. of Conf. on Nucl. Data for Science and Technology, Juelich, 355(1991)
[35] Y.Ikeda et al., JAERI-M-91-032 (1991)
[36] D. L. Smith et al., Proc. of Conf. on Nucl. Data for Science and Technology, Juelich, 282(1991)
[37] S. Chiba et al., RCM / BEIJING94 / P1 (1994)
[38] D. L. Smith et al., International Reactor Dosimetry File (IRDF-90)
[39] T. B. Ryves et al., NEANDC(E)-212,8, 79(1980)
[40] D. B. Gayther et al., Proc. of Conf. on Nuclear Data for Science and Technology, Mito, 1842(1988)
[41] M. Wagner et al., Annual of Nuclear Energy 15, 363(1980)
[42] M. Wagner et al., Proc. of Conf. on Nuclear Data for Science and Technology, Mito, 1049(1988)
[43] M. Wagner et al., Annual of Nuclear Energy 20, 1(1993)

Evaluation of the (n,α) Cross Sections for $^{58,60\sim62,64}Ni$ and ^{Nat}Ni

Ma Gonggui Wang Shiming Zhang Kun

(Institute of Nuclear Science and Technology,
Sichuan University, Chengdu)

Introduction

The cross section of the (n,α) reaction is very important for fusion reactor for monitoring neutron field in the context of radiation induced material damage, radiation safety, neutron dosimetry, etc.

The natural nickel consists of five stable isotopes, i. e. ^{58}Ni, $^{60\sim62,64}Ni$. Their abundances and threshold energies are given in Table 1.

Table 1 Isotopic abundances and their reaction threshold energies of nickel

isotope	58	60	61	62	64
abun. / (%)	68.27	26.1	1.13	3.59	0.91
thre. / MeV	0.0	0.0	0.0	0.4445	2.4805

For (n,α) cross section measurement there are some difficulties due to no good neutron source and other numerous reactions in sample. The data were only measured in the energy range below 10.0 MeV and around 14.0 MeV. Here the evaluations of these cross sections are given in Figs. 1～4 with experimental data.

1 Evaluation of Cross Section

1.1 $^{58}Ni(n,\alpha)^{55}Fe$ Reaction

The experimental data were measured by Baba(94), Goverdovski(94), Wattecamps(94), Qaim(84, 76), Graham(87, 79) and Paulsen(81)[2~9] in the energy range below 10.0 MeV and around 14.0 MeV, respectively. The evaluated data at 14.1 MeV was taken from Zhou(91)[10]. Below 14.0 MeV, the cross sec-

tion was obtained by fitting experimental data. Above 14.0 MeV, the recommended data were taken from theoretical calculations, and normalized to the fitting measured value of 112.0 mb at 14.0 MeV.

1.2 $^{62}Ni(n,\alpha)^{59}Fe$ Reaction

The experimental data were measured by Wang(90), Qain(84), Lees(79), Fukuda(78), Welgel(75), Levkovskij(68), and Yu(67)[5, 11~16] in the energy range from 6.4 to 9.5 MeV and around 14.0 MeV, respectively. The evaluated datum at 14.1 MeV was taken from Zhou(91). Below 14.0 MeV, the data were obtained by fitting experimental data. Above 14.0 MeV, the experimental fitting value of 20.6 mb at 14.0 MeV was used to normalize corresponding calculated result.

1.3 $^{64}Ni(n,\alpha)^{61}Fe$ Reactions

The experimental data were measured by Kobayashi(91), Ribansky(85), Bahal(85), Qain(84) and Levkovskij(68)[5, 15, 17~19] in the energy range from 7.0 to 9.6 MeV and around 14.0 MeV, respectively. The evaluated datum at 14.1 MeV was taken from Zhou(91). Below 14.0 MeV, the cross sections were given by fitting experimental data. Above 14.0 MeV, the recommended data were taken from calculated result, and normalized to the fitting measured datum of 502 mb at 14.0 MeV.

1.4 $^{60,61}Ni(n.\alpha)^{57,58}Ni$ Reaction

Due to ^{60}Ni and ^{61}Ni have no experimental data, the data were taken from theoretical calculation results. The evaluated data of 63 mb and 42 mb at 14.1 MeV by Zhou(91) were used to normalize corresponding model calculated values for ^{60}Ni and ^{61}Ni, respectively.

1.5 The (n,α) Reaction for Natural Nickel

For natural Ni, the experimental data were measured by Wattecamps(83), Kneff(86), Grimes(79) and Paulsen(81)[9, 20~22] around 14.5 MeV and in the energy range from 4.89 to 9.97 MeV, respectively. The α particles were measured at five angles with telescope detectors in a reaction chamber.

The (n,α) cross section of natural Ni was obtained from summing the isotopic data weighted by the isotopic abundance. The comparison of experi-

mental data with evaluated ones are shown in Fig. 4. It is found that the present evaluation is in very good agreement with the experimental data.

2 Summary

Based on experimental data and theoretical calculation, the (n,α) cross sections for Ni isotope and natural nickel were evaluated in the neutron energy region up to 20 MeV. The present evaluated data were compared with ENDF / B–6, JENDL–3, BROND–2 and EFF–2. It was shown that the present evaluations reproduce the measured data of natural nickel and its isotopes well.

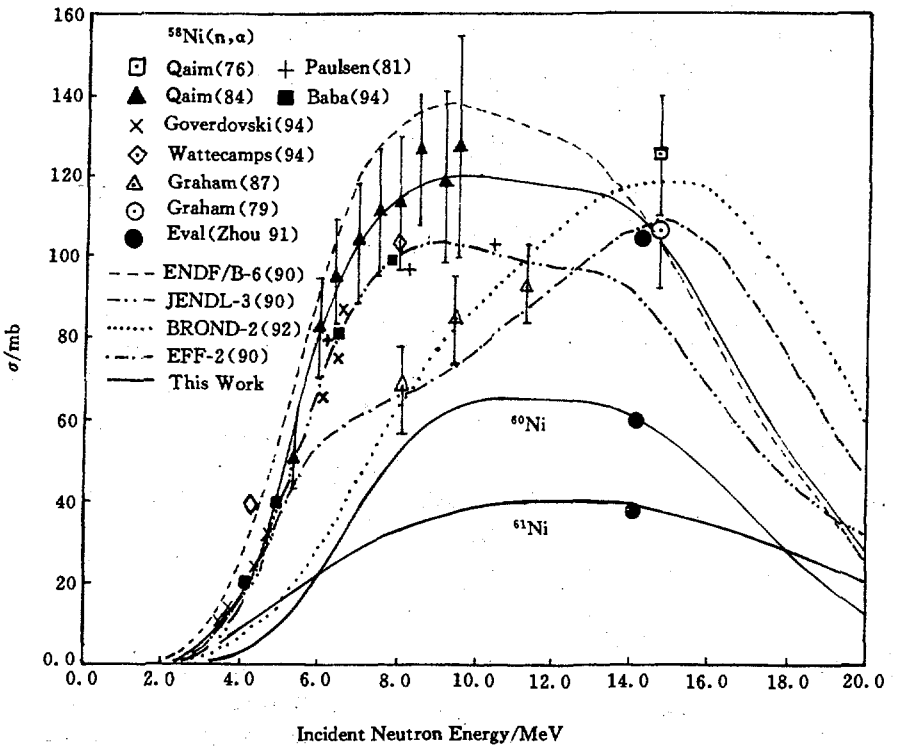

Fig. 1 (n,α) cross section for ^{58,60,61}Ni

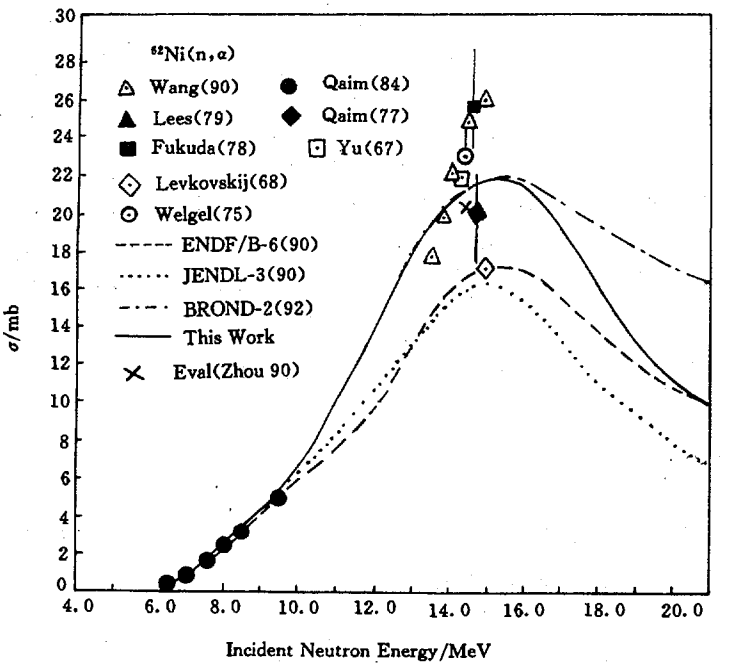

Fig. 2 (n,α) cross section for ^{62}Ni

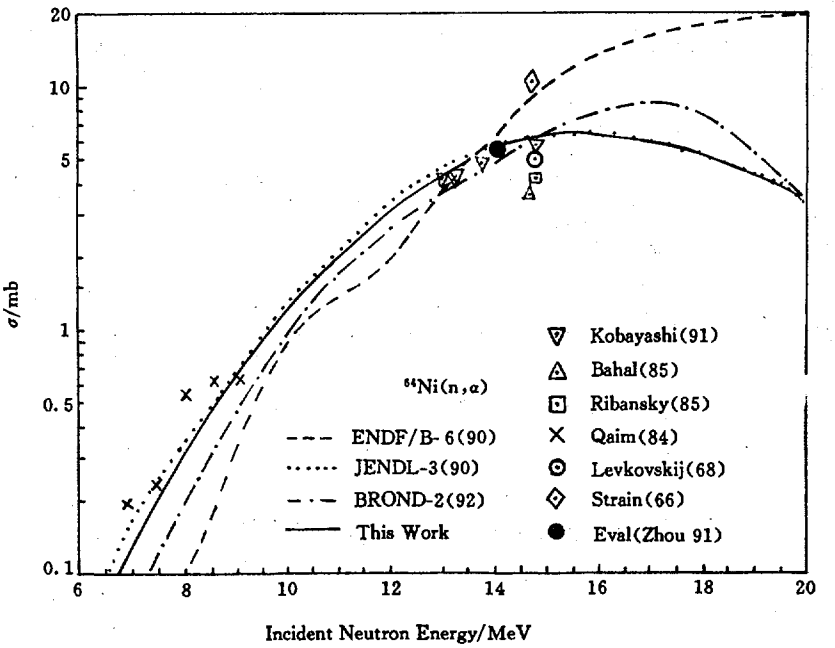

Fig. 3 (n,α) cross section for ^{64}Ni

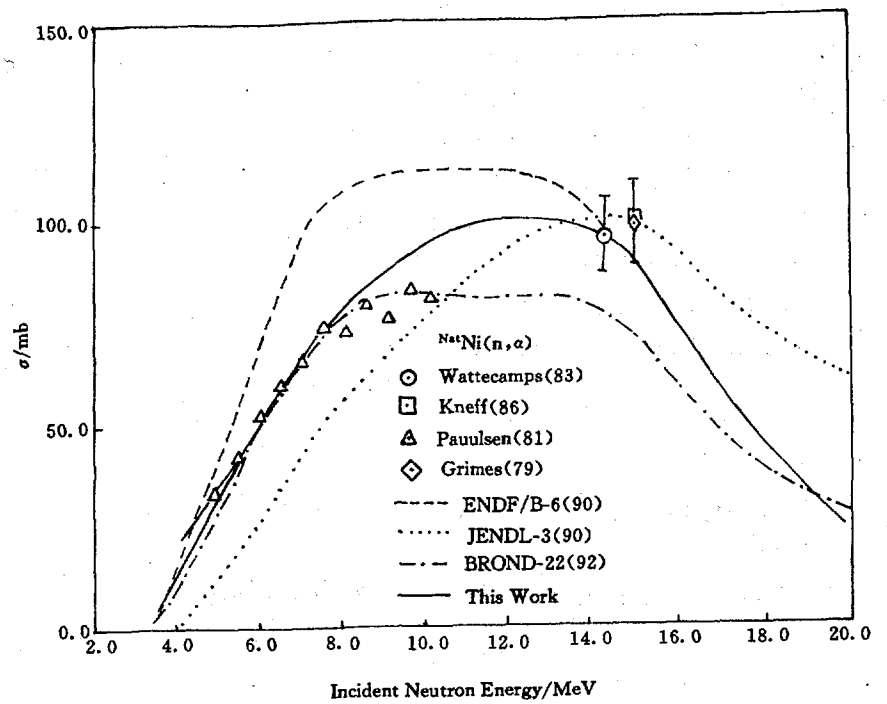

Fig. 4 (n,α) cross section for natural Ni

References

[1] Zhang Jingshang, Nucl. Sci. Eng., 114, 55, 1993

[2] M. Baba et al., Nucl. Instr. Meth., A337, 474, 1994

[3] A. Goverdovski et al., Proc. Int. Cong. on Nucl. Data, Gatlinburg, Tennessee, May 9 ~13, p. 117, 1994

[4] E. Wattecamps et al., Proc. Int. Conf. on Nucl. Data, Gatlinburg, Tennessee, May 9~13, p. 282, 1994

[5] S. M. Qaim et al., Nucl. Sci. Eng., 88, 143, 1984

[6] S. M. Qaim et al., Proc. of the Ninth Symp. on Fusion Tech., Garmisch, 589, 1976

[7] S. L. Graham et al., Nucl. Sci. Eng., 95(1), 60, 1987

[8] S. L. Graham et al., Phys. Rev. C19, 2127, 1979

[9] A. Paulsed et al., Nucl. Sci. Eng., 78, 377, 1981

[10] Zhou Delin et al., A Progress Report to FENDL Meeting, 1991

[11] Wang Yongchang et al., High Energy Physics and Nuclear Physics, 14, 1117, 1990

[12] E. W. Lees et al., R. AERE-R-9390, 6, 1979

[13] K. Fukuda et al., Japanese Reports to Nucl. Eng., Agency Nucl. Data Comm. Documents-566 / U, 44, 1978

[14] H. Weigel et al., J. Radiochimica, 22, 11, 1975
[15] V. N. Levkovskij et al., Yadernaja Fizika, 8(1), 7, 1968
[16] Yu Yuwen et a., Nucl. Phys., A98, 451, 1967
[17] K. Kobayashi et al., JAERI-M-91-032, 265, 1991
[18] I. Ribansky et al., INDC(CSR)-7, 1985
[19] B. M. Bahal et al., NEANDC(E)-252 / U, 5, 28, 1984
[20] E. Wattecamps et al., 83ANTWER, 159, 1983
[21] D. Kneff et al., Nucl. Sci. Eng., 92, 491, 1986
[22] S. M. Grimes et al., Phys. Rev., C19, 2127, 1979

Evaluation of Activation Cross Sections for (n,2n) Reactions on Some Nuclei

Yu Baosheng

(China Nuclear Data Center, CIEA)

Abstract

The evaluations of activation cross sections of (n,2n) reaction for ^{58}Ni, ^{87}Rb, ^{89}Y, ^{90}Zr, ^{140}Ce and ^{169}Tm were performed in order to update the previous evaluated data. The cross sections are recommended based on the recent experimental data, especially the new measured results in CIAE. The present evaluated data are compared with other evaluated data.

The activation cross sections are very useful in fusion research and other applications such as radiation safety, environmental, neutron dosimetry and material damage. More efforts are required to identify and resolve the differences and discrepancies in the existing activation cross sections from different laboratories. The main characteristics of the evaluated activation cross sections in this work are as follows :

1 Most of the activation cross sections mentioned above have been measured

in CIAE. A project of activation cross sections measurements and evaluation have been under–way in CIAE for a long period. The new measured data could contribute to this evaluated work and modify the recommended data.

2 The activation cross section in the so–called 'gap' energy region 5～12 MeV are being researched using the activation method with quasi–energetic neutron produced by the $^{1}H(^{11}B,n)^{11}C$ reaction at JAERI and by D(d,n) reaction using D–D gas target at variable energy compact Cyclotron CV 28 FRG (Julich, Federal Republic of Germany). These newly measured data could supplement the scarce data in this energy region, and modify the previous evaluation.

3 In order to eliminate the discrepancies in the existing activation cross sections, the background neutron yield from both "gas–out" effect and D–D breakup needs to be accurately determined and abstracted. It was noted that both effects increase with the neutron energy and strongly depend on the threshold of the specific reaction. Recently, the accurate experimental data have been obtained in many laboratories.

(1) ^{58}Ni

The cross sections for $^{58}Ni(n,2n)^{57}Ni$ reaction above 15 MeV were measured mainly by Paulsen[1], Bayhurst[2], Zhao Wenrong[3] and Pavlik[4]. there are large discrepancy among these measured data sets.

Paulsen[1] measured the data early, Pavlik[4] measured in 1982 and revised in 1985. Meanwhile, the new data of Pavlik[4] span a wide energy region from threshold to 19 MeV.

The half–life of residual nuclei ^{57}Ni are known very well (36 h), the characteristic gamma ray 1378 keV has a branching ratio 0.779, which are adopted in the world after 1982. The corrections for the characters of gamma ray of ^{57}Ni are negligible.

The recommended data above 15 MeV were determined based on measured data by Pavlik[4]. The evaluated data are shown in Fig. 1.

(2) ^{87}Rb

For $^{87}Rb(n,2n)$ cross section, the experimental data are scarce. At present, the cross section was evaluated based on the experimental data and theoretically calculated data. The evaluated data are compared with those from

ENDF / B–6. Both evaluated data are consistence with each other in their tend. However, the discrepancies exist in the energy region from 13 to 15 MeV. Present evaluated data shown in Fig. 2 are consistent with the existing measured data given by R. Pepelinik[5] and Yuan Xialin[6].

(3) ^{89}Y

For ^{89}Y(n,2n)^{88}Y reaction there exist lots of measured data. The measured data by Zhao Wenrong[3] cover the energy region from 13 to 18 MeV and consist with the new measured data. At present work, the cross section was evaluated based on new experimental data, especially the measured data in CIAE from 13 to 18 MeV. The previous evaluation is modified and the data are shown in Fig. 3.

(4) ^{90}Zr

For this nuclide, there are many new experimental data. The evaluated data (Fig. 4) were based on these new measured data by Csicki[7], Ikeda[8], Kobayushi[9], Palvik[10] around threshold and above 18 MeV energy region. The evaluated data are compared with other evaluated data from ENDF / B–6, JENDL–3, BRON–2 (Fig. 5).

(5) ^{140}Ce

The experimental data[2] exist only from 12 to 20 MeV. The cross section was evaluated based on these measured data (mainly from CIAE) and systematic (below 12 MeV). The evaluated data are shown in Fig. 6.

(6) ^{169}Tm

The cross section was evaluated based on experimental data. The existing experimental data from 8 to 13 MeV were measured by Frehaurst[11] with liquid tank method. The cross sections were measured relatively to the known cross sections of ^{238}U(n,f) reaction. In the measurements, the different ^{238}U(n,f) standard cross sections were used. Now, the cross sections, especially from 11 to 12 MeV energy region, were renormalized by using the new ^{238}U(n,f) cross section from ENDF / B–6. The new corrected values supersede the earlier data. The previous evaluated data are modified and the evaluated data are shown in Fig. 7.

Acknowledgements

The authors are indebted to IAEA (International Atomic Energy Agency), CNNC (Chinese National Nuclear Corporation) and CIAE for their supports, and thank to Drs. A. B. Pashchenko, T. Benson, O. Schwerer, Lu Hanlin and Zhao Wenrong for their kind helps and suggestions.

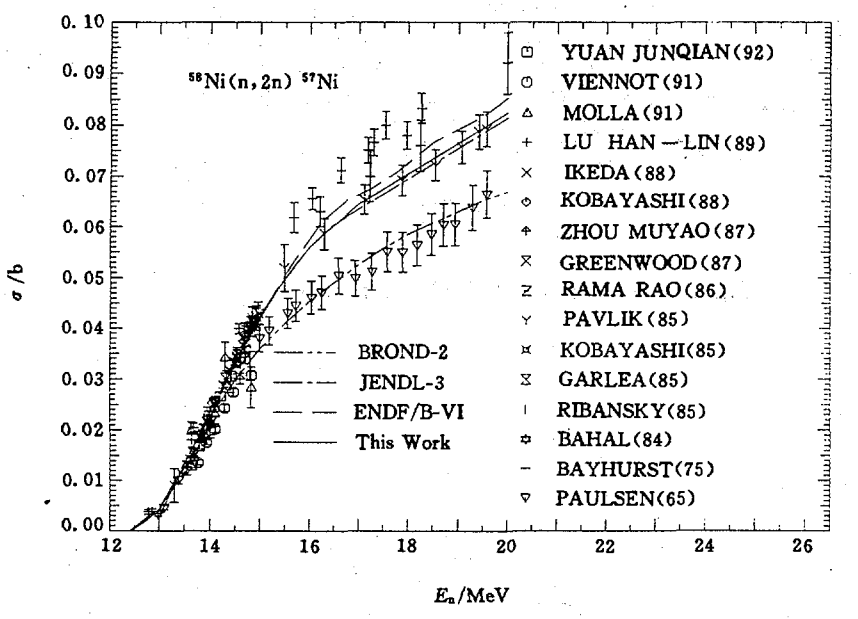

Fig. 1 The evaluated ^{58}Ni(n,2n) cross section

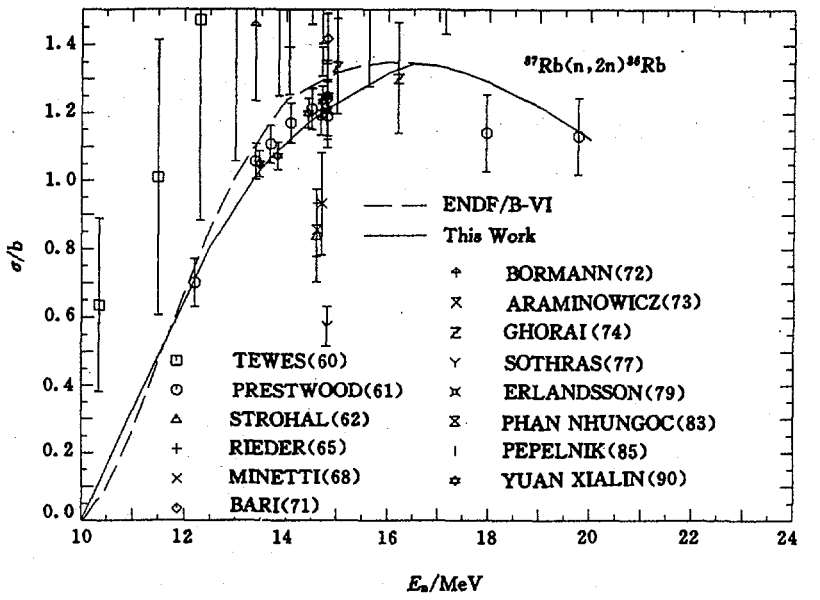

Fig. 2 The evaluated ^{87}Rb(n,2n) cross section

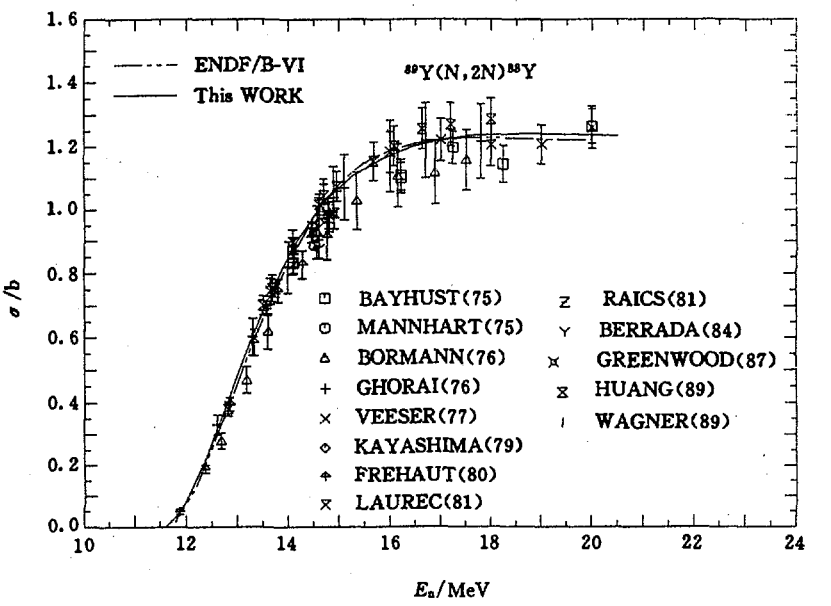

Fig. 3 The evaluated ^{89}Y(n,2n) cross section

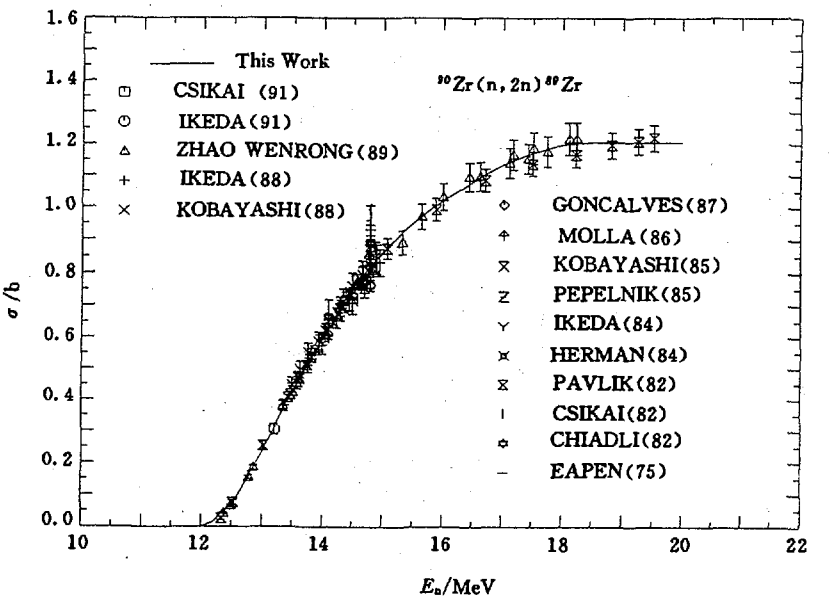

Fig. 4 The evaluated ^{90}Zr(n,2n) cross section

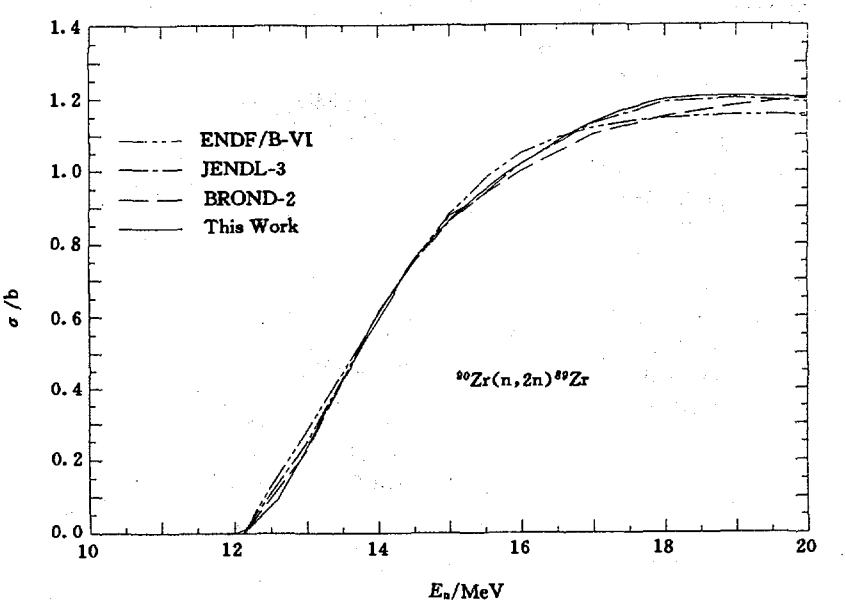

Fig. 5 Comparison between the evaluated data for ^{90}Zr(n,2n) reaction

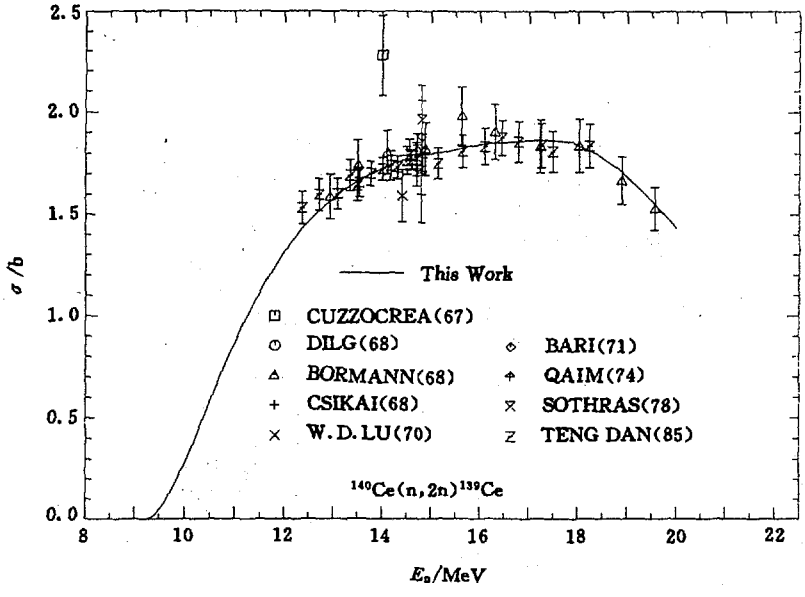

Fig. 6 The evaluated ^{140}Ce(n,2n) cross section

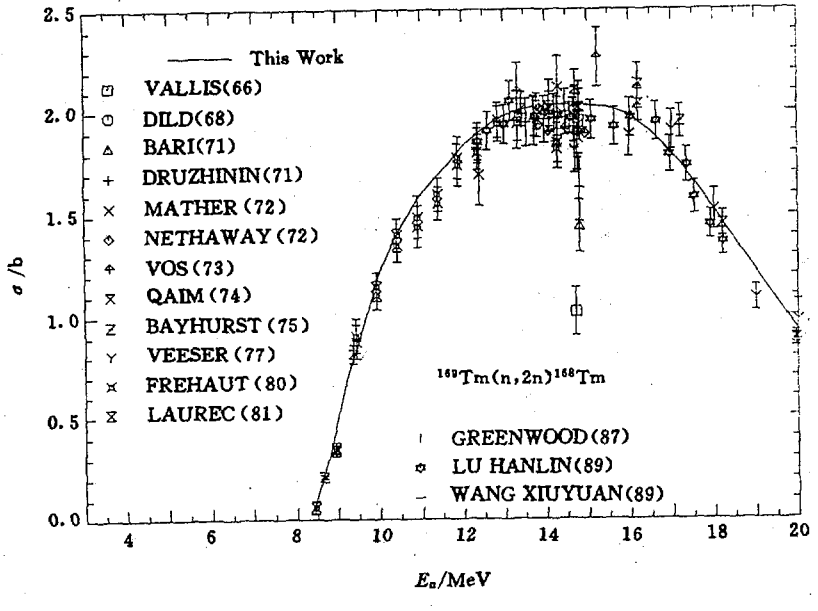

Fig. 7 The evaluated ^{169}Tm(n,2n) cross section

References

[1] A. Paulsen et al., EXFOR Data No. 20386002 (1965)
[2] B. P. Bayhurst et al., Phys. Rev., C, 12, 451(1975)
[3] Zhao Wenrong, Lu Hanlin et al., INDC(CPR)–16 (1989)
[4] A. Pavlik et al., Nucl. Sci. and Eng., 90, 186(1985)
[5] R. Pepelnik et al., NEANDC(E)–262, 32(1985)
[6] Yuan Xialin et al., China Journal of Nucl. Phys., 12, 4(1990)
[7] J. Csikai et al., Annual Nuclear Energy, 18, 1(1991)
[8] Y. Ikedaet al., JAERI–M–91–032, (1991)
[9] K. Kobayushi et al., NEANDC(J)–155, 52(1990)
[10] A. Pavlik et al., EXFOR Data No. 21807002 (1988)
[11] J. Frehaut et al., Nuclear Cross Section and Tech., 425, 855(1975)

Sensitivity of *Logft* on ε Branching to Ground State of ^{197}Au in Decay of ^{197}Hg

Zhou Chunmei

(China Nuclear Data Center, CIAE)

The decay scheme of ^{197}Hg (64.14 h) is fairly established[1], as shown in Fig. 1. In the decay scheme adopted in the Table of Isotopes (7th edition) [2] there is no electron capture branching to the ground state of ^{197}Au and ε transition proceeds by 99% and 1% to the 77.35 and 268.71 keV states respectively. The later evaluation of decay data for $A = 197$[1] attributed about 5.6% feeding to the ground state of ^{197}Au. The evaluated value is estimated from the assumption that the β–transition rate logft of ^{197}Hg (ground state) → ^{197}Au (ground state) is equal to β^-–transition rate logft of ^{197}Pt (ground state)→ ^{197}Au (ground state) ($logft = 7.33 \pm 0.12$ is known[1]). Its I_ε value is obtained from Fig. 2 where *logft*–values are calculated by using LOGFT code[3].

Recently the ε branching is estimated directly from the accurate measurement[4] of K x–ray and γ–ray intensity in the decay of ^{197}Hg (64.14 h)

and using the measured K–electron capture probabilities (P_K)[5] for the different states of ^{197}Au of this decay. The recent evaluated I_ε branching to different states of ^{197}Au for ^{197}Hg decay (64.14 h) are shown in the Table 1.

From Fig. 2 it can be seen that the logft–values are not much sensitive to small change in the value of the ε–transition branching. The changing *logft*–values for the ground state from 7.4 to 7.6 cause the values of the ε–transition branching changes from 5% to 7%. This shows that one should be very careful in using *logft*–value to deduce the decay branching.

Table 1 Evaluated ε data from ^{197}Hg decay (64.14 h)[6]

E(level) / keV	I_ε / %	*logft*
268.714	> 1.42	< 7.5
77.351	>96.71	< 6.1
0	< 1.87	> 8.0

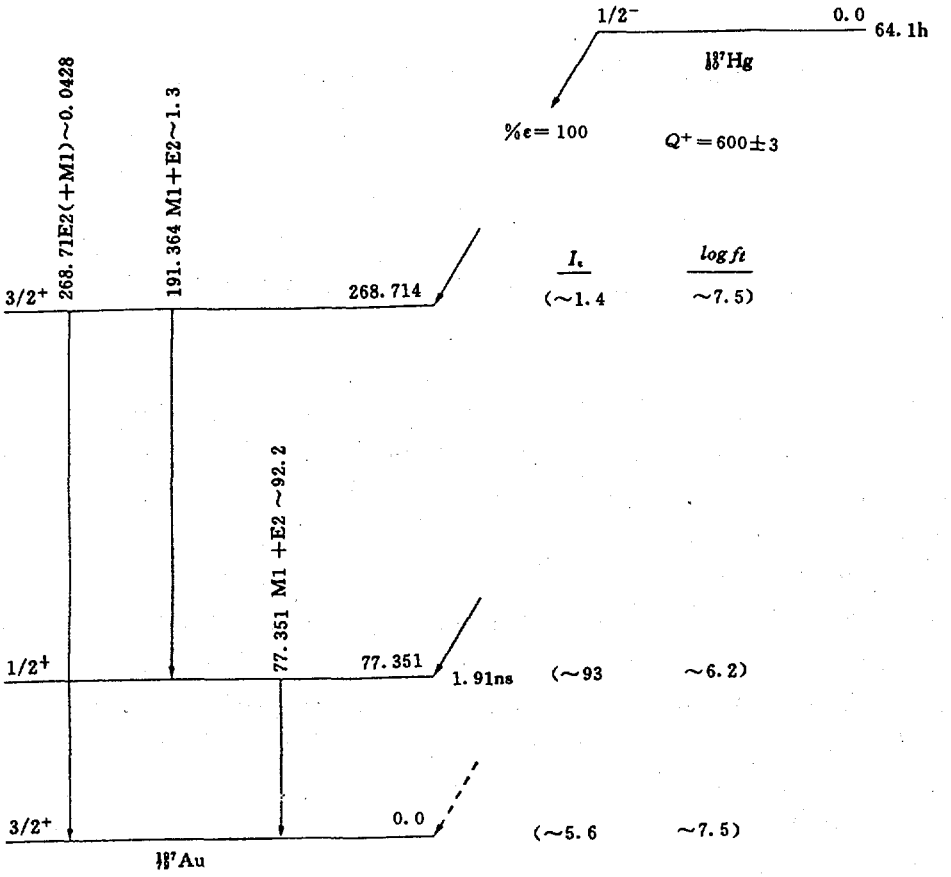

Fig. 1 Decay scheme of ^{197}Hg (64.14 h)

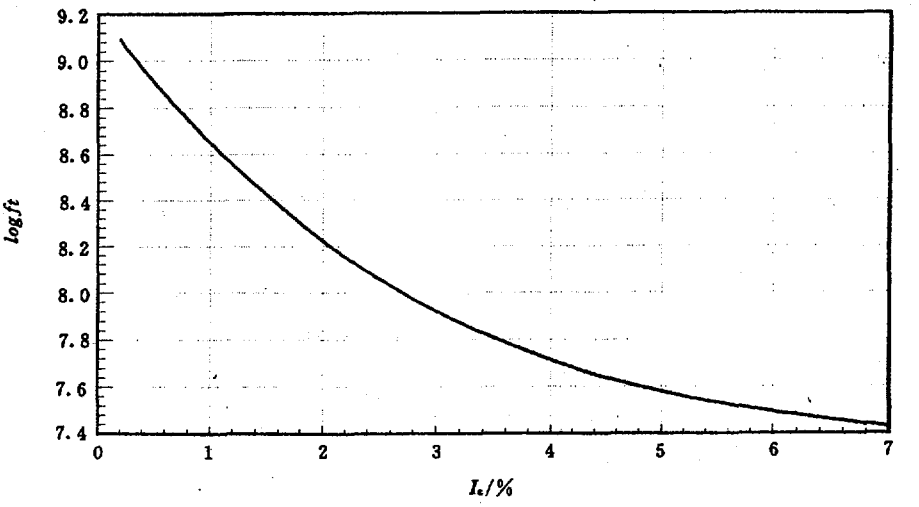

Fig. 2 Variation of logft with I_ε branching to ground state of ^{197}Au for ^{197}Hg decay (64.14 h)

References

[1] Zhou Chunmei, Nuclear Data Sheets, 62, 441, 1991

[2] C. M. Lederer et al., Table of Isotopes (7th Edition) John Willey and Sons Inc., New York, 1987

[3] T. W. Burrows, Private Communication (1992)

[4] B. Dasmahapatra et al., App. Rad. Isot., 45, 803, 1994

[5] B. Dasmahapatra et al., Z. Phys., A343, 161, 1992

[6] Zhou Chunmei, Nuclear Data Sheets Update for $A = 197$ (to be published, 1995)

IV ATOMIC AND MOLECULAR DATA

Evaluated Particle Reflection Data Base

Yao Jinzhang Yu Hongwei

(China Nuclear Data Center, CIAE)

Introduction

Data on the reflection of light ions from solid surfaces are important in various fields of research and application, especially for the development of fusion energy device. The particle reflection is characterized by two parameters. First, the number reflection coefficient, R_n, defined as the ratio of all particles backscattered from the surface to the number of the incident particles; second, the energy reflection coefficient, R_e, defined as the energy carried away by the reflected particles divided by the energy of the projectiles. Some reviews of study on the reflection have been published. Recent two reports were presented by E. W. Thomas et al.[1] and W. Eckstein[2].

Generally speaking, the particle reflection coefficient is high at low energy which approach to 1 at minimun energy of projectiles and decrease monotonically as incident energy increases. However, Baskes[3], using the Embedded Atom Method (EAM), showed that for the hydrogen particle the energy reflection coefficients do not reach unity at very low energy. Instead, the reflection coefficients decrease again when the kinetic energy approaches the chemical binding energy of surface atoms. Eckstein[4], using the Monte Carlo program TRIM–SP, indicated that the decrease starts below 10 eV and depends strongly on the binding energy. Z. Luo[5], using the modified bipartition model in which the chemical binding energy of surface atoms is taken into account, calculated the reflection coefficients of combinations for light ions projectile on twelve species solid surfaces. Our recommended data indicated that reflection coefficients have a drastic decrease with decreasing energy below 100 eV. Data in this energy region are urgently needed in designing Tokamak–type fusion devices.

1 Data Sources

In present evaluation of reflection coefficient, the data were taken from experimental measurements[6~9] up to the end of 1994, also the data were calculated with modified bipartition model and modified empirical formula, which is shown as

$$Q_e = \frac{\frac{0.705}{f}}{\left(1+\left(\frac{\varepsilon}{0.047}\right)^{0.597}+\left(\frac{\varepsilon}{0.619}\right)^{1.5}\right)} \tag{1}$$

$$R_e = Q_e - \exp\left(-\pi\varepsilon\left(M_1+M_2\right)\right)$$

$$R_n = \frac{R_e}{\gamma_e}$$

$$\gamma_e = \frac{1}{\left(1+\left(\frac{\varepsilon}{0.133}\right)^{0.285}\right)} + \frac{0.530}{\left(1+\left(\frac{\varepsilon}{85}\right)^{-1.46}\right)}$$

$f = F(Z_1, Z_2, M_1, M_2, \varepsilon)$ defined in Ref. [6];

The reduced energy is

$$\varepsilon = \frac{0.032534\ M_2 E_0}{Z_1 Z_2\left(M_1+M_2\right)\left(Z_1^{\frac{2}{3}}+Z_2^{\frac{2}{3}}\right)^{\frac{1}{2}}}$$

Where Z_1, M_1, Z_2 and M_2 represent the charge and mass of projectile and target, respectively. E_0 is energy of incident particle.

Experimental studies are mainly confined to energies between 1 and 10 keV in which beams are easy to produce, reflected species are easy to detect. The accuracy of measurement is quoted as 10% to 30%. Under some conditions, it is up to 50%. The precision of data calculated by bipartition model depends on approachability of Boltzmann equation, choice of potentials and other relevant parameters. For elemental targets, the empirical formula is reasonably in good agreement with the experimental and calculated data with bipartition model, covering almost the whole energy region above 10 eV for various combinations

of the projectiles and targets. The relative deviations of the data from empirical formula follow approximately the normal distribution; the standard deviation is 26% for the experimental data and 30% for the data computed by bipartition collision approximation. No significant difference in the standard deviation can be seen for the different projectiles.

2 Evaluation Procedure

Our recommended data are determined by fitting composite data with optimal weights by spline function[10]. In order to suit a format of atomic and molecular library (ALADDIN)[11], the recommended data are put into the scale expression

$$R_n(\text{ or } R_e) = \frac{A_1 \ln(A_2\varepsilon + e)}{1 + A_3\varepsilon^{A_4} + A_5\varepsilon^{A_6}}\left(1 - \frac{A_7}{\varepsilon}\right) \tag{2}$$

Where ε is reduced energy as mentioned above, $e=2.7183$, the optimal values of parameter $A_1 - A_7$ can be produced by method of generalized least-square. The coefficients of R_n and R_e depended on incident energies can be calculated by the formula (2) with parameters A_1, A_2, A_3, A_4, A_5, A_6, and A_7.

At present, our data base of particle reflections include H^+, D^+, $^3He^+$ and $^4He^+$ projectiles and Be, B, C, Al, Si, Ti, Fe, Ni, Cu, Mo, W and Au twelve monoatom solid surfaces. Figs. 1～4 show some examples of evaluation results. In the figures, Exp is experimental measurements, Luo is calculation result by Luo Zhengming, Emp is the result calculated by modified empirical formula (1) and solid line shows the recommended data.

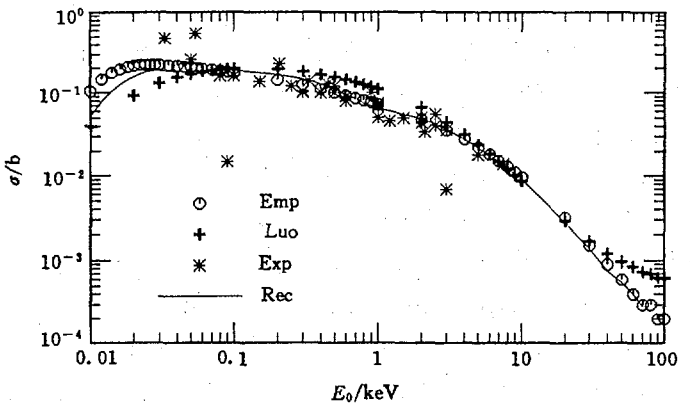

Fig. 1 R_n vs E_0 for D^+ on C solid surface

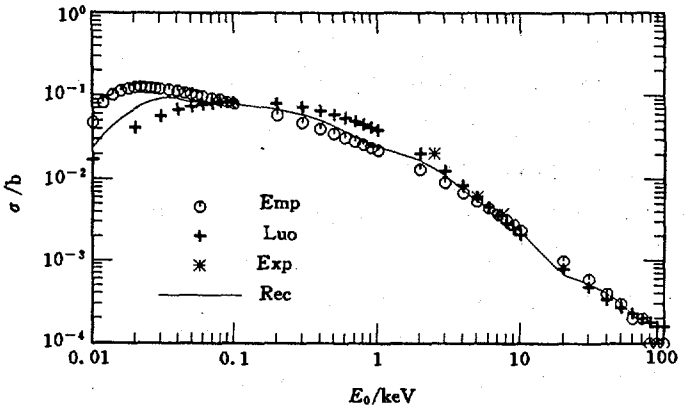

Fig. 2 R_n vs E_0 for D^+ on C solid surface

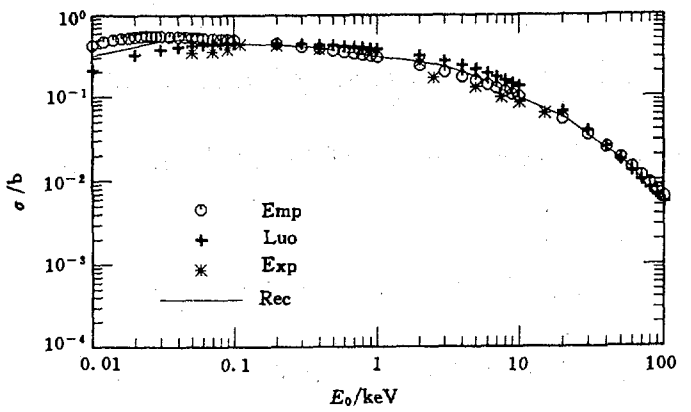

Fig. 3 R_n vs E_0 for D^+ on Ni solid surface

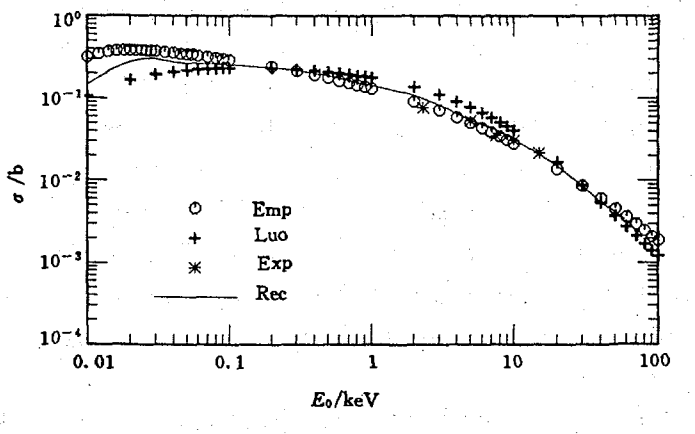

Fig. 4 R_n vs E_0 for D^+ on Ni solid surface

References

[1] E. W. Thomas et al., INDC(NDS)-249 (1991)
[2] W. Eckstein, Supplement to the Journal Nuclear Fusion Vol. 1, 17 (1991)
[3] M. I. Baskes, J. Nucl. Mater. 128-129, 676 (1984)
[4] W. Eckstein et al., Appl. Phys. A38, 123 (1985)
[5] Z. Luo, Nucl. Instr. & Methods in Phys. Rev. B48, 435 (1990)
[6] R. Ito et al., IPPJ-AM-41 (1985)
[7] C. K. Chen et al., Appl. Phys. A31, 37 (1983)
[8] R. Aratari et al., Nucl. Instr. & Methods in Phys. Res. B42, 11 (1989)
[9] A. Narmann et al., Nucl.Instr. & Methods in Phys. Res. B69, 158 (1992)
[10] J. B. Ahorsley et al., Nucl. Instr. Methods, 62, 29 (1968)
[11] IAEA-NDS-AM-17 (1989)

Physical Sputtering Simulated Calculation by TRIM-91 Program

Yao Jinzhang Yu Hongwei

(China Nuclear Data Center, CIAE)

The TRIM program is a Monte Corlo Transport Code. The original version of TRIM was presented by J. P. Biesack et al.. The details of the program have already been described in Ref. [1]. The TRIM program is based on the assumption of an amorphous target material. The incident ions and the recoil atoms are followed throughout their slowing-down process until their energy falls below a predetermined energy. The total sputtering yields include the sputterings by incident and reflected ions. The TRIM program assumes the validity of the binary encounter model, i. e. the projectiles (incident ion or recoil atoms) encounter target atoms sequentially one by one. The same assumption is also implicitly inherent in all analytic theories which are based on linearized Boltzmann equations.

We performed firstly calculation for D^+ ion projectile on nickel target using TRIM-91 Code on microcomputer with the following output : (a) total

sputtering yields by incident and reflected ions, (b) ion reflection (back scattering), (c) sputtered particle distributions in energy, and (d) two–dimensional distribution on polar and azimuthal angles,and angle–energy correlations. (c) and (d) are not presented here.

The results are indicated in the following table.

Total number of projectile particle is taken as 15000

The surface binding energy E_s = 4.46 eV

incident energy / keV	0.1	0.3	0.5	0.8	1	3	5	7	10	15
sputtering yield (TRIM–91)	0.0153	0.0306	0.0383	0.0404	0.0469	0.0356	0.0249	0.0167	0.0179	0.01
mean energy of sputtered particle (eV / atom)	0.1	0.2	0.3	0.3	0.4	0.4	0.4	0.3	0.2	0.2
number of ion reflection	4581	4312	4199	5102	3582	2411	1815	1399	1007	659

The sputtering yields depend on the incident energies, shown in Fig. 1. In Fig. 1, the solid line is the fit results of experimental measurements and our calculations using Bohdansky's formula[2] by spline function. The experimental values are taken from IPP 9 / 82 (1993)[3]. The results calculated by TRIM–91 are in good agreement with our recommended data (solid line) in the region of incident energies from 0.2 to 10 keV within the range of measurement errors. The precision of calculation with TRIM–91 is better than 10%.

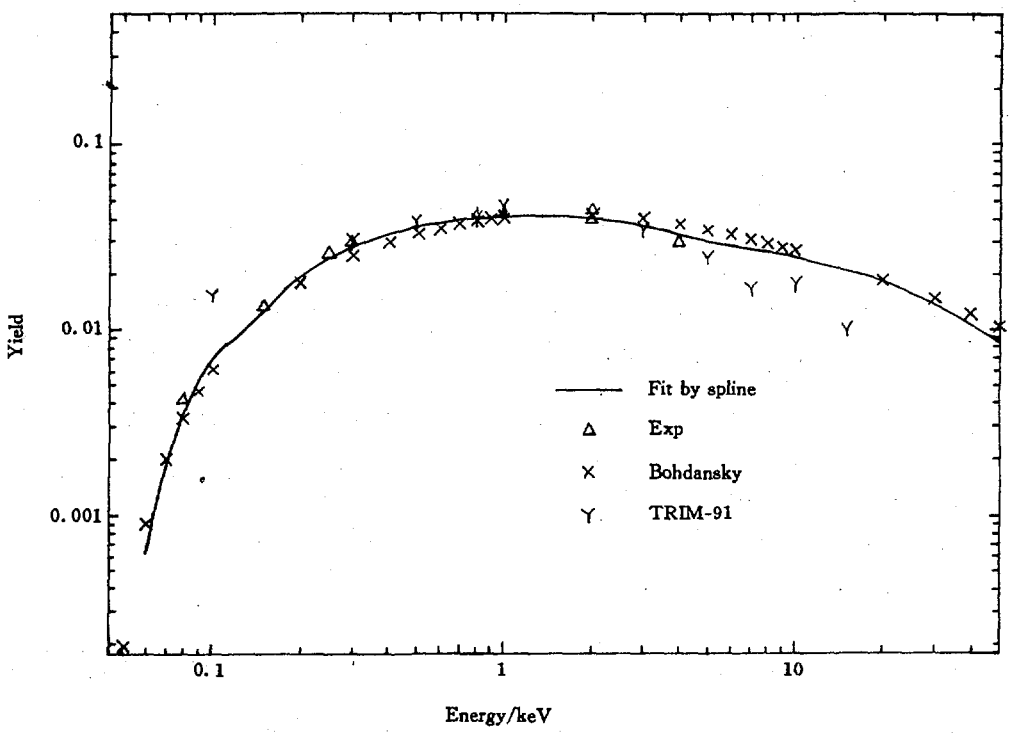

Fig. 1 Sputtering yield of Ni by D^+

References

[1] J. P. Biersack et al., Nuclear Instrum. Methods 174, 257 (1980)
[2] Yu Hongwei et al., CNDC No. 12, 91 (1994)
[3] W. Eckstein et al., IPP 9 / 32 (1993)

V PARAMETER AND PROGRAM LIBRARIES

The Management–Retrieval Code of Nuclear Level Density Sub–Library (CENPL–NLD)*

Ge Zhigang Su Zongdi

(China Nuclear Data Center, CIAE)

Huang Zhongfu Dong Liaoyuan

(Department of Physics, Guangxi Univ.)

Abstract

The management–retrieval code of the Nuclear Level Density (NLD) is presented. It contains two retrieval ways : single nucleus (SN) and neutron reaction (NR). The latter contains four kinds of retrieval types. This code not only can retrieve level density parameter and the data related to the level density, but also can calculate the relevant data by using different level density parameters and do comparison of the calculated results with related data in order to help user to select level density parameters.

Introduction

As we know that the level density parameters are crucial ingredient in the nuclear statistical theory. Three kinds of the level density formulae, the composite four–parameter formula, i. e. Gelbert–Cameron model (G–C)[1], back–shifted Fermi gas model (BS)[2] and Generalized Superfluid Model (GSM)[3], are widely used in the nuclear model calculations. The Nuclear Level Density library (NLD), which is a sub–library of Chinese Evaluated Nuclear Parameter Library (CENPL), has been set up at China Nuclear Data Center, the data file of the sub–library consists of two parts : eight sets of popular level

density parameters for three kinds of the level density formulae and the data related to level density, such as the S–wave average level spacing D_0 at the neutron separation energy and cumulative number N_0 of low lying level[4], which are used to help user to select the required level density parameter. The management–retrieval code of NLD has been developed. It not only can retrieve the level density parameters and the data related to the level density, but also can calculate the D_0 and N_0 values, so that the calculated results with different level density parameters can be compared with ones in data file and the required parameters can be selected.

1 Data Files

The NLD sub–library contains two data files, one is LRD file, which contains the data relevant to level density :

D_0 : S–wave average level spacing at neutron separation energy.

N_0 : Cumulative number of low–lying level.

S_0 : S–wave neutron strength function.

GW_0 : S–wave average radioactive capture width at neutron separation energy.

D_0, N_0 and S_0 values were recommended by Huang Zhongfu et al. in 1993[4], GW_0 values were taken from Ref. [5]. These values are denoted by label 'LRD' in the sub–library. Another is LDP file, which contains eight sets of level density parameters. Three of them, recommended by Su et al. [6] (denoted by label ' GC–Su'), Gilbert–Cameron[1] (' GC–GC ') and Cook et al.[2] respectively, are used for the Gilbert–Cameron level density formula. Three of them comes from Huang[7] ('BS–H') and Dilg et al.[8] ('BS–HRB' and 'BS–RB') and for Back–Shifted Fermi gas formula. Other two sets were recommended by Lu et al.[9] in 1994 (' GSM–I') and Ignatyuk et al.[3] ('GSM–I') and for Generalized Superfluid Model.

2 The Management–Retrieval Code

The management–retrieval code of NLD sub–library is used for retrieving the required data. In addition, It also displays the basic information in LRD, LDP data file and NLD–sub–library and can calculate D_0 and N_0 values, and compare the calculated results.

NLD code provides the following two retrieval ways :

A. Retrieving for single nucleus (SN)

In this case, user can retrieve D_0, N_0, S_0 and GW_0 and / or level density

parameters for single nucleus. Also can calculate D_0 and N_0 by using the different level density and compare them.

B. Retrieving for a neutron induced reaction (NR)

NR way can be used to retrieve the level density parameters for four types of fast neutron calculation codes respectively, which is the same as Ref. [10].

At present, there are two versions of this code, one is used on personal computer and another on Micro–VAX II computer.

User can start the code by running "NLD", the information concerned are displayed and then the corresponding "answer" chosen by you is input. The retrieving results are displayed on the screen and stored in data file "OUTNLP.DAT".

3 Conclusion

The NLD sub–library (Version 1) has been set up at CNDC, and used for nuclear model calculations and other fields. NLD sub–library contains the data relevant to the level density and level density parameters. It can provide eight sets of level density parameters for three popularly used level density formulae. The comparison can be done to help user to choose the parameters. The parameters in the data file were cumulated in past different periods. Since they were obtained by fitting the experimental data in those age, so they could not reproduce present experimental data well. The change tendency of the three kinds formulae mentioned above with energy is different. Therefore, it is necessary to recommend new level density parameters by using the update experimental data. Since there are no systematic parameters for B–S and GSM formulae, so their uses are limited. We'll do the study on the systematics for B–S and GSM formulae in near future.

* The project is supported in part by the International Atomic Energy Agency and the National Natural Science Foundation of China.

References

[1] A. Gilbert et al., Can. J. Phys., 43, 1446(1965)

[2] J. L. Cook et al., Ausit. J. Phys., 20, 477(1967)

[3] A. V. Ignatyuk et al., Sov. Nucl. Phys., 1979, v. 29, p. 450

[4] Huang Zhongfu et al., to be published

[5] S. F. Mughabghab et al., Neutron Cross Section, 1981

[6] Su Zongdi et al., INDC(CPR)-2, 1985
[7] Huang Zhongfu et al., Chinese J. Nucl. Phys., 13, 147(1991)
[8] W. Dilg et al., Nucl. Phys., A217, 296(1973)
[9] Lu Guoxiong et al., to be published
[10] Su Zongdi et al., CNDP, 12, 80(1994)

The Sub-library of Atomic Mass and Characteristic Constants of Nuclear Ground State (CENPL-MCC 1.1) (III)*

Su Zongdi Sun Zhengjun Ma Lizhen

(China Nuclear Data Center, CIAE)

The sub-library MCC 1.1 of atomic mass and characteristic constants of nuclear ground state (MCC, Version 1.1), which is a sub-library of the Chinese Evaluated Nuclear Parameter Library (CENPL), is an updated edition of MCC-1. The mass excess, atomic mass and total binding energy have been updated in the data file.

It consists of experimental and systematics mass excesses, atomic masses and total binding energies for 2650 nuclides compiled and recommended by Audi and Wapstra[1] in 1993, and calculated mass excesses for 2121 nuclides by Moller et al.[2] using a nuclear mass formula with a finite-range droplet macroscopic model and the folded-Yukawa single particle microscopic model in 1994. The few of them (181 nuclides), calculated by Moller et al. in 1991[3], are also collected.

In addition, MCC-1.1 data file also contains half-life and abundance, spin and parity of nuclear ground state. Most of these data were taken from Refs. [4, 5], the few of them were collected and compiled by us.

The format of the data file, the functions and running processes of the management-retrieval code for MCC-1.1 sub-library are just the same as MCC-1 (Version 1) sub-library[6, 7].

The authors would like to thank NDS / IAEA and NNDC / BNL for providing us the data tapes with mass excesses, ENSDF and so on.

* The project is supported in part by the International Atomic Energy Agency and the National Natural Science Foundation of China.

References

[1] G. Audi et al., Nucl. Phys. A565, 1 (1993) and A565, 66(1993)
[2] P. Moller et al., (1 August 1994), At. Nucl. Data Tables
[3] P. Moller et al., At. Nucl. Data Tables, 39, 281(1988) (File as of 1991)
[4] Evaluated Nuclear Structure Data File—a computer file of evaluated experimental nuclear structure data maintained by the National Nuclear Data Center, Brookhaven National Laboratory. (File as of March 1991)
[5] N. E. Holden, Table of the Isotopes, 71st edition (1990)
[6] Su Zongdi et al., Commu. Nucl. Data Progress, 11, 103(1994)
[7] Su Zongdi et al., Commu. Nucl. Data Progress, 12, 80(1994)

The Sub–Library of Giant Dipole Resonance Parameters for γ–ray (CENPL–GDP–1.1) (II) *

Liu Jianfeng

(Department of Physics, Zhengzhou University, Zhengzhou)

Su Zongdi

(China Nuclear Data Center, CIAE)

Zuo Yixin

(Department of Mathematics, Nankai University, Tianjin)

Introduction

In this paper, the experimental data of the photonuclear reactions for the nuclides ^{12}C, ^{14}N, ^{16}O, ^{27}Al and ^{28}Si[1] were fitted with the Lorentz curves describing the giant dipole resonances of the photonuclear reactions and the giant dipole resonance parameters (GDRP) of these nuclides were extracted. These GDRP were compiled in the sub–library of the giant dipole resonance parameters for γ–ray (GDP). An updated edition GDP–1.1 (Version 1.1) has been set up and used in the nuclear model calculation widely.

1 The GDRP for $A < 50$

First of all, the collected experimental data of photoneutron reaction cross sections for the nuclides ^{12}C, ^{14}N, ^{16}O, ^{27}Al and ^{28}Si were fitted with the Lorentz curve, and the GDRP of these nuclides were extracted. In the next place, the integrated cross sections (ICS), the first moments (FM) and the second moments (SM) of the integrated cross sections of the photonuclear reaction giant dipole resonances of these nuclides have been calculated by using these parameters, and adjusting these parameters a little, the better coincidences of the integrated cross sections and the excitation curves of these nuclides with the experimental data have been reached. The reliability of the extracted GDRP have further been assured.

The determined GDRP for these nuclides are listed in Table 1.

Table 1 The giant dipole resonance parameters of ^{12}C, ^{14}N, ^{16}O, ^{27}Al and ^{28}Si

Z	A	E_g/ MeV	g/ MeV	g/ mb	E_g/ MeV	g/ MeV	g/ mb
6	12	22.60	1.90	6.30	26.50	8.60	2.60
7	14	20.60	4.30	2.90	23.50	4.50	13.90
8	16	24.50	6.20	6.50			
13	27	21.10	6.10	12.50	29.50	8.70	6.70
14	28	20.10	3.90	10.50	26.50	8.70	3.70

In Table 2 are listed the comparisons of the ICS, FM, SM calculated by using the GDRP listed in Table 1 for these nuclides with the experimental data which are all taken from Ref. [1].

Table 2 The comparisons of the calculated results (cal.) with the experimental data (exp.)

Z	A	ICS / mb, MeV		FM / mb		SM / (mb/MeV)	
		cal.	exp.	cal.	exp.	cal.	exp.
6	12	45.9	46.8	1.859	1.83	0.0781	0.073
			51.6		2.08		0.085
7	14	104.8	98.0	4.534	4.36	0.202	0.200
8	16	53.4	41.5	2.186	1.76	0.0928	0.075
			62.9		2.40		0.094
			61.5		2.51		0.105
13	27	169.7	167.0	7.128	7.17	0.317	0.320
			151.0		6.77		0.310
14	28	97.2	105.0	4.338	4.46	0.203	0.200

2 GDP–1.1

The GDP sup–library was extended (updated edition GDP–1.1). Up to now, it contains the GDRP of 107 nuclides ranging from ^{12}C to ^{239}Pu, among them, 102 nuclides ranging from ^{51}V to ^{239}Pu were taken from Ref. [2]. The format of the data file, the functions and running processes of the management–retrieval code for GDP–1.1 sub–library are just the same as GDP–1 (Version 1) sub–library[3].

Since the GDRP of five nuclides added in this sub–library are all based on the experimental data, the nuclear mass region of the experimental values of the giant dipole resonance parameters have been extended from $A=51$ to $A=12$. This is useful for both model calculations of the nuclear reactions and for the systematics approaches of the GDRP.

* The project is supported in part by the International Atomic Energy Agency and the National Natural Science Foundation of China.

References

[1] A. I. Blokhin et al., INDC (CCP)–337, 1991

[2] S. S. Dietrich et al., Atomic Data and Nuclear Data Tables, 38, 199(1988)

[3] Zuo Yixin et al., Commu. Nucl. Data Progress, 11, 95(1994)

Computer Program Library Status

Liu Ruizhe Zhang Limin

(China Nuclear Data Center, CIAE)

There are two sublibraries in Program Library Relative to Nuclear Data (PLRND, called CPL before). One is called Chinese Program Sublibrary (CNDCP). Another is called Foreign Program Sublibrary. This paper is about the first one.

With the development of nuclear data, some programs have been designed and developed by Chinese. The task of Computer Program Library is collecting, managing, distributing and exchanging the programs. The collection range is the programs for nuclear theory calculation, experimental data evaluation, multigroup constant generation and library management.

In order to ensure the quality of the programs collected by PLRND, a series rules for collecting, testing and evaluating have been made. Under the rules, three meetings for program evaluation were held in 1989, 1992 and 1994, respectively. More than 20 experts from universities and China Nuclear Data Center participated the meetings. All store programs in PLRND were determined on one of these meetings.

For each collected program, materials such as source program, examples and some test cases should be submitted by the author. Then one or two experts are invited to review the program on physics and numerical methods, and to run it for testing all cases given by the author. After that, the examination and acceptance activities could be done at one of the meeting mentioned above.

Up to now, 46 programs in total developed by Chinese have been collected in PLRND. The alphabetic index of them is in Table 1.

Index of Programs in CNDCP Library

Program-name(s), Description	ABST-ID	DATE
ABCC,ADIABATIC-BORN APPROX & COUPLING CHANNEL THEORY	CNDCP0037	0494
ADLFIT,EXTRACTION OF ADLER-ADLER PARAMETERS FROM 1-3 KINDS OF CROSS SEC	CNDCP0005	1189
APCOM,SEARCHING OPTIMAL P D T HE3 HE4 OPTICAL POTENTIAL BELOW 50MEV	CNDCP0024	1092
AUJP,SEARCHING OPTIMUM N-OPTICAL MODEL PARAM BY CALC SEC & ANGL DISTR	CNDCP0012	1189
AVBWFT,EXTRACTION OF UNRESOLVED RESON PARAMETERS FROM CROSS SECTIONS	CNDCP0009	1189
AVRPES,ESTIMATION OF UNRESOLVED PARAMETERS FROM RESOLVED PARAMETERS	CNDCP0010	1189
CBWFIT,EXTRACTION OF MODIFIED SLBW PARAMETERS WITH MULTILEVEL INTERFERENCE	CNDCP0008	1189
CCOM,N DIRECT ELAST & INELAST SCAT CROSS SEC CALC FOR DEFORMED NUCLEUS	CNDCP0004	1189
CFUP1,CALC N P D T HE3 HE4 REACTN FISSILE NUCLEI ENERGY 1-33MEV	CNDCP0026	0692
CMUP,CHARGED PARTICLE CROSS SEC CALC OF MEDIUM-HEAVY NUCLEI	CNDCP0013	1189
CMUP2,CALC N P D T HE3 HE4 REACTN MEDIUN-HEAVY NUCLEI ENERGY 1-50MEV	CNDCP0025	0692
DDCS,DDX CALC INDUCED BY N P He4 D T He3 UP TO TENS OF MEV	CNDCP0035	0794
DDXB1,PROCESSING DATA FROM ENDF / B LIBRARY,PLOTING,EDX & DDX	CNDCP0031	1192
DPPM,THE PRE- AND POST-MANAGEMENT OF CODE DWUCK4	CNDCP0036	0694
DRM,CALC NEWTRON DATA BY DWAB & OPTICAL MODEL FOR 1P SHELL NUCLEI	CNDCP0022	0492
ERES,EXFOR NUCL DATA ENTERING,EDITING,RETRIEVING AND CHECKING	CNDCP0033	0594
FBP,RETRIEVE FISSION BARRIER PARAMETER FROM CENPL-FBP	CNDCP0042	0794
FUP1,A PROGRAM FOR CALCULATING ALL FAST NEUTRON DATA OF FISSION NUCLEUS	CNDCP0046	0395
GDP,RETRIEVE GIANT DIPOLE PARAMETER FROM CENPL-GDP	CNDCP0043	0794
HFTT,EXCITATION FUNC CALC FOR PARTICLE INDUCED NUCL REACTN BY STATIST MODEL	CNDCP0011	1189
IPEET-103,N INDUCED REACTN X-SEC FOR FISSILE NUCLIDES,PRE EQUILIBRIUM MODEL	CNDCP0002	1189
KORP-1,(N,P) OR (P,N) REACTION X-SEC & DIFF X-SEC BY DWBA	CNDCP0021	0692
LIANG,CALC ON N X-SEC,SPECTRA & ANGL DISTR WITH H-F	CNDCP0001	1189
LSQXY,CURVE FITTING WITH UNCERTAINTY WEIGHTING	CNDCP0039	0694
MADEX,MAKE PROGRAM INDEX OF ALPHABETIC SUBJECT & KEYWORD	CNDCP0044	0794
MAINPLT,PROCESSING & PLOTTING FOR ENDF / B DATA OR EXP. DATA	CNDCP0040	0794
MCC,RETRIEVE NUCL MASS & BASIC CONST FROM CENPL-MCC	CNDCP0041	0794
MSDR,CALC DOUBLE DIFFERENTIAL CROSS SECTION	CNDCP0027	0692
MUP2,FAST N NUCL REACTION X-SEC OF MEDIUM-HEAVY NUCLEI	CNDCP0014	1189
MUP3,FAST N X-SEC,SCAT & NERGY ANGL DISTR BY OM,H-F & PRE-EQUILIBRIUM	CNDCP0020	1192
NDCP-1,CALC. NEUTRON DATA & MORE ATTENTION TO GAMMA PRODUCTION DATA	CNDCP0038	0794
NG1,CALC OF (N,GAMMA) X-SEC WITH SYSTEMATICS PARAMETERS IN EN = 1KEV - 20 MEV	CNDCP0007	1189
NX1,CALC OF (N,P),(N,ALPHA) X-SEC WITH SYSTEMATICS PARAMETERS IN EN = < 20MEV	CNDCP0006	1189
PLOT,EVALUATED EXPERIMENTAL DATA POINTS WITH ERROR BAR ON PC	CNDCP0030	1092
RETRIEVE,RETRIEVE CODES FROM PRGRAM LIBRARY IN INDC	CNDCP0045	0794
ROP,CALC X-SEC & ANGL DISTR BY MULTILEVEL MULTICHANNEL R-MATRIX THEORY	CNDCP0015	1189
SCAT,CENERAL THERM N SCAT LAW FOR VARIED MODERATORS	CNDCP0016	1189
SC2N3NN,CALC OF (N,2N),(N,3N) X-SEC WITH SYSTEMATICS PARAMETERS IN EN < 25MEV	CNDCP0003	1189
SCPLOT,SMALL 2-D GRAPHIC SOFTWARE PACKAGE USING IN DISPLAY SCIENTIFIC DATA	CNDCP0028	1192
SESP,SIMULTANEOUS EVALUATION SPLINE FIT CODE FOR CROSS SEC AND RATIOS	CNDCP0019	0692
SPC,SPLINE FIT,MULTI-SET CORRELATIVE DATA,KNOT OPTIMIZATION	CNDCP0018	0692
SPEC,N P He4 D T He3 INDUCED REACTIONS UP TO TENS OF MEV	CNDCP0034	0794
SPF,DATA COMBINE,POLYNOMIALS & PHYS FORMULAS FIT & CALC & COVARIANCE,TREAT	CNDCP0029	1192
UNIFY,X-SEC AND ANGL DIST BELOW 20 MEV BY UNIFIED MODEL	CNDCP0017	0492
UNF92,FAST N X-SEC DDX &GAMMA PROD CALC FOR STRUC MAT BELOW 20MEV	CNDCP0023	0592

The programs are grouped into 12 categories[1] according to the subject. The percentage of each category is shown in Fig. 1, which was plotted by program PERSN, developed at CNDC .

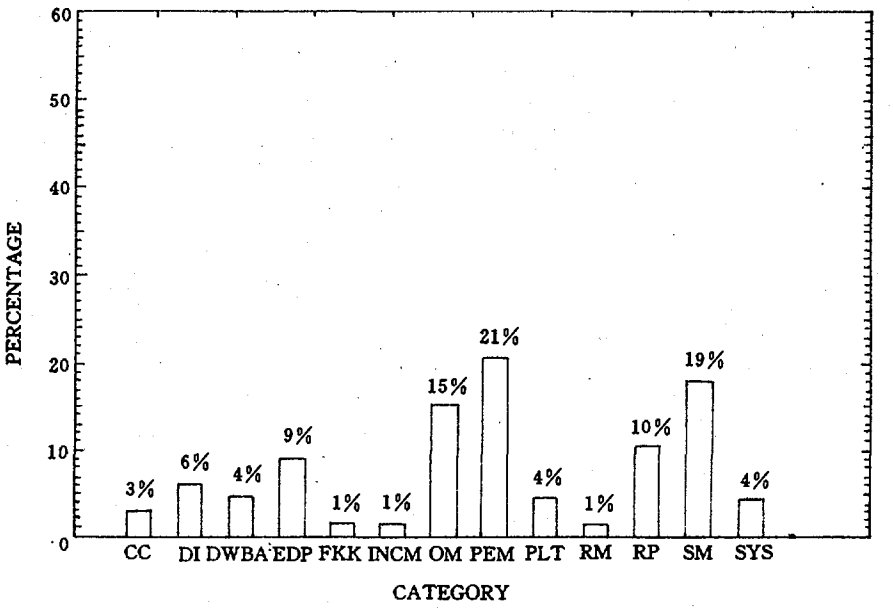

Fig. 1 Category

Reference

[1] Liu Ruizhe, Program MADEX Creating Index for PLRND at CNDC

CINDA INDEX

Nuclide	Quantity	Energy (eV)		Lab	Type	Documentation			
		Min	Max			Ref	Vol	Page	Date
^{23}Na	(n,2n)	1.35+7	1.48+7	LNZ	Expt	Jour CNDP	14	5	Dec 95
^{56}Fc	Evaluation		1.41+7	AEP	Eval	Jour CNDP	14	34	Dec 95
Ni	(n,α)	Thrsh	2.0 +7	SIU	Eval	Jour CNDP	14	53	Dec 95
^{58}Ni	(n,α)	Thrsh	2.0 +7	SIU	Eval	Jour CNDP	14	53	Dec 95
	(n,2n)	Thrsh	2.0 +7	AEP	Eval	Jour CNDP	14	58	Dec 95
^{60}Ni	(n,α)	Thrsh	2.0 +7	SIU	Eval	Jour CNDP	14	53	Dec 95
^{61}Ni	(n,α)	Thrsh	2.0 +7	SIU	Eval	Jour CNDP	14	53	Dec 95
^{62}Ni	(n,α)	Thrsh	2.0 +7	SIU	Eval	Jour CNDP	14	53	Dec 95
^{64}Ni	(n, α)	Thrsh	2.0 +7	SIU	Eval	Jour CNDP	14	53	Dec 95
^{64}Zn	(n,γ)	1.56+5	1.15+6	BJG	Expt	Jour CNDP	14	1	Dec 95
^{87}Rb	(n,2n)	Thrsh	2.0 +7	AEP	Eval	Jour CNDP	14	58	Dec 95
^{89}Y	(n,2n)	Thrsh	2.0 +7	AEP	Eval	Jour CNDP	14	58	Dec 95
	Calculation	1.0 +5	2.0 +7	ZHN	Theo	Jour CNDP	14	8	Dec 95
^{90}Zr	(n,2n)	1.0 +5	2.0 +7	AEP	Theo	Jour CNDP	14	58	Dec 95
^{93}Nb	(n,2n)	1.0 +5	2.0 +7	AEP	Theo	Jour CNDP	14	45	Dec 95
	(n,n')	1.0 +5	2.0 +7	AEP	Theo	Jour CNDP	14	45	Dec 95
^{92}Mo	(n,p)	1.34+7	1.48+7	LNZ	Expt	Jour CNDP	14	5	Dec 95
^{94}Mo	(n,2n)	1.34+7	1.48+7	LNZ	Expt	Jour CNDP	14	5	Dec 95
^{98}Mo	(n,p)	1.35+7	1.48+7	LNZ	Expt	Jour CNDP	14	5	Dec 95
Ba	(n,x)	1.35+7	1.48+7	LNZ	Expt	Jour CNDP	14	5	Dec 95
^{134}Ba	(n,2n)	1.35+7	1.48+7	LNZ	Expt	Jour CNDP	14	5	Dec 95
^{137}Ba	(n,p)		1.42+7	LNZ	Expt	Jour CNDP	14	5	Dec 95
^{140}Cc	(n,2n)	1.35+7	1.48+7	LNZ	Expt	Jour CNDP	14	5	Dec 95
	(n,2n)	Thrsh	2.0 +7	AEP	Eval	Jour CNDP	14	58	Dec 95
^{142}Ce	(n,2n)	1.35+7	1.48+7	LNZ	Expt	Jour CNDP	14	5	Dec 95
^{169}Tm	(n,2n)	Thrsh	2.0 +7	AEP	Eval	Jour CNDP	14	58	Dec 95
Lu	Calculation	1.0 +3	2.0 +7	AEP	Theo	Jour CNDP	14	16	Dec 95
^{175}Lu	Calculation	1.0 +3	2.0 +7	AEP	Theo	Jour CNDP	14	16	Dec 95
^{176}Lu	Calculation	1.0 +3	2.0 +7	AEP	Theo	Jour CNDP	14	16	Dec 95
^{179}Hf	(n,2n)		1.44+7	LNZ	Expt	Jour CNDP	14	5	Dec 95
^{209}Bi	(n,2n)		1.46+7	LNZ	Expt	Jour CNDP	14	5	Dec 95

Author, Comments
Kong Xiangzhong+, SIG, TBL, ACTIV
Zhou Delin, SIG
Ma Gonggui+, SIG
Ma Gonggui+, SIG
Yu Baosheng, SIG
Ma Gonggui+, SIG
Ma Gonggui+, SIG
Ma Gonggui+, SIG
Ma Gonggui+, SIG
Chen Jinxiang+, TBL, ACTIV
Yu Baosheng, SIG
Yu Baosheng, SIG
Liu Jianfeng+, CALC, with NDCP-1
Yu Baosheng, SIG
Yu Baosheng, SIG, NB-92 M
Yu Baosheng, SIG, NB-93 M
Kong Xiangzhong+, SIG, TBL, ACTIV
Kong Xiangzhong+, SIG, TBL, ACTIV
Kong Xiangzhong+, SIG, TBL, ACTIV
Kong Xiangzhong+, SIG, TBL, ACTIV, CS-134
Kong Xiangzhong+, SIG, TBL, ACTIV
Kong Xiangzhong+, SIG, TBL, ACTIV
Kong Xiangzhong+, SIG, TBL, ACTIV
Yu Baosheng, SIG
Kong Xiangzhong+, SIG, TBL, ACTIV
Yu Baosheng, SIG
Han Yinlu+, with UNF CODE
Han Yinlu+, with UNF CODE
Han Yinlu+, with UNF CODE
Kong Xiangzhong+, SIG, TBL, ACTIV
Kong Xiangzhong+, SIG, TBL, ACTIV

（京）新登字 077 号

图书在版编目 (CIP) 数据

中国核科技报告：核数据进展通讯 = CNIC：COMMUNICATION OF NUCLEAR DATA PROGRESS：英文／刘廷进等. —北京：原子能出版社, 1995, 12

ISBN 7-5022-1433-X

I. 中 … II. 刘 … III. ①核技术-研究报告-中国 ②核电子学-数据处理-系统-连续性出版物 IV. ① TL-24 ② TL822-55

中国版本图书馆 CIP 数据核字 (95) 第 19573 号

原子能出版社出版发行

责任编辑：李曼莉

社址：北京市海淀区阜成路 43 号 邮政编码：100037

核科学技术情报研究所印刷

开本 787×1092 1／16 · 印张 5 1／2 · 字数 80 千字

1995 年 12 月北京第一版 · 1995 年 12 月北京第一次印刷